

Arctic Report Card: Update for 2014

Tracking recent environmental changes

Home About Printouts Previous Report Cards NOAA Arctic Theme Page Contacts

HOME

Executive Summary

VITAL SIGNS

Air Temperature

Terrestrial Snow Cover

Greenland Ice Sheet

Sea Ice

Sea Surface Temperature

Ocean Primary Productivity

Tundra Greenness

INDICATORS

Polar Bears

FROSTBITES

Climate, Herbivores & Ecosystem Function

Depicting Arctic Change

What's new in 2014?

Rising air and sea temperatures continue to trigger changes in the Arctic. *The Arctic is warming at twice the rate of anywhere else on Earth.*

However, natural variation remains, such as the slight increase in March 2014 sea ice thickness and only a slight decrease in total mass of the Greenland ice sheet in summer 2014.



Arctic Report Card 2014

Highlights

The warming Arctic atmosphere was strongly connected to lower latitudes in early 2014 causing cold air outbreaks into the eastern USA and warm air intrusions into Alaska and northern Europe.

Snow cover extent in April 2014 in Eurasia was the lowest since 1967 and **sea ice extent** in September was the 6th lowest since 1979.

Polar bears numbers in western Hudson Bay and the southern Beaufort Sea are decreasing in connection with a decrease in the availability of sea ice.

The tundra is "browning" as the length of the growing season is decreasing in Eurasia, but maximum tundra greenness and biomass are increasing across the Arctic.

Sea surface temperatures and primary production are increasing as the sea ice retreats throughout the Arctic Ocean.

On the Greenland ice sheet nearly 40% of the surface experienced melting conditions in summer 2014 and the albedo (reflectivity) reached a new record low value in August.



[DOC](#) | [NOAA](#) | [NOAA Arctic Research Program](#)
[Disclaimer](#) | [Privacy Policy](#) | [Webmaster](#)

December 2014

www.arctic.noaa.gov/reportcard

Citing the complete report:

M. O. Jeffries, J. Richter-Menge, and J. E. Overland, Eds., 2014: Arctic Report Card 2014, <http://www.arctic.noaa.gov/reportcard>.

Citing an essay (example):

Derksen, C. and R. Brown, 2014: Snow [in Arctic Report Card 2014], <http://www.arctic.noaa.gov/reportcard>.

Table of Contents

Authors and Affiliations	3
Executive Summary.....	6
Air Temperature.....	9
Terrestrial Snow Cover.....	16
Greenland Ice Sheet.....	22
Sea Ice	33
Arctic Ocean Sea Surface Temperature	40
Arctic Ocean Primary Productivity	45
Tundra Greenness.....	56
Polar Bears: Status, Trends and New Knowledge	61
Climate and Herbivore Body Size Determine How Arctic Terrestrial Ecosystems Work.....	68
Depicting Arctic Change: Dependence on the Reference Period	71

Authors and Affiliations

- D. Berteaux, Université du Québec à Rimouski and Centre d'études nordiques, Rimouski, QC, Canada
- J. Bêty, Université du Québec à Rimouski and Centre d'études nordiques, Rimouski, QC, Canada
- U. S. Bhatt, Geophysical Institute, University of Alaska Fairbanks, Fairbanks, AK, USA
- P. A. Bieniek, Geophysical Institute, University of Alaska Fairbanks, Fairbanks, AK, USA
- J. E. Box, Geological Survey of Denmark and Greenland, Copenhagen, Denmark
- R. Brown, Climate Processes Section, Environment Canada, Montreal, QC, Canada
- M.-C. Cadieux, Département de Biologie and Centre d'études nordiques, Université Laval, Québec City, QC, Canada
- J. Cappelen, Danish Meteorological Institute, Copenhagen, Denmark
- J. C. Comiso, Cryospheric Sciences Laboratory, NASA Goddard Space Flight Center, Greenbelt, MD, USA
- L. W. Cooper, Chesapeake Biological Laboratory, University of Maryland Center for Environmental Science, Solomons, MD, USA
- C. Derksen, Climate Research Division, Environment Canada, Toronto, ON, Canada
- H. E. Epstein, Department of Environmental Sciences, University of Virginia, Charlottesville, VA, USA
- X. Fettweis, University of Liege, Liege, Belgium
- K. E. Frey, Graduate School of Geography, Clark University, Worcester, MA, USA
- G. Gauthier, Département de Biologie and Centre d'études nordiques, Université Laval, Québec City, QC, Canada
- S. Gerland, Norwegian Polar Institute, Fram Centre, Tromsø, Norway
- S. J. Goetz, Woods Hole Research Center, Falmouth, MA, USA
- R. R. Gradinger, Institute of Marine Research, Tromsø, Norway
- D. Gravel, Département de Biologie, Université du Québec à Rimouski, Rimouski, QC, Canada
- J. M. Grebmeier, Chesapeake Biological Laboratory, University of Maryland Center for Environmental Science, Solomons, MD, USA
- K. C. Guay, Woods Hole Research Center, Falmouth, MA, USA
- E. Hanna, Department of Geography, University of Sheffield, Sheffield, UK
- I. Hanssen-Bauer, Norwegian Meteorological Institute, Blindern, Oslo, Norway
- S. Hendricks, Alfred Wegener Institute, Bremerhaven, Germany

R. A. Ims, Department of Arctic and Marine Biology, University of Tromsø, Tromsø, Norway

M. O. Jeffries, Office of Naval Research, Arlington, VA, USA

G. J. Jia, Institute of Atmospheric Physics, Chinese Academy of Sciences, Beijing, China

S.-J. Kim, Korea Polar Research Institute, Incheon, Republic of Korea

C. J. Krebs, Department of Zoology, University of British Columbia, Vancouver, BC, Canada

N. Lecomte, Université du Québec à Rimouski and Centre d'études nordiques, Rimouski, QC, Canada; Department of Arctic and Marine Biology, University of Tromsø, Tromsø, Norway; Department of Biology, University of Moncton, Moncton, NB, Canada

P. Legagneux, Département de Biologie and Centre d'études nordiques, Université Laval, Québec City, QC, Canada; Université du Québec à Rimouski and Centre d'études nordiques, Rimouski, QC, Canada

S. J. Leroux, Department of Biology, Memorial University of Newfoundland, St John's, NL, Canada

M. Loreau, Centre for Biodiversity Theory and Modelling, CNRS, Moulis, France

K. Luojus, Arctic Research Centre, Finnish Meteorological Institute, Helsinki, Finland

W. Meier, NASA Goddard Space Flight Center, Greenbelt, MD, USA

R. I. G. Morrison, National Wildlife Research Centre, Environment Canada, Carleton University, Ottawa, ON, Canada

T. Mote, Department of Geography, University of Georgia, Athens, Georgia, USA

L. Mudryk, Department of Physics, University of Toronto, Toronto, ON, Canada

M. Nicolaus, Alfred Wegener Institute, Bremerhaven, Germany

J. E. Overland, National Oceanic and Atmospheric Administration, Pacific Marine Environmental Laboratory, Seattle, WA, USA

D. Perovich, ERDC-Cold Regions Research and Engineering Laboratory, Hanover, NH, USA; Thayer School of Engineering, Dartmouth College, Hanover, NH, USA

J. Pinzon, Biospheric Science Branch, NASA Goddard Space Flight Center, Greenbelt, MD, USA

A. Proshutinsky, Woods Hole Oceanographic Institution, Woods Hole, MA, USA

M. K. Raynolds, Institute of Arctic Biology, University of Alaska Fairbanks, Fairbanks, AK, USA

D. Reid, Wildlife Conservation Society Canada, Whitehorse, YT, Canada

J. Richter-Menge, ERDC-Cold Regions Research and Engineering Laboratory, Hanover, NH, USA

S.-I. Saitoh, Graduate School of Fisheries Sciences, Hokkaido University, Hokkaido, Japan

N. M. Schmidt, Arctic Research Centre, Aarhus University, Aarhus, Denmark

C. J. P. P. Smeets, Institute for Marine and Atmospheric Research Utrecht, Utrecht University, Utrecht, The Netherlands

M. Tedesco, City College of New York, New York, NY, USA; National Science Foundation, Arlington, VA, USA

M.-L. Timmermans, Yale University, New Haven, CT, USA

J.-É. Tremblay, Québec-Océan and Takuvik, Biology Department, Université Laval, Québec City, QC, Canada

M. Tschudi, Aerospace Engineering Sciences, University of Colorado, Boulder, CO, USA

C. J. Tucker, Biospheric Science Branch, NASA Goddard Space Flight Center, Greenbelt, MD, USA

R. S. W. van de Wal, Institute for Marine and Atmospheric Research Utrecht, Utrecht University, Utrecht, The Netherlands

D. Vongraven, Norwegian Polar Institute, Fram Centre, Tromsø, Norway

J. Wahr, Department of Physics and Cooperative Institute for Research in Environmental Sciences, University of Colorado, Boulder, CO, USA

D. A. Walker, Institute of Arctic Biology, University of Alaska Fairbanks, Fairbanks, AK, USA

J. Walsh, International Arctic Research Center, University of Alaska Fairbanks, Fairbanks, AK, USA

M. Wang, Joint Institute for the Study of the Atmosphere and Ocean, University of Washington, Seattle, WA, USA

N. G. Yoccoz, Department of Arctic and Marine Biology, University of Tromsø, Tromsø, Norway

G. York, Polar Bears International, Bozeman, MT, USA

H. Zeng, Institute of Atmospheric Physics, Chinese Academy of Sciences, Beijing, China

Executive Summary

Martin O. Jeffries¹, Jacqueline Richter-Menge², James E. Overland³

¹Office of Naval Research, Arlington, VA, USA

²ERDC-Cold Regions Research and Engineering Laboratory, Hanover, NH, USA

³National Oceanic and Atmospheric Administration, Pacific Marine Environmental Laboratory, Seattle, WA, USA

December 2, 2014

The Arctic Report Card (www.arctic.noaa.gov/reportcard/) considers a range of environmental observations throughout the Arctic, and is updated annually. As in previous years, the 2014 update to the Arctic Report Card describes the current state of different physical and biological components of the Arctic environmental system and illustrates that change continues to occur throughout the system.

Mean annual air temperature continues to increase in the Arctic, at a rate of warming that is more than twice that at lower latitudes. In winter (January-March) 2014, this Arctic amplification of global warming was manifested by periods of strong connection between the Arctic atmosphere and mid-latitude atmosphere due to a weakening of the polar vortex. In Alaska this led to statewide temperature anomalies of +10°C in January, due to warm air advection from the south, while temperature anomalies in eastern North America and Russia were -5°C, due to cold air advection from the north.

Evidence is emerging that Arctic warming is driving synchronous pan-Arctic responses in the terrestrial and marine cryosphere. For instance, during the period of satellite passive microwave observation (1979-2014), reductions in Northern Hemisphere snow cover extent in May and June (-7.3% and -19.8% per decade, respectively) bracket the rate of summer sea ice loss (-13.3% per decade decline in minimum ice extent), and since 1996 the June snow and September sea ice signals have become more coherent.

In April 2014, a new record low snow cover extent for the satellite era (1967-2014) occurred in Eurasia and, in September 2014, minimum sea ice extent was the 6th lowest in the satellite record (1979-2014). But, in 2014, there were modest increases in the age and thickness of sea ice relative to 2013. The eight lowest sea ice extents since 1979 have occurred in the last eight years (2007-2014).

There is growing evidence that polar bears are being adversely affected by the changing sea ice in those regions where there are good data. Thus, for example, between 1987 and 2011 in western Hudson Bay, Canada, a decline in polar bear numbers, from 1,194 to 806, was due to earlier sea ice break-up, later freeze-up and, thus, a shorter sea ice season. In the southern Beaufort Sea, polar bear numbers had stabilized at ~900 by 2010 after a ~40% decline since 2001. However, survival of sub-adult bears declined during the entire period. Polar bear condition and reproductive rates have also declined in the southern Beaufort Sea, unlike in the

adjacent Chukchi Sea, immediately to the west, where they have remained stable for 20 years. There are also now twice as many ice-free days in the southern Beaufort Sea as there are in the Chukchi Sea.

As the sea ice retreats in summer and previously ice-covered water is exposed to solar radiation, sea surface temperature (SST) and upper ocean temperatures in all the marginal seas of the Arctic Ocean are increasing; the most significant linear trend is in the Chukchi Sea, where SST is increasing at a rate of 0.5°C/decade. In summer 2014, the largest SST anomalies, as much as 4°C above the 1982-2010 average, occurred in the Barents Sea and in the Bering Strait region, which includes the Chukchi Sea.

Declining summer sea ice extent is also leading to increasing ocean primary production due to solar radiation being available over a larger area of open water. The greatest increases in primary production during the period of SeaWiFS and MODIS satellite observation (1998-2010) occurred in the East Siberian Sea (+112.7%), Laptev Sea (+54.6%) and Chukchi Sea (+57.2%). In 2014, the greatest primary production occurred in the Kara and Laptev seas north of Eurasia. Regional variations in primary production are strongly dependent on the availability of nutrients in the near-surface water layer that receives sufficient solar radiation for photosynthesis to occur.

On land, peak tundra greenness, a measure of vegetation productivity that is strongly correlated with above-ground biomass, continues to increase. The trend in peak greenness indicates an average tundra biomass increase of approximately 20% during the period (1982-2013) of AVHRR satellite observation. On the other hand, greenness integrated over the entire growing season indicates that a browning and a shorter growing season have occurred over large areas of the tundra since 1999. In Eurasia, in particular, these conditions have coincided with a decline in summer air temperatures.

Ice on land, as represented by the Greenland Ice Sheet, experienced extensive melting again in 2014. The maximum extent of melting at the surface of the ice sheet was 39.3% of its area; for 90% of the summer the extent of melting was above the long-term (1981-2010) average; and the number of days of melting in June and July exceeded the 1981-2010 average over most of the ice sheet. Average albedo (reflectivity) during summer 2014 was the second lowest in the period of MODIS satellite observation (2000-2014), and a new, ice sheet-wide record low albedo occurred in August 2014. These signals contrast with the total ice mass, which did not change significantly between 2013 and 2014.

In summary, Arctic Report Card 2014 shows that change continues to occur in both the physical and biological components of the Arctic environmental system. However, it is a complex system and there are spatial and temporal variations in the magnitude and direction of change, and there are some apparent mixed signals. For example, peak tundra greenness increased between 1982 and 2013, but over the length of the growing season there has been an apparent browning of the tundra since 1999, particularly in Eurasia. And, most recently, between 2013 and 2014 there was a modest increase in the age and thickness of sea ice, while mass loss

from the Greenland ice sheet was negligible. Nevertheless, overall the long-term trends provide evidence of continuing and often significant change related to Arctic amplification of global warming.

Air Temperature

J. Overland¹, E. Hanna², I. Hanssen-Bauer³, S.-J. Kim⁴, J. Walsh⁵, M. Wang⁶, U. S. Bhatt⁷

¹NOAA/PMEL, Seattle, WA, USA

²Department of Geography, University of Sheffield, Sheffield, UK

³Norwegian Meteorological Institute, Blindern, Oslo, Norway

⁴Korea Polar Research Institute, Incheon, Republic of Korea

⁵International Arctic Research Center, University of Alaska Fairbanks, Fairbanks, AK, USA

⁶Joint Institute for the Study of the Atmosphere and Ocean, University of Washington, Seattle, WA, USA

⁷Geophysical Institute, University of Alaska Fairbanks, Fairbanks, AK, USA

December 2, 2014

Highlights

- The annual surface air temperature anomaly (+1.0°C relative to the 1981-2010 mean value) for October 2013-September 2014 continues the pattern of increasing positive anomalies since the late 20th Century.
- On a number of occasions in winter (January-March) 2014 there were strong connections between Arctic and mid-latitude weather patterns. A high amplitude (sinuous) jet stream sent warm air northward into Alaska and northern Europe, and cold air southward into eastern North America and central Russia.
- As a consequence of the sinuous jet stream in early 2014, extreme monthly temperature anomalies of +10°C were reported in Alaska, and -5°C over eastern North America and much of Russia.
- An Arctic Dipole pattern, with high pressure on the North American side of the central Arctic and low pressure on the Siberian side, contributed to low sea ice extent in summer 2014.

Arctic air temperatures are both an indicator and driver of regional and global changes. Although there are year-to-year and regional differences in air temperatures due to natural random variability, the magnitude and Arctic-wide character of the long-term temperature increase is a major indicator of global warming. Increases in Arctic temperatures cause, and are in turn influenced by, a set of feedbacks involving many parts of the Arctic environmental system: loss of sea ice and snow, changes in land ice and vegetation cover, permafrost thaw, black carbon (soot) in the atmosphere and on snow and ice surfaces, and atmospheric water vapor.

Mean Annual Surface Air Temperature

The mean annual surface air temperature anomaly (+1.0°C relative to the 1981-2010 mean value) for October 2013-September 2014 for land stations north of 60°N continues the pattern of increasing positive anomalies since the late 20th Century (**Fig. 1.1**). Note that 1981-2010 is the current reference period used by the World Meteorological Organization and individual national

agencies such as NOAA. The 12-month period October 2013-September 2014 is the time elapsed since annual air temperature anomalies were last reported in the Arctic Report Card (Overland et al. 2013), and September 2014 is the most recent month for which data were available at the time of writing. The same applies to the next section describing seasonal air temperature variability.

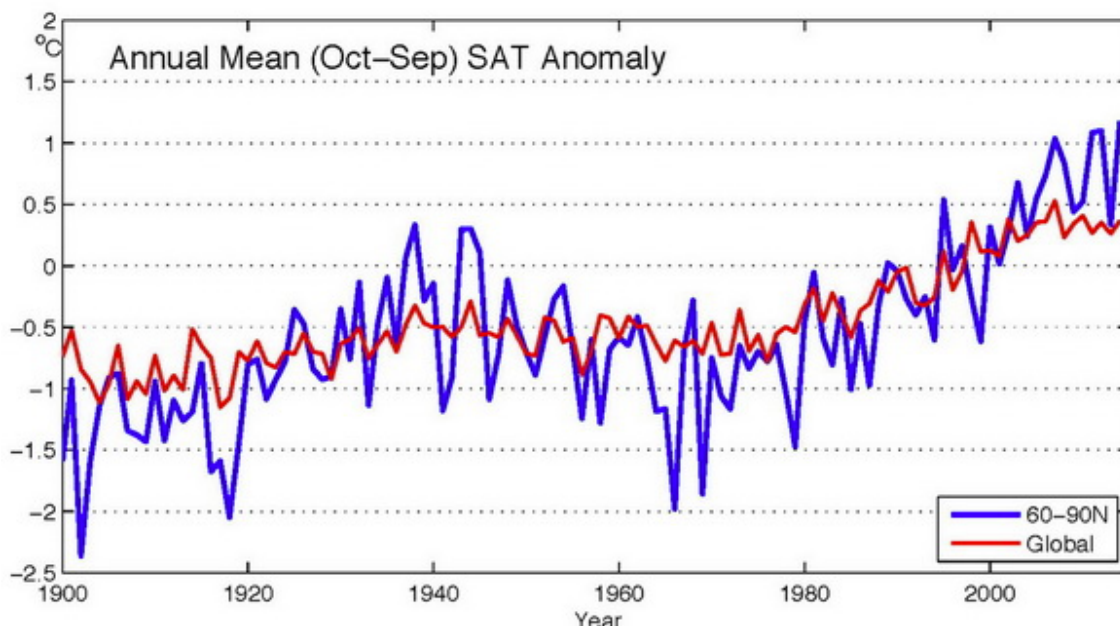


Fig. 1.1. Arctic and global mean annual surface air temperature (SAT) anomalies (in °C) for the period 1900-2014 relative to the 1981-2010 mean value. The Arctic data are for land stations north of 60°N; note that there were few stations in the Arctic prior to 2014, particularly in northern Canada. Since a full year of 2014 data was not available at the time of writing the reporting year is October-September. The data are from the CRUTEM4v dataset, which is available at www.cru.uea.ac.uk/cru/data/temperature/.

The global rate of temperature increase has slowed in the last decade (Kosaka and Xie 2013), but Arctic temperatures continued to increase, such that the Arctic is warming at more than twice the rate of lower latitudes, as is evident in **Fig. 1.1**. The rapid warming in the Arctic is known as Arctic Amplification and is due to feedbacks involving many parts of the Arctic environment: loss of sea ice and snow cover, changes in land ice and vegetation cover, and atmospheric water vapor content (Serreze and Barry 2011).

The spatial distribution of near-surface temperatures in autumn-early winter (October-December) during recent years (2009-2014) has been warmer than the final 20 years of the 20th Century (1981-2000) in all parts of the Arctic (**Fig. 1.2**). These Arctic-wide positive (warm) anomalies are an indication that the early 21st Century temperature increase in the Arctic is due to global warming rather than natural regional variability (Overland 2009, Jeffries et al. 2013a).

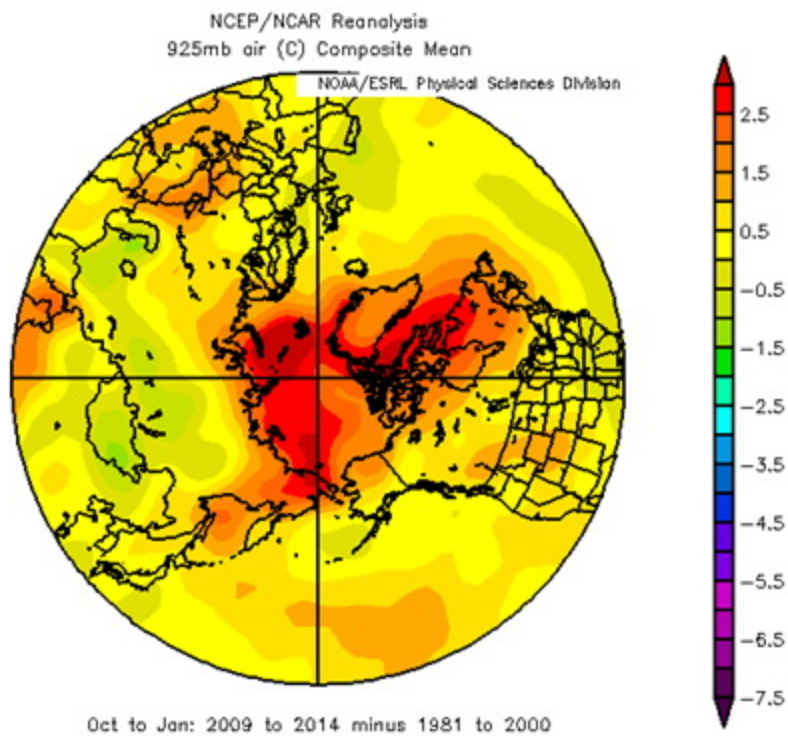


Fig. 1.2. October - January average near-surface air temperature anomalies (in °C) for the years 2009-2014 relative to the final 20 years of the 20th Century (1981-2000). Data are from NOAA/ESRL, Boulder, CO, and can be found at <http://www.esrl.noaa.gov/psd/>.

Seasonal Surface Air Temperature Variability, October 2013 to September 2014

Seasonal air temperature variations are described for the period October 2013 to September 2014, which is divided by season into autumn 2013 (October, November, December), and winter (January, February, March), spring (April, May, June) and summer (July, August, September) of 2014 (**Fig. 1.3**).

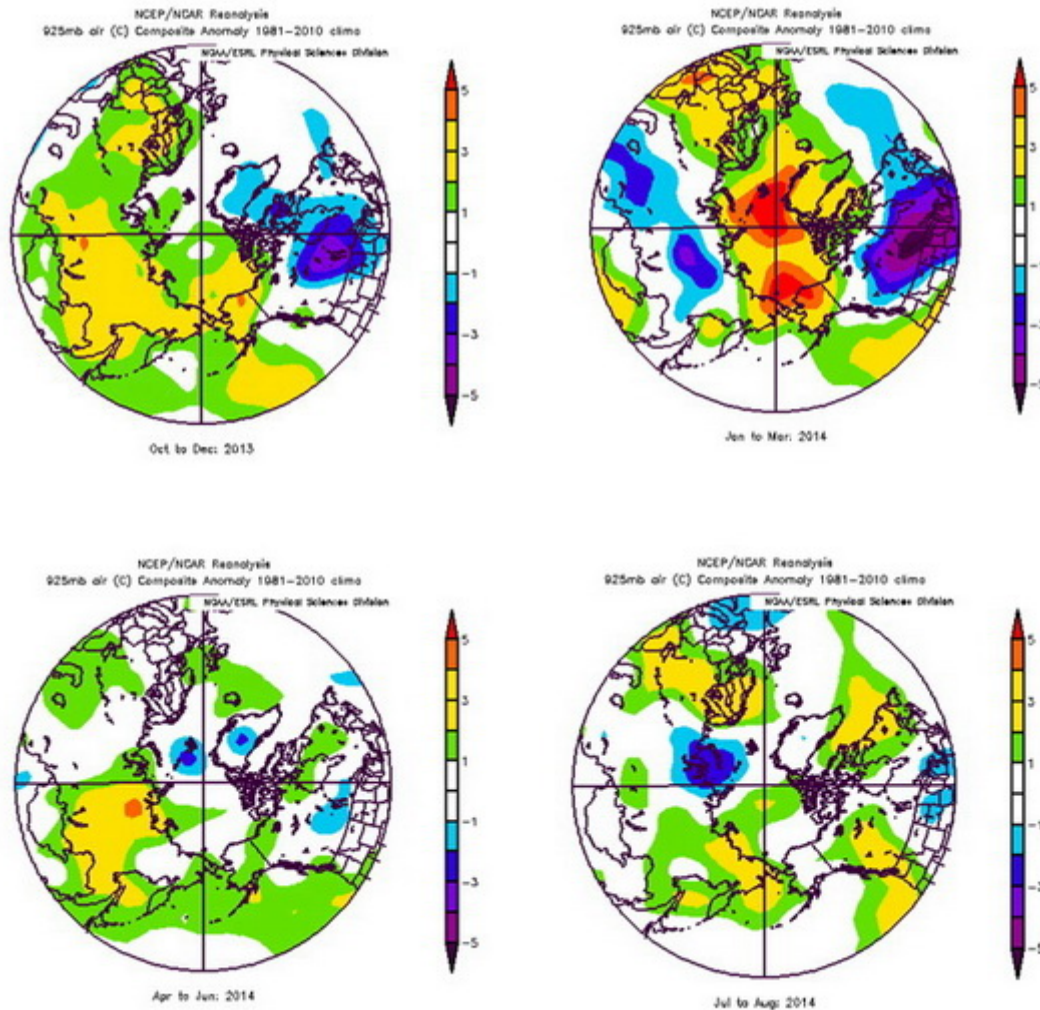


Fig. 1.3. Seasonal anomaly patterns for near surface air temperatures (in °C) in 2014 relative to the baseline period 1981-2010 in (a, top left) autumn 2013, (b, top right) winter 2014, (c, bottom left) spring 2014, and (d, bottom right) summer 2014. Temperature analyses are from slightly above the surface layer (at 925 mb level) that emphasizes large spatial patterns rather than local features. Data are from NOAA/ESRL, Boulder, CO, at <http://www.esrl.noaa.gov/psd/>.

Autumn 2013 was characterized by considerable month-to-month and regional variability in individual weather features that are masked by the 3-month composite (**Fig. 1.3a**). For example, there were anomalously high air temperatures in October over Alaska due to a strong Aleutian low pressure system, while low pressure in the Atlantic sector in November and December (similar to the winter pattern illustrated in **Fig. 1.4**) caused relatively warm temperatures in Siberia and cold temperatures in Greenland and Canada.

For winter 2014, each of the three months had similar regional temperature extremes (**Fig. 1.3b**). Extreme monthly temperature anomalies in excess of +5°C over the central Arctic spread south over Europe and Alaska. Svalbard Airport, for example, was 8°C above the 1981-2010 January-March average. Statewide, Alaska temperature anomalies were +10°C in late January

2014. Warm temperatures broke the 7-year (2007-2013) string of cold anomalies and extensive sea ice cover in the Bering Sea. Temperature anomalies were 5°C below normal in January and February over eastern North America and in January, February and March over much of Russia. Northern Siberia was relatively cool, and warm anomalies were observed in far eastern Asia. This pattern resulted from fewer storms connecting central Asia to northern Europe and was perhaps related to the greater sea ice loss that occurred in winter 2014 over the Barents and Kara seas (Kim et al. 2014).

On a number of occasions in January, February and March 2014 Arctic and mid-latitude weather patterns were strongly linked due to a high amplitude (more sinuous) "wave number 2" jet stream pattern (**Fig. 1.4**). This sent warm air from the south northward into Alaska and northern Europe, and cold air from the Arctic southward into eastern North America. A sinuous jet stream pattern is often associated with a negative Arctic Oscillation (AO) climate pattern, as evidenced by the higher geopotential heights north of Alaska and central Greenland (**Fig. 1.4**). The wave number 2 pattern had low heights over Iceland, where record low sea level pressures and warm temperatures occurred. In January, the North Atlantic Oscillation (NAO) was positive, while the AO was negative; this is unusual, as the AO and NAO often have the same sign. The wavy pattern over eastern North America and the positive NAO over the North Atlantic Ocean contributed to January flooding in the UK (Slingo et al. 2014).

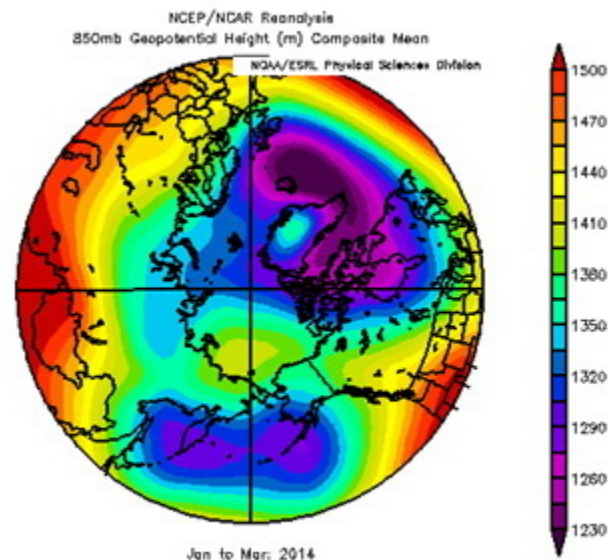


Fig. 1.4. Geopotential height (in dynamic meters) field for winter (JFM) 2014. Wind flow is counter-clockwise along the geopotential height contours. Data are from NOAA/ESRL, Boulder, CO, at <http://www.esrl.noaa.gov/psd/>.

Apart from low pressure over the Kara Sea causing warmer temperatures in central Siberia, which contributed to a record low April snow cover extent in Eurasia (see the essay on [Snow](#)), no major anomalies were observed in spring 2014 (**Fig. 1.3c**). Air temperatures were near normal during summer 2014 (**Fig. 1.3d**) relative to recent climatology (1981-2010), which

includes a number of warm years. Summer temperatures in Greenland were above the 1981-2010 average (see the essay on the [Greenland Ice Sheet](#)), but were not unusually warm compared to the last decade. Summer 2014 was the warmest ever measured at many weather stations in Scandinavia. The Arctic Dipole (AD) (Wang et al. 2009, Overland et al. 2012) pattern dominated summer sea level pressure, with higher pressures on the North American side of the central Arctic and low pressures on the Siberian side (**Fig. 1.5**). In summer, this pattern tends to favor lower sea ice extent. Consistent with this observation, the minimum ice extent in September 2014 was the sixth lowest in the satellite record (see the essay on [Sea Ice](#)). Low atmospheric pressure over the eastern Aleutian Islands (**Fig. 1.5**) contributed to a wetter than normal summer in Interior Alaska.

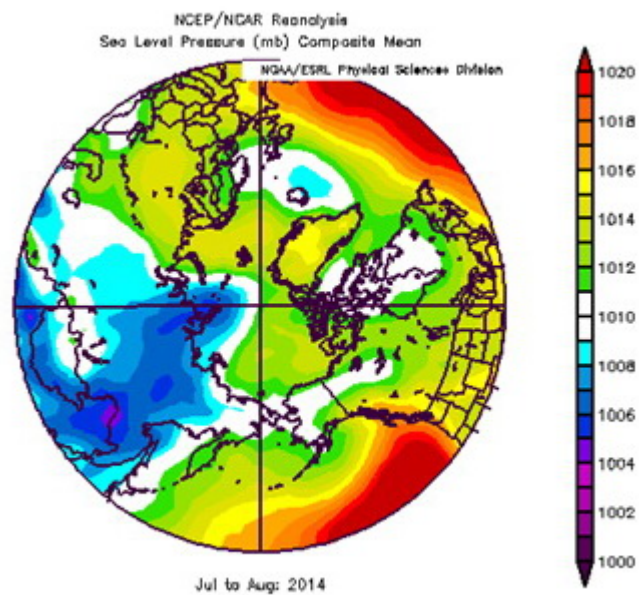


Fig. 1.5. Sea level pressure (in millibars) field for summer (JA) 2014 illustrates the Arctic Dipole pattern, with higher pressure on the North American side of the Arctic than on the Eurasian side. Data are from NOAA/ESRL, Boulder, CO, at <http://www.esrl.noaa.gov/psd/>.

References

- Jeffries, M. O., J. E. Overland, and D. K. Perovich, 2013a: The Arctic shifts to a new normal. *Physics Today*, 66(10), 35-40.
- Kim, B.-M., S.-W. Son, S.-K. Min, J.-H. Jeong, S.-J. Kim, X. Zhang, T. Shim, and J.-H. Yoon, 2014: Weakening of the stratospheric polar vortex by arctic sea-ice loss. *Nature Communications*, 5, doi: 10.1038/ncomms5646.
- Kosaka, Y., and S.-P. Xie, 2013: Recent global-warming hiatus tied to equatorial Pacific surface cooling. *Nature*, 501, 403-407.

Overland, J. E., 2009: The case for global warming in the Arctic. In *Influence of Climate Change on the Changing Arctic and Sub-Arctic Conditions*, J. C. J. Nihoul and A. G. Kostianoy (eds.), Springer, 13-23.

Overland, J. E., J. A. Francis, E. Hanna, and M. Wang, 2012: The recent shift in early summer Arctic atmospheric circulation. *Geophys. Res. Lett.*, 39, L19804, doi:[10.1029/2012GL053268](https://doi.org/10.1029/2012GL053268).

Overland, J. E., E. Hanna, I. Hanssen-Bauer, B.-M. Kim, S.-J. Kim, J. Walsh, M. Wang, and U. Bhatt, 2013: Air Temperature, in *Arctic Report Card: Update for 2013*, http://www.arctic.noaa.gov/report13/air_temperature.html.

Serreze, M., and R. Barry, 2011: Processes and impacts of Arctic amplification: A research synthesis. *Global and Planetary Change*, 77, 85-96.

Slingo, J, S. Belcher, A. Scaife, M. McCarthy, A. Saulter, K. McBeath, A. Jenkins, C. Huntingford, T. Marsh, J. Hannaford, and S. Parry. 2014: The Recent Storms and Floods in the UK. Synopsis Report CSc 04, Centre for Ecology and Hydrology, Natural Environment Research Council & Meteorological Office, UK, 28 pp.

Wang, J., J. Zhang, E. Watanabe, M. Ikeda, K. Mizobata, J. E. Walsh, X. Bai, and B. Wu, 2009: Is the Dipole anomaly a major driver to record lows in Arctic summer sea ice extent? *Geophys. Res. Lett.*, 36, L05706, doi:[10.1029/2008GL036706](https://doi.org/10.1029/2008GL036706).

Terrestrial Snow Cover

C. Derksen¹, R. Brown², L. Mudryk³, K. Luojus⁴

¹Climate Research Division, Environment Canada, Toronto, ON, Canada

²Climate Processes Section, Environment Canada, Montreal, QC, Canada

³Department of Physics, University of Toronto, Toronto, ON, Canada

⁴Arctic Research Centre, Finnish Meteorological Institute, Helsinki, Finland

December 2, 2014

Highlights

- Snow cover extent (SCE) across the Arctic land surface during spring 2014 (April, May, June) was below the long-term mean of 1981-2010. A new record low April SCE for the satellite era (1967-2014) was established for Eurasia, and June SCE in North America was the 3rd lowest in the record. June SCE in both the North American and Eurasian sectors of the Arctic was below average for the 10th consecutive season.
- Below average winter snow accumulation in western Russia, Scandinavia, the Canadian subarctic tundra and western Alaska, combined with above-normal spring temperatures, contributed to 3-4 week earlier than normal spring snow disappearance over these regions.
- Evidence is emerging that Arctic warming is driving synchronous pan-Arctic responses in the terrestrial and marine cryosphere: reductions in May and June SCE (-7.3% and -19.8% per decade, respectively) bracket the rate of summer sea ice loss (-13.3% per decade) over the 1979-2014 period for which satellite derived sea ice extent is available.

Snow overlying the Arctic land surface plays a significant role in the radiative forcing component of the Earth's energy budget by reflecting a high proportion of incident solar radiation back to space. This contributes to the cooling influence of the cryosphere on the global climate system, with the proportion of cooling attributable to terrestrial snow approximately the same as Arctic sea ice (Flanner et al. 2011). From an energy budget perspective, the transition seasons of autumn and spring are of particular interest because the Arctic is always completely snow covered in winter. Variability in temperature and precipitation during these shoulder seasons is closely coupled with the timing of the onset of snow in the autumn (Brown and Derksen, 2013) and snow-free conditions in the spring (Wang et al., 2013). Like the albedo difference between open water and sea ice in summer, the timing of spring snow melt is particularly significant because the low albedo of snow-free ground is coupled with increasing solar radiation during the lengthening days of the high latitude spring. Snow is also a very effective insulator, so variability in snow cover onset and snow melt, as well as snow accumulation during the cold Arctic winter, influences the thermal state of the soil beneath the snowpack (deeper snow = warmer soil).

Previous analysis of the satellite derived weekly NOAA snow chart Climate Data Record (CDR; maintained at Rutgers University and described in Brown and Robinson, 2011), which extends from 1967 through 2014, identified a dramatic loss of Northern Hemisphere spring snow cover extent (SCE) over the period 2007 through 2012 (Derksen and Brown, 2012). SCE anomalies for spring 2014, computed separately for the North American and Eurasian sectors of the Arctic (land areas north of 60°N), were consistent with these reductions (**Fig. 2.1**). Below normal SCE was observed for each month and region, with the exception of North America in April.

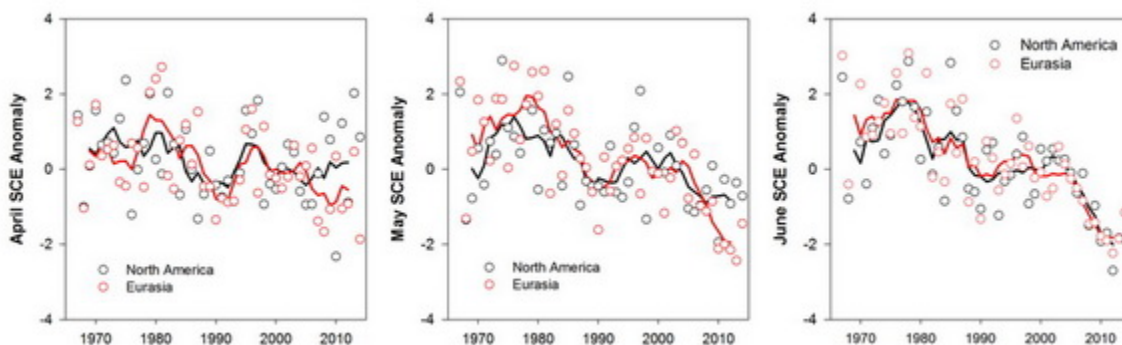


Fig. 2.1. Monthly Northern Hemisphere snow cover extent (SCE) standardized (and thus unitless) anomaly time series (with respect to 1981-2010) from the NOAA snow chart CDR for (a, left) April (b, center) May and (c, right) June 2014. Solid black and red lines depict 5-yr running means for North America and Eurasia, respectively.

In 2014, a new record low April SCE for the satellite era was established for Eurasia, driven by strong positive surface temperature anomalies over eastern Eurasia (see **Fig. 1.3c** in the essay on [Air Temperature](#)) and anomalously shallow snow depth over western Eurasia and northern Europe (**Fig. 2.3a**). The low snow accumulation across Europe and western Russia is consistent with warm temperature anomalies and reduced precipitation associated with the positive phase of the East Atlantic (EA) teleconnection pattern, which was strongly positive (mean index value of 1.43) from December 2013 through March 2014 (<http://www.cpc.ncep.noaa.gov/data/teledoc/ea.shtml>). Across North America, April SCE was above average (standardized anomaly of 0.86) as colder than normal surface temperatures extended across the Canadian Arctic and subarctic (see **Fig. 1.3b** in the essay on [Air Temperature](#)). Temperature anomalies shifted to positive in some regions during May (particularly in a dipole pattern over the eastern Canadian Arctic and Alaska), and were extensively warmer than average by June (see **Fig. 1.3c** in the essay on [Air Temperature](#)). This drove June SCE in North America to the 3rd lowest in the satellite record in spite of the positive SCE anomalies in April.

For both the North American and Eurasian sectors of the Arctic, below average SCE was observed during May for the ninth time in the past ten spring seasons, and for the 10th consecutive June. This loss of spring snow cover is reflected in the monthly SCE trends computed for 1967 through 2014 (**Table 2.1**). The rate of loss of spring SCE (-19.8% per decade) exceeds the rate of September sea ice loss (-13.3%) over the 1979-2014 period of the satellite passive microwave sea ice record (see the essay on [Sea Ice](#)), adding to the compelling

evidence of the observed rapid response of both the terrestrial and marine cryosphere to Arctic amplification in surface temperature trends (Derksen et al. 2014; also see the essay on [Air Temperature](#)).

Table 2.1. Linear trends (1967-2014) in snow cover extent (SCE) derived from the NOAA snow chart CDR using the Mann-Kendall (MK) statistic following the removal of serial correlation. **Bold:** significant at 95%; **bold italics:** significant at 99%. Updated from Derksen and Brown (2012).

	SCE Trend (km ² x 10 ⁶ x decade ⁻¹)	
	North America	Eurasia
April	-0.13	-0.41
May	-0.22	<i>-0.77</i>
June	<i>-0.45</i>	<i>-0.84</i>

Snow cover duration (SCD) departures derived from the NOAA daily Interactive Multisensor Snow and Ice Mapping System (IMS) snow cover product (Helfrich et al., 2007) show snow cover onset 10 to 20 days earlier than the average across northwestern Russia, northern Scandinavia, the Canadian Arctic Archipelago and the north slope of Alaska, with later snow onset over northern Europe and the Mackenzie River region in northwestern Canada (**Fig. 2.2a**). The spring SCD departures (**Fig. 2.2b**) are consistent with the April snow depth anomaly pattern (**Fig. 2.3b**; derived from the Canadian Meteorological Centre daily gridded global snow depth analysis described in Brasnett 1999) with below-normal snowpack and 20 to 30 day earlier melt over northern Europe, Siberia and the central Canadian Arctic. Above-normal snowpack conditions were observed during early spring over much of northern Russia (**Fig. 2.3**) but did not translate into later than normal spring snow cover due to above-normal spring temperatures that contributed to rapid ablation. This finding is consistent with the observation of Bulygina et al. (2010) of a trend toward increased winter snow accumulation and a shorter, more intense spring melt period over large regions of Russia.

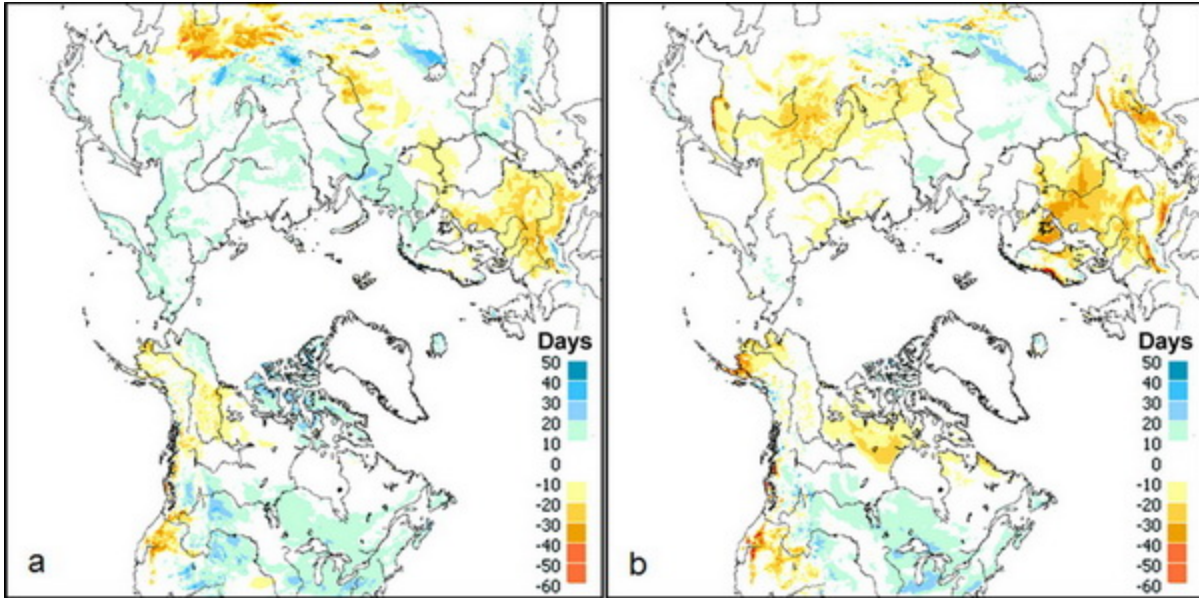


Fig. 2.2. Snow cover duration (SCD in days) departures (with respect to 1998-2010) from the NOAA IMS data record for the 2013-2014 snow year: (a, left) autumn; and (b, right) spring.

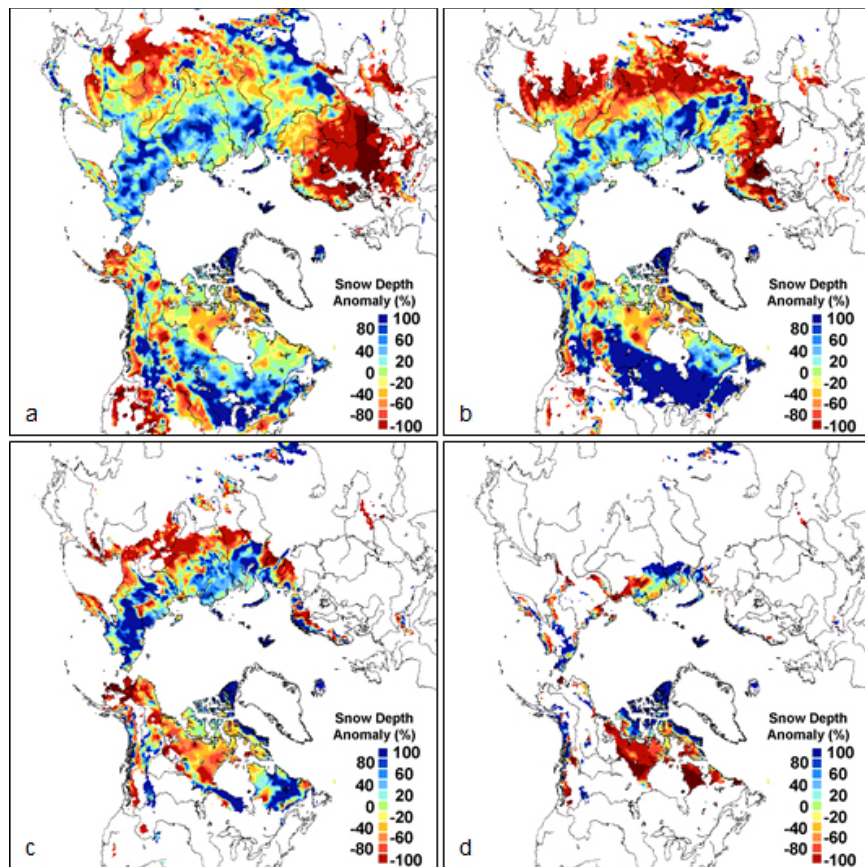


Fig. 2.3. 2014 snow depth anomaly (% of the 1999-2010 average) from the CMC snow depth analysis for (a, top left) March, (b, top right) April, (c, bottom left) May, and (d, bottom right) June.

While rigorous connections between changes in Arctic terrestrial snow and sea ice remain to be made, evidence is emerging that Arctic warming is driving synchronous pan-Arctic responses in the terrestrial and marine cryosphere (**Fig. 2.4**). De-trended correlation analysis of June SCE (from the NOAA CDR) with September sea ice extent (nsidc.org/data/seaice_index/) between 1979 and 2014 identified a correlation of 0.31 (statistically significant only at 90%). When the time series is divided into two parts, a de-trended correlation near zero for the first half of the record (1979-1995) increases to 0.57 (significant at 99%) for the second half (1996-2014). The latter indicates coherent snow and sea ice inter-annual variability (independent of the long term trend) over the past two decades, which was not present in the earlier portion of the satellite records.

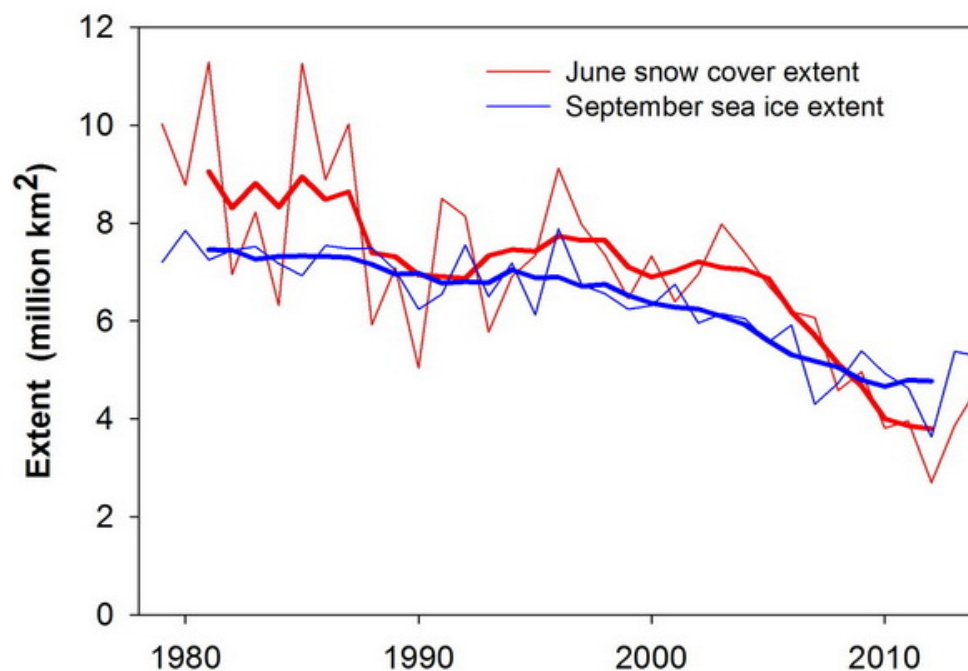


Fig. 2.4. Northern Hemisphere June snow cover extent and September Arctic sea ice extent, 1979-2014 (updated from Derksen and Brown, 2012). Bold red and blue lines are 5-year running means of the original snow and sea ice extent records, respectively. Vertical dashed line denotes the 1996 division of the time series into two parts for de-trended correlation analysis.

References

- Brasnett, B., 1999: A global analysis of snow depth for numerical weather prediction. *J. Appl. Meteorol.*, 38, 726-740.
- Brown, R., and D. Robinson, 2011: Northern Hemisphere spring snow cover variability and change over 1922-2010 including an assessment of uncertainty. *Cryosphere*, 5, 219-229.
- Brown, R., and C. Derksen, 2013: Is Eurasian October snow cover extent increasing? *Environmental Research Letters. Env. Res. Lett.*, 8, 024006 doi:10.1088/1748-9326/8/2/024006.

Bulygina, O. N., P. Y. Groisman, V. N. Razuvaev, and V. F. Radionov, 2010: Snow cover basal ice layer changes over Northern Eurasia since 1966. *Environ. Res. Lett.*, 5, 015004, doi:10.1088/1748-9326/5/1/015004.

Derksen, C., and R. Brown, 2012: Spring snow cover extent reductions in the 2008-2012 period exceeding climate model projections. *Geophys. Res. Lett.*, 39, doi:10.1029/2012GL053387.

Derksen, C., R. Brown, and K. Luojus, 2014: Terrestrial Snow (Arctic). In State of the Climate in 2013, *Bull. Am. Met. Soc.*, 95, S132-S133.

Flanner, M., K. Shell, M. Barlage, D. Perovich, and M. Tschudi, 2011: Radiative forcing and albedo feedback from the Northern Hemisphere cryosphere between 1979 and 2008. *Nature Geosci.*, 4, 151-155, doi:10.1038/ngeo1062.

Helfrich, S., D. McNamara, B. Ramsay, T. Baldwin, and T. Kasheta, 2007: Enhancements to, and forthcoming developments in the Interactive Multisensor Snow and Ice Mapping System (IMS). *Hydrolog Process.*, 21, 1576-1586.

Wang, L., C. Derksen, and R. Brown, 2013: Recent changes in pan-Arctic melt onset from satellite passive microwave measurements. *Geophys. Res. Lett.*, 40, doi:10.1002/grl.50098.

Greenland Ice Sheet

M. Tedesco^{1,2}, J. E. Box³, J. Cappelen⁴, X. Fettweis⁵, T. Mote⁶,
R. S. W. van de Wal⁷, C. J. P. P. Smeets⁷, J. Wahr⁸

¹City College of New York, New York, NY, USA

²National Science Foundation, Arlington, VA, USA

³Geological Survey of Denmark and Greenland, Copenhagen, Denmark

⁴Danish Meteorological Institute, Copenhagen, Denmark

⁵University of Liege, Liege, Belgium

⁶Department of Geography, University of Georgia, Athens, Georgia, USA

⁷Institute for Marine and Atmospheric Research Utrecht, Utrecht University, Utrecht, The Netherlands

⁸Department of Physics and Cooperative Institute for Research in Environmental Sciences,
University of Colorado, Boulder, CO, USA

December 2, 2014

Highlights

- Melt extent, above the 1981-2010 average for 90% of summer 2014, reached a maximum of 39.3% of the ice sheet area on 17 June 2014. The number of days of melting in June and July 2014 exceeded the 1981-2010 average over most of the ice sheet.
- Average surface mass balance (the difference between annual snow accumulation and annual melting) measured along the K-transect in west Greenland for the period 2013-2014 was slightly below the 1990-2010 average, while the equilibrium line altitude (~1,730 m a.s.l., the lowest altitude at which winter snow survived) was at a higher elevation than the 1990-2010 average of 1,545 m.
- A negligible ice mass loss of 6 Gt between June 2013 and June 2014, in contrast to the largest annual loss (474 Gt) observed in the GRACE record in 2012, indicates a slowing of the rate of ice loss.
- Average albedo during summer 2014 was the second lowest in the period of record that began in 2000; a new record low albedo occurred in August 2014.
- Summer 2014 in Greenland was the warmest on record at Kangerlussuaq, west Greenland, where the average June temperature was 2.3°C above the 1981-2010 average. In January 2014, the average temperature at Illoqqortoormiut, east Greenland and Upernavik, west Greenland were 7.5°C and 8.7°C above the 1981-2010 means, respectively.

With an area of 1.71 million km² and volume of 2.85 km³, the Greenland ice sheet is the second largest glacial ice mass on Earth. Only the Antarctic ice sheet is larger. The freshwater stored in the Greenland ice sheet has a sea level equivalent of +7.4 m. The discharge of the ice to the ocean by melting and runoff, and iceberg calving would not only increase sea level, but also likely alter the ocean thermohaline circulation and global climate. The high albedo (reflectivity) of the ice sheet surface (together with that of snow-covered and bare sea ice, and snow on land)

plays an important role in the regional surface energy balance and the regulation of global air temperatures.

Surface Melting

Estimates of the spatial extent of melting across the Greenland ice sheet (**Fig. 3.1**), derived from brightness temperatures measured by the Special Sensor Microwave Imager/Sounder (SSM/I/S) passive microwave radiometer (e.g., Mote 2007, Tedesco et al. 2013a, 2013b), show that melt extent for the period June through August (JJA, hereafter referred to as the summer) 2014 was above the 1981-2010 average 90% of the time (83 of 92 days, **Fig. 3.1d**). Melting occurred over 4.3% more of the ice sheet, on average, than in summer 2013, but 12.8% less than the exceptional summer of 2012 (**Fig. 3.1d**). Melt extent exceeded two standard deviations above average, reaching a maximum of 39.3% of the total ice sheet area on 17 June (**Fig. 3.1b**). Similar values occurred on 9 July and 26 July (**Fig. 3.1c**). Melt extent exceeded the 1981-2010 average on 28 days in June, 25 days in July, and 20 days in August 2014. For a brief period in early August there was below average melt extent, but by 21 August melting areas covered 29.3% of the ice sheet; this exceeded the 1981-2010 average by two standard deviations.

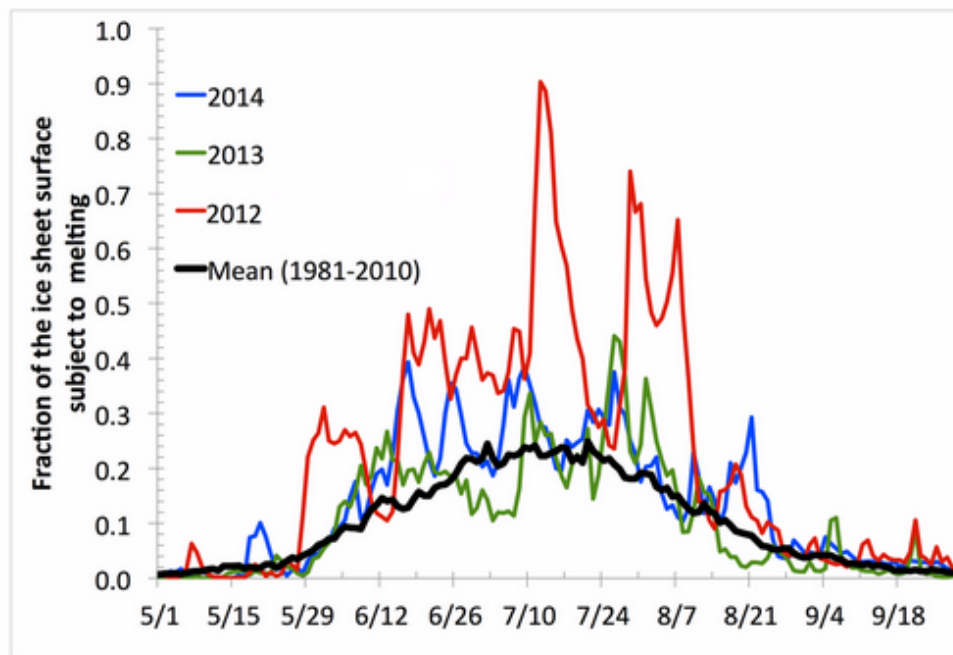
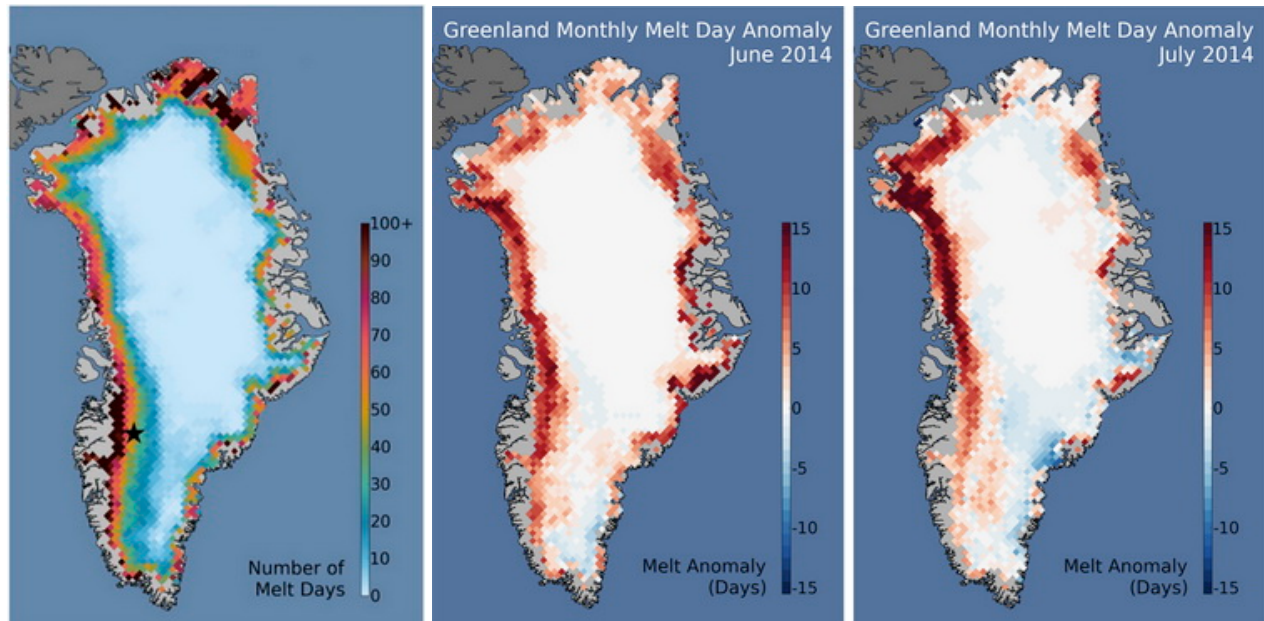


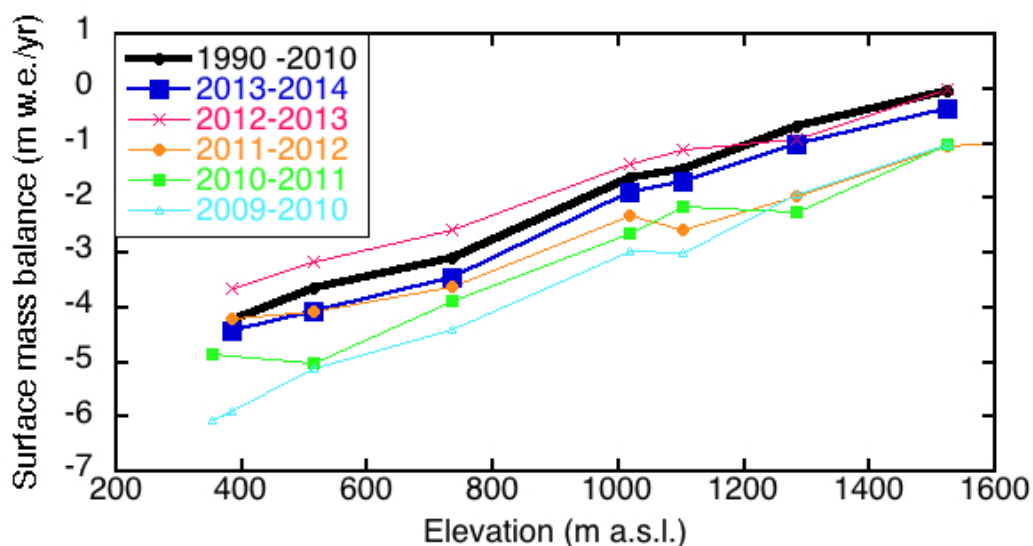
Fig. 3.1. Melting on the Greenland Ice Sheet in 2014 as described by (a, top left) total number of days when melting was detected at the surface between 1 January and 1 October, 2014; (b, top center) June melt anomaly expressed as the number of days melting that month compared to the 1981-2010 average; (c, top right) July melt anomaly expressed as the number of days melting that month compared to the 1981-2010 average; and (d, bottom) the annual cycle of melt extent expressed as a fraction of the total ice sheet area where melting was detected. In (d), melt extent in 2014 is represented by the blue line and the long-term average is the black line. Black star in (a, top left) indicates the position of the K-transect (discussed in the surface mass balance section).

The number of days of surface melting in June and July 2014 exceeded the 1981-2010 average across most of the ice sheet (**Figs. 3.1b and 3.1c**), particularly on the western margin,

consistent with the above normal temperatures recorded at coastal stations in western Greenland in June and July. Locations with below average days of melting were evident in southeast Greenland (**Figs. 3.1b and 3.1c**), consistent with below normal temperatures in that region (see **Fig. 1.3d** in the essay on [Air Temperature](#), which shows lower temperatures in southeast Greenland than along the western margin of the ice sheet).

Surface Mass Balance

Average surface mass balance (the difference between annual snow accumulation and annual melting) measured along the K-transect in West Greenland (Van de Wal et al. 2005, 2012) for the period 2013-2014 was slightly below the mean for 1990-2010 (measurements began in 1990; thus it is not possible to use the standard 1981-2010 reference period) (**Fig. 3.2a**). The equilibrium line altitude (the lowest altitude at which winter snow survives), estimated to be 1,730 m above sea level [a.s.l.] in 2014, was at a higher elevation than the 1990-2010 mean (1,545 m). During summer 2014, melt rates below the equilibrium line were not as high as they were in some recent years, e.g., 2010 and 2012.



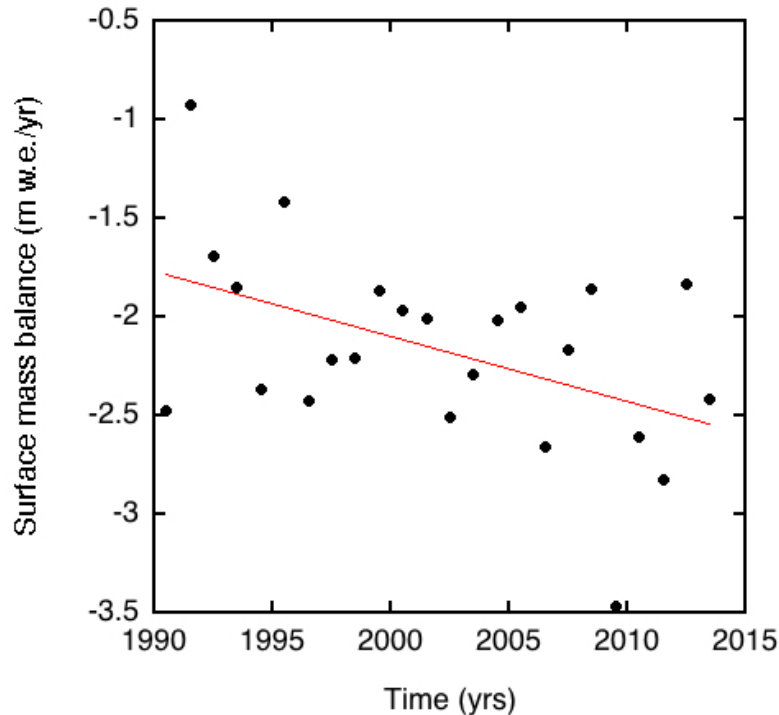


Fig. 3.2. (a, top) Surface mass balance as a function of elevation along the K-transect for 2013-2014 (large blue squares), the previous four years, and the 20-year (1990-2010) average. (b, bottom) Average surface mass balance for sites located between 400 m and 1500 m a.s.l. A linear regression (red line) of the data gives a correlation coefficient (r) of 0.46 (significant at a 97.5% confidence level).

Figure 3.2a shows the mass balance profiles for the last five years and the long-term mean obtained from stations at different elevations. **Figure 3.2b** shows the average surface mass balance for sites between 400 m and 1500 m a.s.l altitude, and the corresponding linear trend. There was slightly more melt in 2013-2014 than the 1990-2010 average; 2013-2014 had the 7th most negative mass balance of the 24 consecutive mass balance years in the observational record. The trend in the mean mass balance over the ablation area is -3.3 cm per year.

Total Ice Mass

GRACE (Gravity Recovery and Climate Experiment) satellite gravity solutions are used to estimate monthly changes in the total mass of the Greenland ice sheet (Velicogna and Wahr 2006; **Fig. 3.3**). Between the beginning of June 2013 and the beginning of June 2014, which corresponds closely to the period between the onsets of the 2013 and 2014 melt seasons, there was virtually no net change in cumulative ice sheet mass. The very small 6 Gt (Gigatonne) loss during that 12 month period, just 2% of the mass loss of 294 Gt between 2003 and 2013, indicates a slowing in the rate of ice mass loss. The negligible June 2013 to June 2014 mass loss follows a 474 Gt mass loss between June 2012 and June 2013, the largest annual loss observed in the GRACE record. A GRACE mass estimate cannot be obtained for July 2014, because the GRACE K-Band ranging system was switched off during that month to preserve battery life.

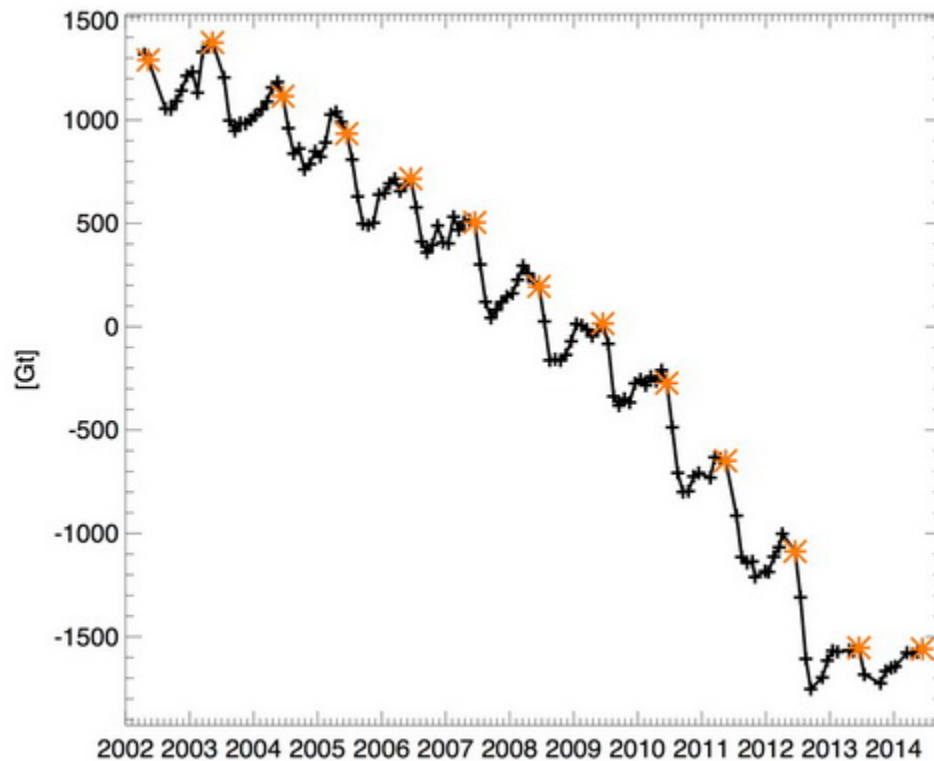


Fig. 3.3. Monthly mass anomalies (in Gigatonnes, Gt) for the Greenland ice sheet since April 2002 estimated from GRACE measurements. The anomalies are expressed as departures from the 2002-2014 mean value for each month. For reference, orange asterisks denote June values (or May for those years when June is missing).

Ice Albedo

Albedo, also referred to as reflectivity, is the ratio of reflected solar radiation to total incoming solar radiation. Here it is derived from the Moderate-resolution Imaging Spectroradiometer (MODIS, after Box et al. 2012). In summer 2014, albedo was below average over most of the ice sheet (**Fig. 3.4a**) and the area-averaged albedo for the entire ice sheet was the second lowest in the period of record that began in 2000 (**Fig. 3.4b**). The area-averaged albedo in August was the lowest on record for that month (**Fig. 3.4c**). August 2014 albedo values were particularly low at high elevations; such low values have not previously been observed so late in the summer. The observed albedo in summer 2014 continues a period of increasingly negative and record low albedo anomaly values (Box et al. 2012, Tedesco et al. 2011, 2013a, Dumont et al. 2014).

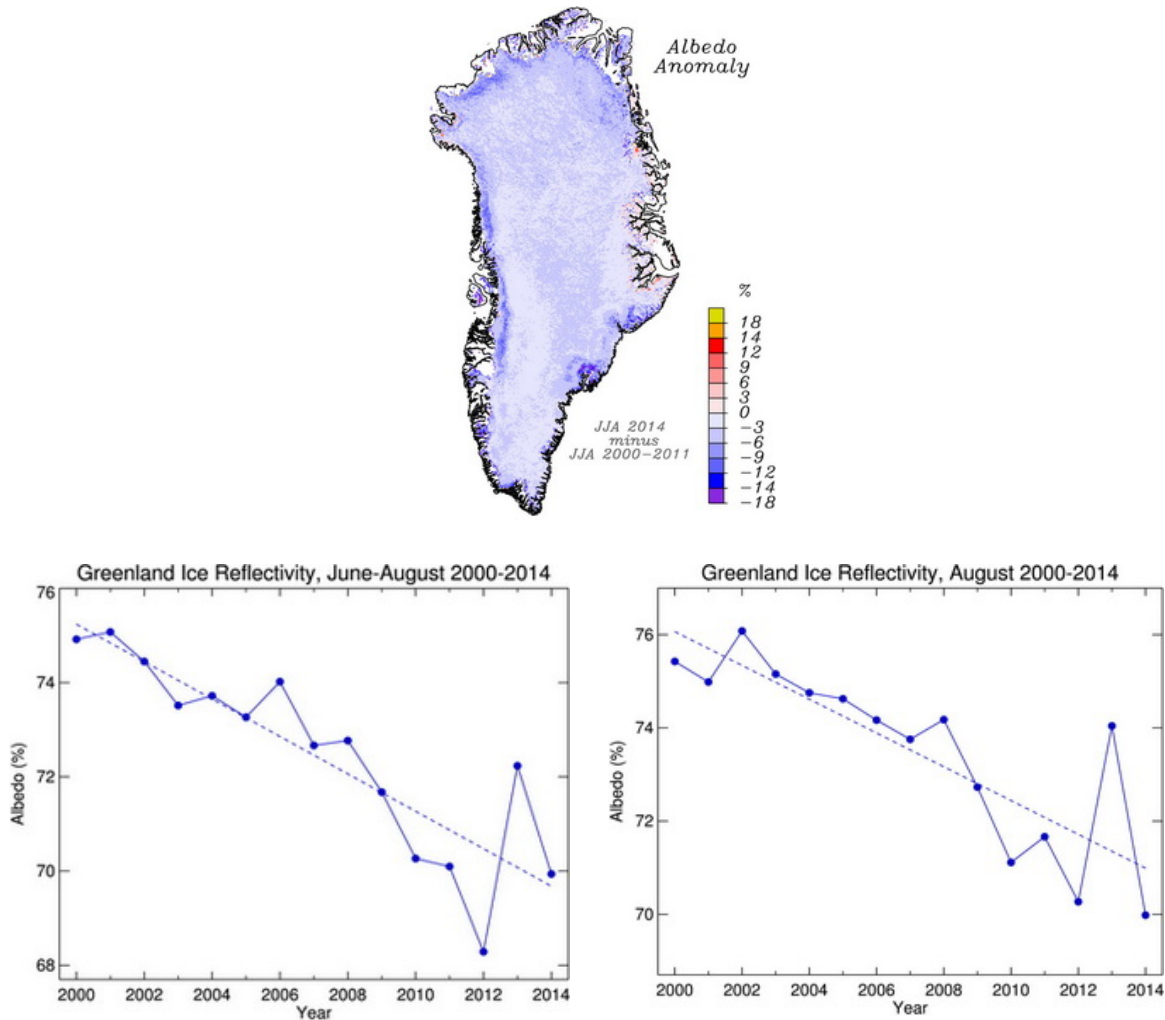


Fig. 3.4. (a, top) Greenland ice sheet surface albedo anomaly for June, July and August (JJA, summer) 2014 relative to the average for those months between 2000 and 2011. (b, lower left) Average surface albedo of the ice sheet each summer between 2000 and 2014. (c, lower right) Average surface albedo of the ice sheet each August between 2000 and 2014. All data are derived from the Moderate-resolution Imaging Spectroradiometer (MODIS).

Weather

Slightly negative (-0.7) North Atlantic Oscillation (NAO) conditions in summer 2014 promoted abnormal anticyclonic conditions over southwest and northwest Greenland; these favored northward advection of warm air along its western margin as far as the northern regions of the ice sheet (see **Fig. 1.3d** in the essay on [Air Temperature](#)). Further, the anticyclonic conditions reduced summer precipitation (snowfall) over south Greenland. The combination of southerly air flow and lower precipitation contributed to the melting, mass balance and albedo observations reported above.

The advection of warm air towards Greenland is reflected in summer air temperatures. Near surface air temperature data recorded by automatic weather stations (**Table 3.1**) indicate that

summer 2014 in Greenland was the warmest on record at Kangerlussuaq, west Greenland, with June temperatures +2.3°C above the 1981-2010 average. Other west Greenland locations also had anomalously warm summer temperatures. For example, the coastal site of Nuuk had its second warmest summer since 1784, with July temperatures 2.9°C above the 1981-2010 mean.

Warming in winter is greater than in summer (**Table 3.1**). At Ittoqqortoormiut, east Greenland, where observations began in 1924, the average air temperature during December 2013 to February 2014 equalled the record high set in the same period in 1947, and January temperatures were 7.5°C above the 1981-2010 average. Upernavik, west Greenland, had its 7th warmest January, 8.7°C above the 1981-2010 average, since observations began in 1873.

Table 3.1. Near-surface temperature anomalies relative to the 1981-2010 average at thirteen stations distributed around Greenland. Standard deviation (SD) values, and the years when record maximum and minimum values occurred are also given. Data are from Cappelen (2014) and from the Danish Meteorological Institute (DMI) for the period January-August 2014.

Location	First year of record	2014 Anomaly (°C) St. Deviation (SD) Max. and Min. Year	SON	DJF	MAM	JJA	June	July	Aug.
				2013 -					
			2013	2014	2014	2014	2014	2014	2014
Pituffik/ Thule AFB	1948	<i>Anomaly (1981-2010)</i>	-0.1	+2.4	+0.8	+0.3	+0.3	-0.2	+0.8
Latitude 76.5°N Longitude 68.8°W		<i>SD</i>	0.1	0.8	0.3	0.3	0.5	-0.0	0.4
		<i>Max. Year</i>	2010	1986	1953	1957	2008	2011	2009
		<i>Min. Year</i>	1964	1949	1992	1996	1986	1972	1996
Upernavik	1873	<i>Anomaly (1981-2010)</i>	-0.4	+4.7	+0.5	+0.6	+1.3	0.0	+0.4
72.8°N 56.2°W		<i>SD</i>	-0.1	1.3	0.1	1.1	1.5	0.5	0.6
		<i>Max. Year</i>	2010	1947	1932	2012	2008	2011	1960
		<i>Min. Year</i>	1917	1983	1896	1922	1894	1916	1873
Kangerlussuaq	1949	<i>Anomaly (1981-2010)</i>	+0.6	+2.1	-0.9	+1.6	+2.3	+1.6	1.0
67.0°N 50.7°W		<i>SD</i>	0.4	0.4	-0.3	1.7	1.5	1.4	0.7
		<i>Max. Year</i>	2010	1986	2005	2014	2014	1968	1960
		<i>Min. Year</i>	1982	1983	1993	1983	1978	1973	1983
Ilulissat	1873	<i>Anomaly (1981-2010)</i>	-0.4	+3.5	+0.1	+0.6	+1.4	+0.5	+0.1
69.2°N 51.1°W		<i>SD</i>	-0.1	1.1	-0.0	1.3	1.4	0.8	0.5
		<i>Max. Year</i>	2010	1929	1932	1960	1997	1960	1960
		<i>Min. Year</i>	1884	1884	1887	1972	1918	1972	1884
Aasiaat	1951	<i>Anomaly (1981-2010)</i>	+0.3	+3.9	+1.2	+1.6	+2.2	+1.3	+1.2
68.7°N 52.8°W		<i>SD</i>	0.4	0.9	0.4	1.5	1.7	1.1	1.0
		<i>Max. Year</i>	2010	2010	2010	2012	2012	2012	1960
		<i>Min. Year</i>	1986	1984	1993	1972	1992	1972	1983
Nuuk	1873	<i>Anomaly (1981-2010)</i>	+0.4	+0.6	-0.9	+2.3	+1.9	+2.9	+2.1
64.2°N 51.8°W		<i>SD</i>	0.6	0.3	-0.8	2.3	1.4	2.6	1.8
		<i>Max. Year</i>	2010	2010	1932	2012	2012	2012	2010
		<i>Min. Year</i>	1898	1984	1993	1914	1922	1955	1884
Paamiut	1958	<i>Anomaly (1981-2010)</i>	+0.9	+0.8	-1.1	+0.7	+0.5	+0.8	+0.9
62.0°N 49.7°W		<i>SD</i>	0.8	0.1	-0.7	0.8	0.6	0.7	0.8
		<i>Max. Year</i>	2010	2010	2005	2010	1987	1958	2010
		<i>Min. Year</i>	1982	1984	1993	1969	1972	1969	1969
Narsarsuaq	1961	<i>Anomaly (1981-2010)</i>	+0.8	+0.9	+0.5	+1.0	+1.4	+0.6	+0.9
61.2°N 45.4°W		<i>SD</i>	0.6	0.1	0.1	1.3	1.3	0.7	0.9
		<i>Max. Year</i>	2010	2010	2010	2012	2012	2012	1987
		<i>Min. Year</i>	1963	1984	1989	1983	1992	1969	1983
Quaqortoq	1873	<i>Anomaly (1981-2010)</i>	+0.5	+0.3	-0.4	+0.6	+0.8	+0.2	+0.8
60.7°N 46.0°W		<i>SD</i>	0.9	0.3	-0.4	0.7	0.5	0.4	0.8
		<i>Max. Year</i>	2010	2010	1932	1929	1929	2012	1960
		<i>Min. Year</i>	1874	1884	1989	1874	1922	1969	1874
Danmarkshavn	1949	<i>Anomaly (1981-2010)</i>	+0.9	+3.9	+0.4	+0.8	+0.3	+1.0	+1.1
76.8°N 18.8°W		<i>SD</i>	0.8	2.1	0.4	1.3	0.3	1.3	1.2
		<i>Max. Year</i>	2002	2005	1976	2008	2008	1958	2003
		<i>Min. Year</i>	1971	1967	1966	1955	2006	1955	1992
Ittoqqortoormiut	1948	<i>Anomaly (1981-2010)</i>	+0.3	+5.3	+1.3	0.0	+0.4		
70.4°N 22.0°W		<i>SD</i>	0.6	2.4	1.1	0.0	0.9		
		<i>Max. Year</i>	2002	2014	1996	1949	1948	1949	1949
		<i>Min. Year</i>	1951	1966	1956	1955	1956	1953	1952
Tasiilaq	1895	<i>Anomaly (1981-2010)</i>	-0.4	+3.0	0.0	+0.6	+0.7	-0.3	+1.2
65.6°N 37.6°W		<i>SD</i>	-0.1	1.7	0.0	0.5	0.3	-0.6	1.5
		<i>Max. Year</i>	1941	1929	1929	2003	1932	1929	2003

		<i>Min. Year</i>	1917	1918	1899	1983	2012	1983	1983
Prins Christian Sund	1951	<i>Anomaly (1981-2010)</i>			+0.5	+1.2	+1.1	+0.9	+1.6
60.0°N 43.2°W		<i>SD</i>			0.6	1.6	1.3	1.0	1.7
		<i>Max. Year</i>			2005	2010	2008	2005	2010
		<i>Min. Year</i>			1989	1970	1993	1969	1992

Note: The more positive or more negative the standard deviation (SD) value, the more extreme the positive or negative temperature anomaly. For example, at Ittoqqortoormiut, where winter 2014 was as warm as the previous warmest winter on record, in 1947, the SD value (2.4) of the winter 2014 temperature anomaly is among the most positive in the table.

Abbreviations: SON: September, October, November; DJF: December, January, February; MAM: March, April, May; JJA: June, July, August.

References

Box, J. E., X. Fettweis, J. C. Stroeve, M. Tedesco, D. K. Hall, and K. Steffen, 2012: Greenland ice sheet albedo feedback: thermodynamics and atmospheric drivers. *The Cryosphere*, 6, 821-839, doi:10.5194/tc-6-821-2012.

Cappelen, J. (ed.), 2014: Greenland - DMI Historical Climate Data Collection 1784-2013, Denmark, The Faroe Islands and Greenland. *Danish Meteorol. Inst. Tech. Rep.*, 14-04, 90 pp. http://www.dmi.dk/fileadmin/user_upload/Rapporter/TR/2014/tr14-04.pdf.

Dumont, M., E. Brun, G. Picard, M. Michou, Q. Libois, J. R. Petit, M. Geyer, S. Morin, and B. Josse, 2014: Contribution of light-absorbing impurities in snow to Greenland's darkening since 200. *Nature Geoscience*, 7, 509-512, doi:10.1038/ngeo2180.

Mote, T., 2007: Greenland surface melt trends 1973-2007: Evidence of a large increase in 2007. *Geophysical Research Letters*, 34, L22507.

Tedesco, M., X. Fettweis, M. R. van den Broeke, R. S. W. van de Wal, W. J. van Berg, M. C. Serreze, and J. E. Box, 2011: The role of albedo and accumulation in the 2010 melting record in Greenland. *Environ. Res. Lett.*, 6, 014005, doi:10.1088/1748-9326/6/1/014005.

Tedesco, M., X. Fettweis, T. Mote, J. Wahr, P. Alexander, J. E. Box, and B. Wouters, 2013a: Evidence and analysis of 2012 Greenland records from spaceborne observations, a regional climate model and reanalysis data. *The Cryosphere*, 7, 615-630, doi:10.5194/tc-7-615-2013.

Tedesco, M., J. E. Box, J. Cappelen, X. Fettweis, T. Jensen, T. Mote, A. K. Rennermalm, L. C. Smith, R. S. W. van de Wal, and J. Wahr. 2013b: [Arctic] Greenland ice sheet [in "State of the Climate in 2012"]. *Bull. Amer. Meteor. Soc.*, 94 (8), S121-S123.

Van de Wal, R. S. W., W. Greuell, M. R. van den Broeke, C.H. Reijmer, and J. Oerlemans, 2005: Surface mass-balance observations and automatic weather station data along a transect near Kangerlussuaq, West Greenland. *Ann. Glaciol.*, 42, 311-316.

Van de Wal, R. S. W., W. Boot, C. J. P. P. Smeets, H. Snellen, M. R. van den Broeke, and J. Oerlemans, 2012; Twenty-one years of mass balance observations along the K-transect, West-Greenland. *Earth Syst. Sci. Data*, 4, 31-35, doi:10.5194/essd-4-31-2012.

Velicogna, I. and J. Wahr. 2006: Significant acceleration of Greenland ice mass loss in spring, 2004: *Nature*, 443, doi:10.1038/nature05168.

Sea Ice

D. Perovich^{1,2}, S. Gerland³, S. Hendricks⁴, W. Meier⁵, M. Nicolaus⁴, M. Tschudi⁶

¹ERDC-Cold Regions Research and Engineering Laboratory, Hanover, NH, USA

²Thayer School of Engineering, Dartmouth College, Hanover, NH, USA

³Norwegian Polar Institute, Fram Centre, Tromsø, Norway

⁴Alfred Wegener Institute, Bremerhaven, Germany

⁵NASA Goddard Space Flight Center, Greenbelt, MD, USA

⁶Aerospace Engineering Sciences, University of Colorado, Boulder, CO, USA

December 2, 2014

Highlights

- The September 2014 Arctic sea ice minimum extent was 5.02 million km², slightly less than the 2013 minimum, but 1.61 million km² greater than the record minimum of 2012. The sixth smallest ice extent of the satellite record (1979-2014) occurred in 2014.
- The coverage of multiyear ice in March 2014 increased to 31% of the ice cover from the previous year's value of 22%.
- Satellite observations indicated an increase of mean thickness in the multi-year sea ice zone north-west of Greenland, from 1.97 m in March 2013 to 2.35 m in March 2014.

The Arctic sea ice cover plays an important role in the global system. From a climate perspective, it serves as both an indicator and an amplifier of climate change. Sea ice is a barrier limiting the exchange of heat, moisture, and momentum between the atmosphere and the ocean, and is host to a rich marine ecosystem. Changes in ice cover affect a wide range of human activities from hunting to shipping to resource extraction.

Sea Ice Extent

There are three key variables used to describe the state of the ice cover; the ice extent, the ice age, and the ice thickness. Sea ice extent is used as the basic description of the state of the Arctic sea ice cover. Satellite-based passive microwave instruments have been used to determine sea ice extent since 1979. There are two months each year that are of particular interest: September, at the end of summer, when the sea ice reaches its annual minimum extent, and March, at the end of winter, when the ice is at its maximum extent. The Arctic sea ice extents in March 2014 and September 2014 are presented in **Fig. 4.1**.

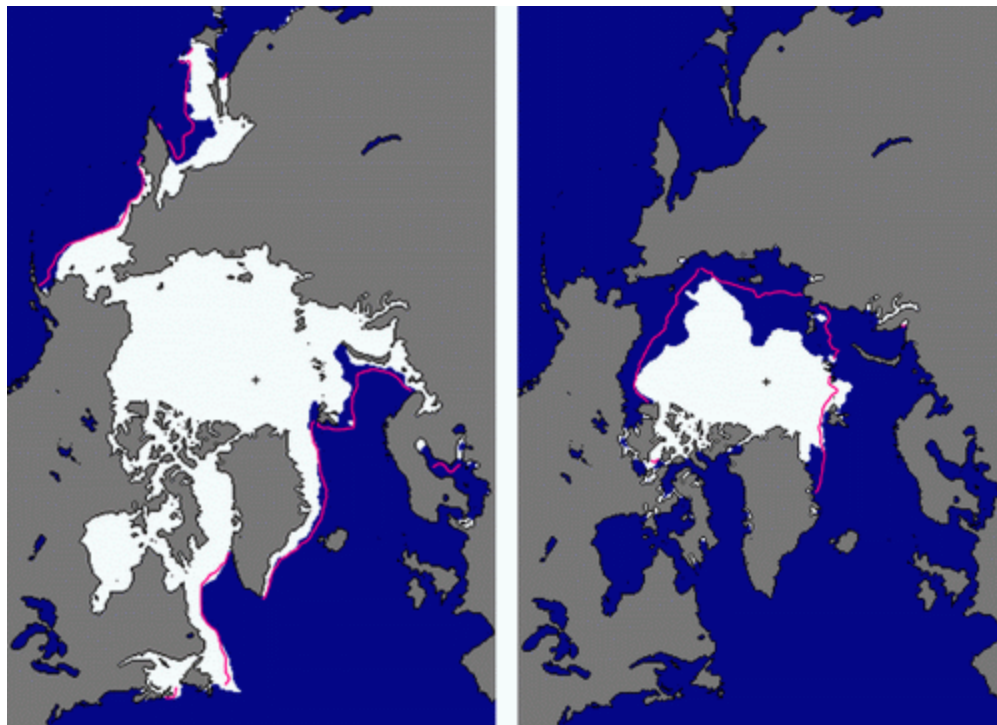


Fig. 4.1. Sea ice extent in March 2014 (left) and September 2014 (right), illustrating the respective monthly averages during the winter maximum and summer minimum extents. The magenta lines indicate the median ice extents in March and September, respectively, during the period 1981-2010. Maps are from NSIDC at nsidc.org/data/seaice_index.

Based on estimates produced by the National Snow and Ice Data Center (NSIDC) the sea ice cover reached a minimum annual extent of 5.02 million km² on September 17, 2014. This was just 80,000 km² below the 2013 minimum, but substantially higher (1.61 million km²) than the record minimum of 3.41 million km² set in September 2012 (**Fig. 4.2**). However, the 2014 summer minimum extent was still 1.12 million km² (23%) below the 1981-2010 average minimum ice extent. In March 2014 ice extent reached a maximum value of 14.76 million km² (**Fig. 4.2**), 5% below the 1981-2010 average. This was slightly less than the March 2013 value, but was typical of the past decade.

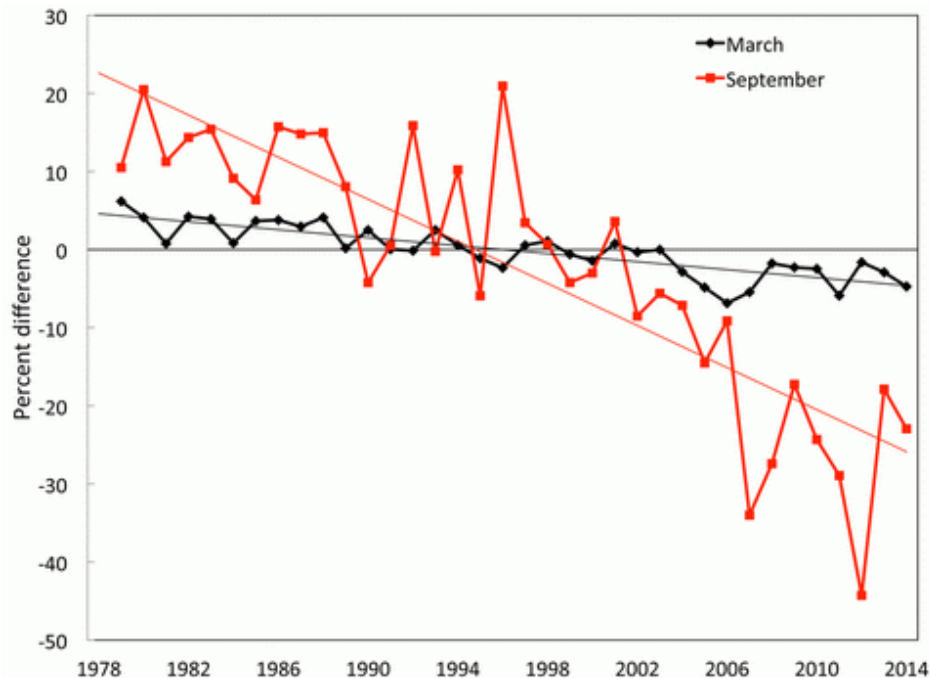


Fig. 4.2. Time series of Arctic sea ice extent anomalies in March (the month of maximum ice extent, black symbols) and September (the month of minimum ice extent, red symbols). The anomaly value for each year is the difference (in %) in ice extent relative to the mean values for the period 1981-2010. The thin black and red lines are least squares linear regression lines. The slopes of these lines indicate ice losses of -2.6% and -13.3% per decade in March and September, respectively.

Sea ice extent had decreasing trends in all months and virtually all regions, the exception being the Bering Sea during winter. The September monthly average trend is now -13.3% per decade relative to the 1981-2010 average (**Fig. 4.2**). The trend is smaller during March (-2.6% per decade), but is still decreasing at a statistically significant rate.

There was a loss of 9.48 million km² of ice between the March and September average extents. This is the smallest seasonal decline since 2006, but is still over 500,000 km² higher than the average seasonal loss. After reaching the March 2014 maximum extent, the seasonal decline began at a rate comparable to the 30-year average, which continued through mid-June 2014. Then, for a few weeks in late-June and early-July, the decrease in ice extent accelerated. Subsequently, the 2014 ice extent tracked the shape of the average ice extent curve for the remainder of the summer melt season, but at a value about one million km² less than the average curve. The retreat of sea ice in summer 2014 and comparisons to previous years and the long-term record are illustrated in the September 2014 report of the Arctic Sea Ice News and Analysis (NSIDC 2014).

Age of the Sea Ice

The age of the sea ice is another descriptor of the state of the sea ice cover. It serves as an indicator for the ice physical properties including surface roughness, melt pond coverage, and thickness. Older ice tends to be thicker and thus more resilient to changes in atmospheric and

oceanic forcing compared to younger ice. The age of the ice can be determined using satellite observations and drifting buoy records to track ice parcels over several years (Tschudi et al. 2010, Maslanik et al. 2011). This method has been used to provide a record of age of the ice since the early 1980s (**Fig. 4.3**).

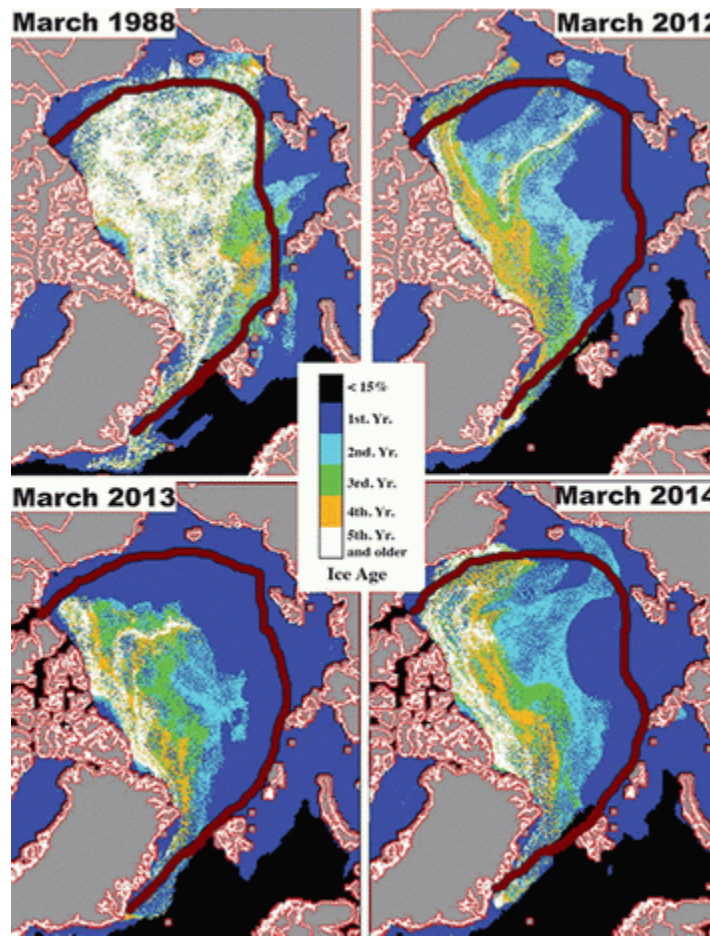


Fig. 4.3. Age of the sea ice in March 1988, 2012, 2013 and 2014, determined using satellite observations and drifting buoy records to track the movement of ice floes. The dark red line denotes the median multiyear ice extent for the period 1981-2010.

The coverage of multiyear ice in March 2014 increased from the previous year, approaching the median multiyear ice extent for 1981-2010. There was a fractional increase in second-year ice, from 8% to 14%. This increase offset the reduction of first-year ice, which decreased from 78% of the pack in 2013 to 69% this year, indicating that a significant portion of first-year ice survived the 2013 summer melt. The oldest ice (4+ years) fraction has also increased, comprising 10.1% of the March 2014 ice cover, up from 7.2% the previous year. Despite these changes, there is still much less of the oldest ice in 2014 compared to, for example, 1988 (**Fig. 4.3**). In the 1980's the oldest ice made up 26% of the ice pack.

After winter 2014, multiyear ice continued to drift through the Beaufort Sea, and remained along the coasts of northwest Greenland and northern Canada. Melt out in the Laptev and Kara Seas

occurred, but first-year ice, with a tongue of second-year ice, remained in the East Siberian Sea, as of August. The nature of this sea ice cover suggests that it will retain older ice as we enter freeze-up in autumn 2014.

Sea Ice Thickness

Ice thickness is an important descriptor of the state of the Arctic sea-ice cover. The CryoSat-2 satellite of the European Space Agency has now produced a time series of radar altimetry data for four successive seasons, with sea ice thickness information available between October and April. However, the algorithms for deriving freeboard (the height of the ice surface above the water level) and its conversion into sea-ice thickness are still being improved (Kurtz et al. 2014, Ricker et al. 2014, Kwok et al. 2014). Recent studies of the impact of snow layer properties on CryoSat-2 freeboard retrieval conclude that radar backscatter from the snow layer may lead to a bias in sea ice freeboard if it is not included in the retrieval process (Ricker et al. 2014, Kwok et al. 2014). Current sea-ice thickness data products from CryoSat-2 are, therefore, based on the assumption that the impact of the snow layer on radar freeboard is constant from year to year and snow depth can be sufficiently approximated by long-term observation values.

With these assumptions, updated radar freeboard and sea-ice thickness maps of the CryoSat-2 data product from the Alfred Wegener Institute (**Fig. 4.4**) show an increase in average freeboard of 0.05 m in March 2014 compared to the two preceding years (2012: 0.16 m, 2013: 0.16 m, 2014: 0.21 m). This amounts to an increase of mean sea-ice thickness of 0.38 m (2012: 1.97 m, 2013: 1.97 m, 2014: 2.35 m). The mean values were calculated for an area in the central Arctic Ocean where the snow climatology is considered to be valid. Excluded are the ice-covered areas of the southern Barents Sea, Fram Strait, Baffin Bay and the Canadian Arctic Archipelago. The main increase of mean freeboard and thickness is observed in the multi-year sea ice zone north-west of Greenland, while first year sea ice freeboard and thickness values remained typical for the Arctic spring.

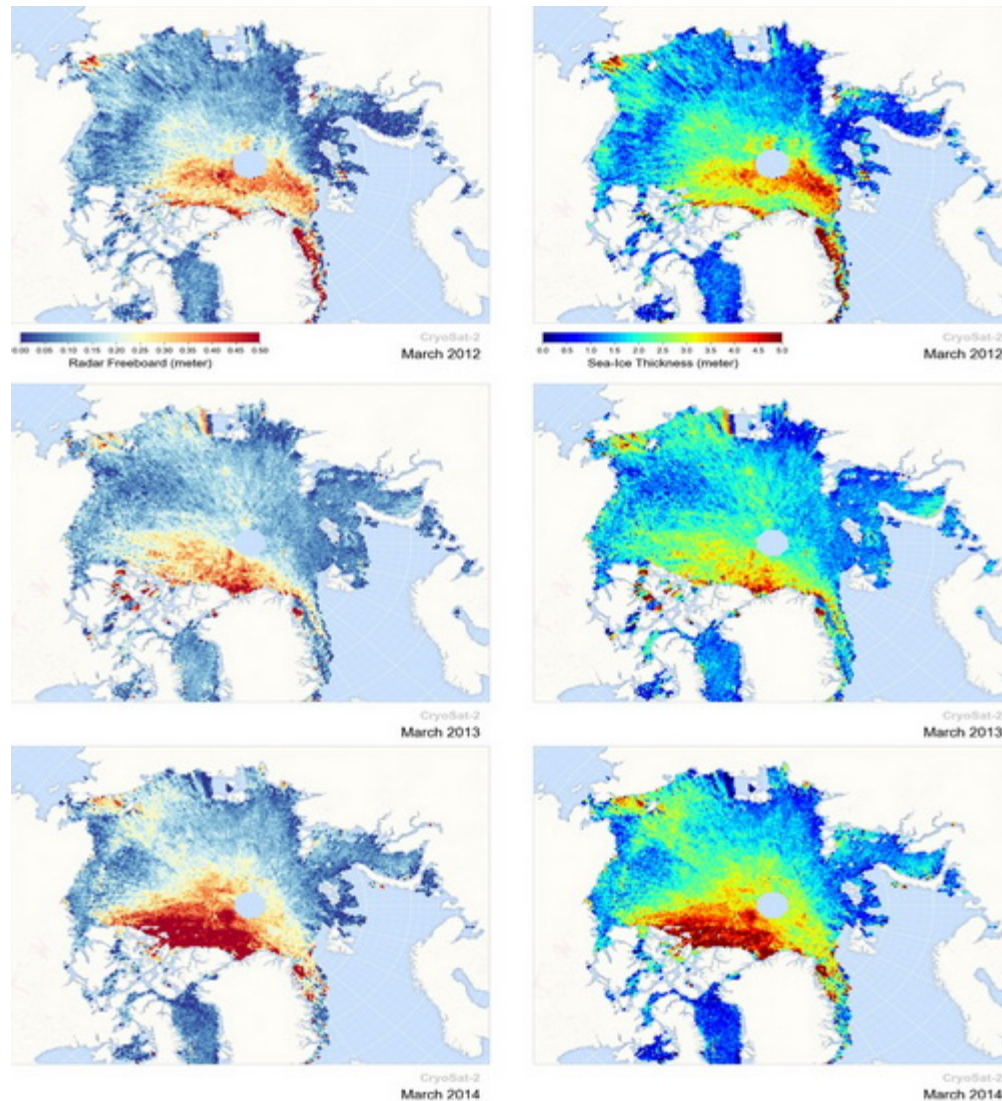


Fig. 4.4. Arctic sea ice freeboard (left) and thickness (right) maps for March retrieved from the ESA CryoSat-2 satellite for the period 2012-2014. The areas with the darkest shading, west and east of Greenland, the Canadian Arctic Archipelago and the Kara Sea, are outside the valid region for long-term snow observations. Freeboard is the height of the ice surface above the water level.

Regionally, thicker sea ice than in previous years has also been observed by airborne electromagnetic survey by the Norwegian Polar Institute in Fram Strait in late summer 2014. Preliminary results show a modal total sea ice thickness of 1.6 m, while the mean total ice thickness is 2.0 m (J. King et al. unpublished data). In surveys in the three years 2010-12, the modal thickness values for the same region and method were between 1.0 m and 1.4 m, and mean thickness values were between 1.1 m and 1.4 m (Renner et al. 2014).

References

Kurtz, N. T., N. Galin, and M. Studinger, 2014: An improved CryoSat-2 sea ice freeboard retrieval algorithm through the use of waveform fitting. *The Cryosphere*, 8, 1217-1237, doi:10.5194/tc-8-1217-2014.

Kwok, R., 2014: Simulated effects of a snow layer on retrieval of CryoSat-2 sea ice freeboard, *Geophys. Res. Lett.*, 41, 5014-5020, doi:10.1002/2014GL060993.

Maslanik, J., J. Stroeve, C. Fowler, and W. Emery, 2011: Distribution and trends in Arctic sea ice age through spring 2011. *Geophys. Res. Lett.*, 38, doi:10.1029/2011GL047735.

NSIDC, 2014: Arctic sea ice reaches minimum extent for 2014. In *Arctic Sea Ice News and Analysis*, National Snow and Ice Data Center (NSIDC), Boulder, CO, <http://nsidc.org/arcticseaicenews/2014/09/>.

Renner, A. H. H., S. Gerland, C. Haas, G. Spreen, J. F. Beckers, E. Hansen, M. Nicolaus, and H. Goodwin, 2014: Evidence of Arctic sea ice thinning from direct observations. *Geophys. Res. Lett.*, 41, 5029-5036, doi:10.1002/2014GL060369.

Ricker, R., S. Hendricks, V. Helm, H. Skourup, and M. Davidson, 2014: Sensitivity of CryoSat-2 Arctic sea-ice freeboard and thickness on radar-waveform interpretation, *The Cryosphere*, 8, 1607-1622, doi:10.5194/tc-8-1607-2014.

Tschudi, M. A., C. Fowler, J. A. Maslanik, and J. A. Stroeve, 2010: Tracking the movement and changing surface characteristics of Arctic sea ice. *IEEE J. Selected Topics in Earth Obs. and Rem. Sens.*, 3, doi: 10.1109/JSTARS.2010.2048305.

Arctic Ocean Sea Surface Temperature

M.-L. Timmermans¹, A. Proshutinsky²

¹Yale University, New Haven, CT, USA

²Woods Hole Oceanographic Institution, Woods Hole, MA, USA

December 2, 2014

Highlights

- Sea surface temperatures (SSTs) in August 2014 were as much as 4°C warmer than the 1982-2010 August mean in the Bering Strait region and the northern Laptev Sea. In the Barents Sea, SST was ~4°C lower than in 2013, and closer to the 1982-2010 August mean.
- In recent years, many Arctic Ocean boundary regions have had anomalously warm August SSTs relative to the 1982-2010 mean; general warming trends are exemplified by the Chukchi Sea, where August SST is increasing at a rate of about 0.5°C/decade.
- Strong spatial and inter-annual variability of SSTs is linked to variability in the patterns of sea ice retreat.



Arctic Ocean sea surface temperature (SST) is an important climate indicator that shows the integrated effect of different factors beyond the seasonal cycle of solar forcing, including heat advection by ocean currents and atmospheric circulation. The distribution of summer SST in the Arctic Ocean largely reflects patterns of sea-ice retreat (see the essay on [Sea Ice](#)) and absorption of solar radiation into the surface layer of the Arctic Ocean, which is influenced by cloud cover, water color and upper ocean stratification. Examination of the magnitude and area of SST anomalies in the Arctic Ocean can be used for predictions of future sea-ice conditions, with positive (negative) summer SST anomalies driving later (earlier) dates of sea ice growth in the autumn.

In this report, we describe August SSTs, an appropriate representation of Arctic Ocean summer SSTs which avoids the cooling and subsequent sea-ice growth that typically takes place in the latter half of September. Mean SSTs in August 2014 in ice-free regions ranged between ~0°C and +7°C, with the highest values in the Chukchi and Barents seas, displaying the same general geographic pattern as the August mean for the period 1982-2010 (**Fig. 5.1**).

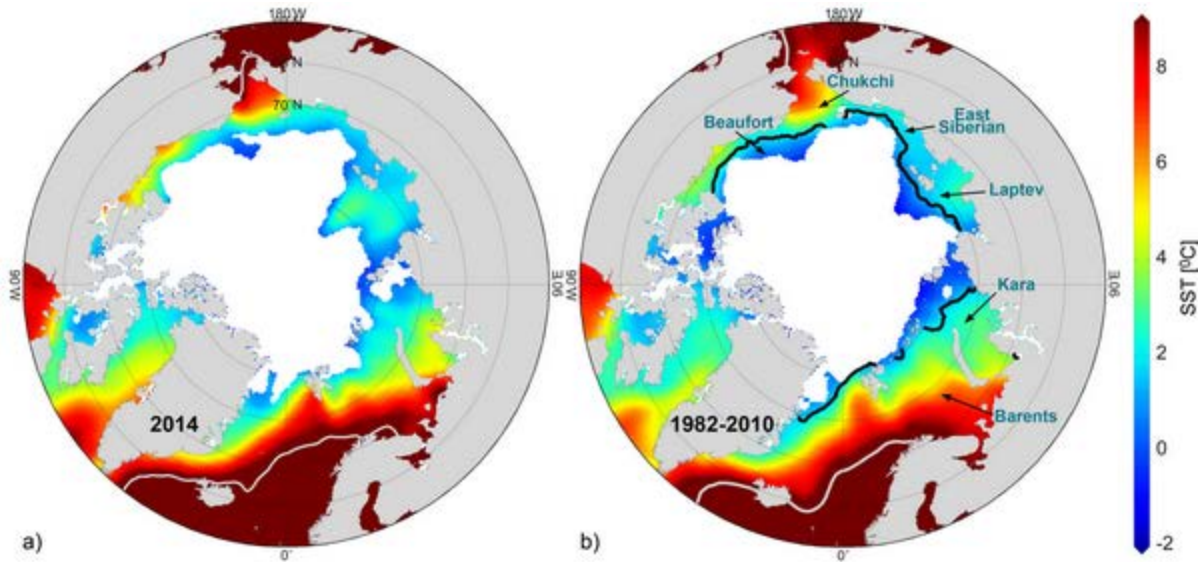


Fig. 5.1. (a) Mean sea surface temperature [SST, °C] in August 2014. White shading is the August 2014 mean sea-ice extent (source: National Snow and Ice Data Center [NSIDC]). (b) Mean SST in August during the period 1982-2010. White shading indicates the August 2010 sea-ice extent and the black line indicates the median ice edge in August for the period 1982-2010. Grey contours in both panels indicate the 10°C isotherm. SST data are from the NOAA Optimum Interpolation (OI) SST V2 product (a blend of in situ and satellite measurements) provided by the NOAA/OAR/ESRL PSD, Boulder, Colorado (<http://www.esrl.noaa.gov/psd/data/gridded/data.noaa.oisst.v2.html>); Reynolds et al. (2002, 2007).

In recent summers, many Arctic Ocean boundary regions have had anomalously warm SSTs in August relative to the 1982-2010 August mean (**Fig. 5.2**). The SST anomaly distribution in August 2007 is notable for the most strongly positive values over large parts of the Chukchi, Beaufort and East Siberian seas since 1982 (**Fig. 5.3**). In August 2007, SST anomalies were up to +5°C in ice-free regions (**Fig. 5.2a** and Steele et al. 2008); warm SST anomalies of this same order were observed in 2008 (not shown) over a smaller region in the Beaufort Sea (Proshutinsky et al. 2009). Anomalously warm SSTs in those summers were related to the timing of sea-ice losses and absorption of incoming solar radiation in open water areas, with ice-albedo feedback playing a principal role (e.g., Perovich et al. 2007).

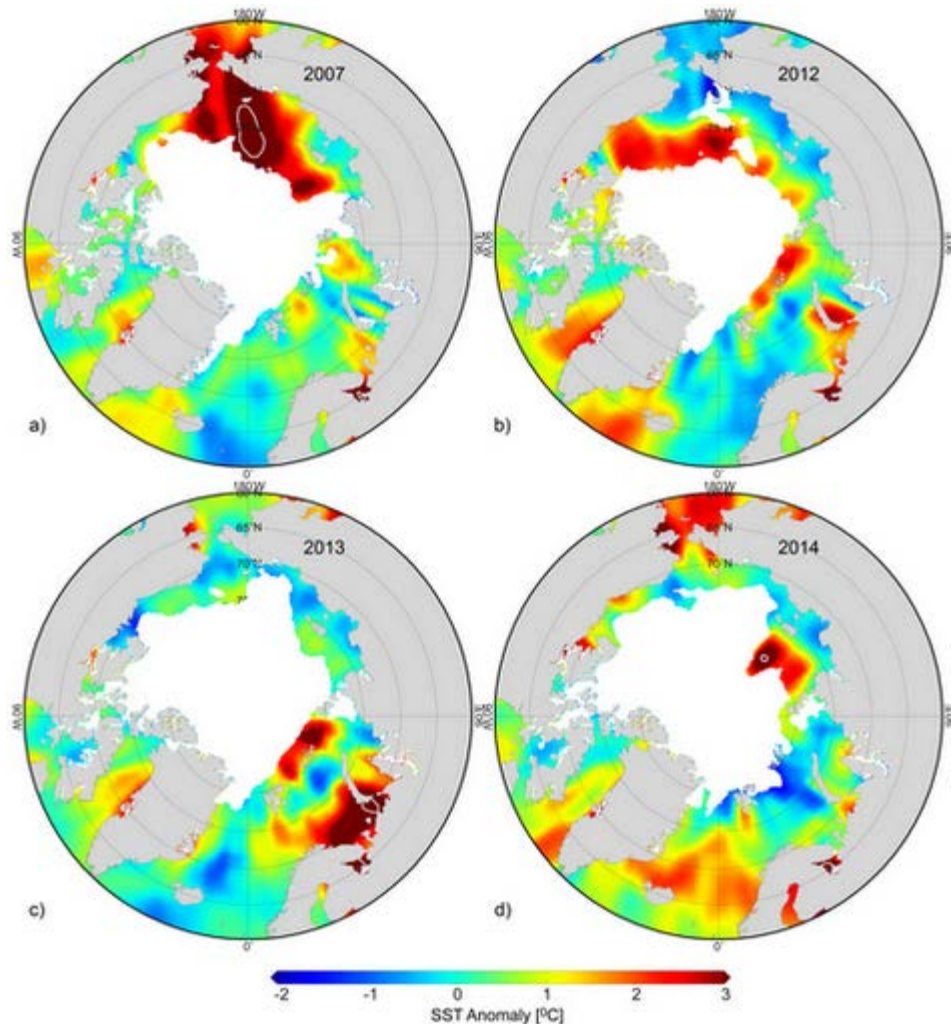


Fig. 5.2. SST anomalies [°C] in (a) August 2007, (b) August 2012, (c) August 2013, and (d) August 2014 relative to the August mean for the period 1982-2010. White shading in each panel indicates August-average sea-ice extent for each year. Grey contours indicate the 4°C isotherm.

In August 2014, the warmest SST anomalies were observed in the vicinity of the Bering Strait and the northern region of the Laptev Sea. SSTs in those regions were the warmest since 2007, with values as much as ~4°C warmer than the 1982-2010 August mean (**Fig. 5.2d**). Other regions of anomalously warm SSTs in recent summers include the Barents and Kara seas, with particularly warm values in August 2013, when the ocean surface was up to 4°C warmer than the 1982-2010 August mean (**Fig. 5.2c**). SSTs in the southern Barents Sea in summer 2013 reached as high as 11°C; warm waters here can be related to earlier ice retreat in these regions and possibly also to the advection of anomalously warm water from the North Atlantic Ocean (Timmermans et al. 2014). August 2014 SSTs returned to cooler values in the vicinity of the Barents and Kara seas (**Figs. 5.1a and 5.2d**), with close to zero area-averaged SST anomalies compared to the 1982-2010 period (**Fig. 5.3**).

Cold anomalies have also been observed in some regions in recent summers (Timmermans et al. 2013, 2014). For example, cooler SSTs in the Chukchi and East Siberian seas in August 2012 and August 2013 were linked to later and less-extensive sea-ice retreat in these regions in those years. In addition, a strong cyclonic storm during the first week of August 2012 (Simmonds 2013), which moved eastward across the East Siberian Sea and the Chukchi and Beaufort seas, caused anomalously cool SSTs as a result of mixing of warm surface waters with cooler deeper waters (Zhang et al. 2013).

Time series of average SST over the Arctic marginal seas, which are regions of predominantly open water in the month of August, are dominated by strong inter-annual and spatial variability linked to variability in the location and timing of sea-ice retreat (**Fig. 5.3**). The high August SSTs in the Chukchi Sea in 2005 and 2007 are notable features of the record, and were due to earlier sea-ice reduction in this region relative to preceding years and prolonged exposure of surface waters to direct solar heating. In other marginal seas, warm August SST anomalies observed in recent years are of similar magnitude to warm anomalies observed in past decades. General warming trends are apparent, however, with the most significant linear trend occurring in the Chukchi Sea, where SST is increasing at a rate of about $0.5^{\circ}\text{C}/\text{decade}$, primarily as a result of declining trends in summer sea-ice extent in the region (e.g., Ogi and Rigor, 2013).

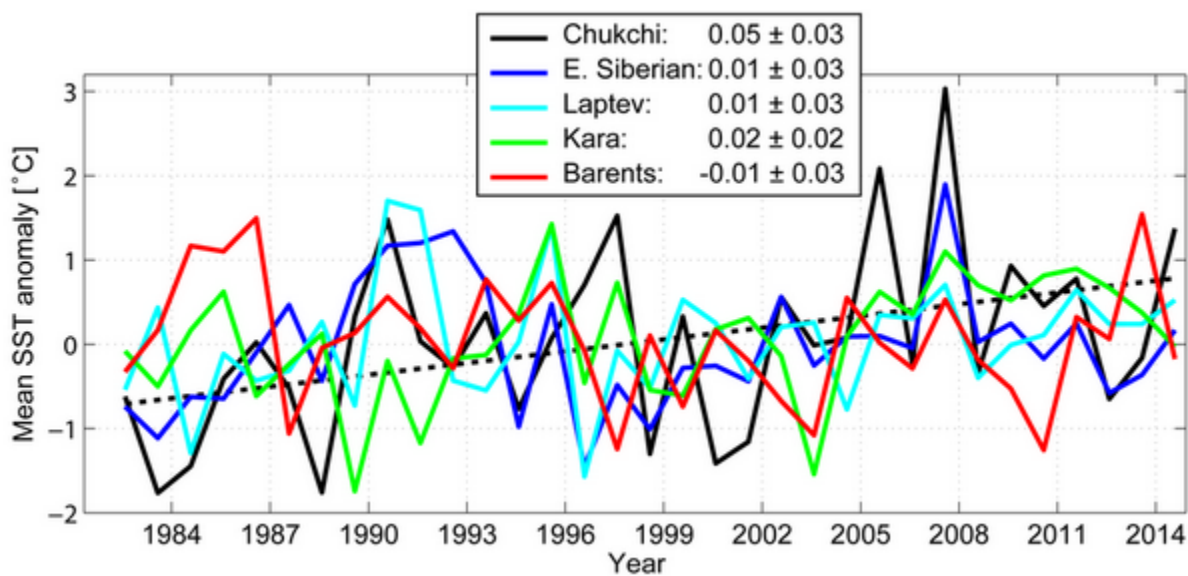


Fig. 5.3. Time series of area-averaged SST anomalies [$^{\circ}\text{C}$] for August of each year relative to the August mean for the period 1982-2010 for each of the marginal seas (see **Fig. 5.1b**) of the Arctic Ocean. The dotted black line corresponds to the linear least-squares fit for the Chukchi Sea record (the only marginal sea to show a trend significantly different from zero). Numbers in the legend correspond to best-fit slopes (with 95% confidence intervals) in $^{\circ}\text{C}/\text{year}$.

References

Ogi, M., and Rigor, I. G., 2013: Trends in Arctic sea ice and the role of atmospheric circulation. *Atmosph. Sci. Lett.*, 14, 97-101, doi: 10.1002/asl2.423.

Perovich, D. K., B. Light, H. Eicken, K. F. Jones, K. Runciman, and S. V. Nghiem, 2007: Increasing solar heating of the Arctic Ocean and adjacent seas, 1979- 2005: Attribution and role in the ice-albedo feedback. *Geophys. Res. Lett.*, 34, L19505, doi:10.1029/2007GL031480.

Proshutinsky, A., R. Krishfield, M. Steele, I. Polyakov, I. Ashik, M. McPhee, J. Morison, M.-L. Timmermans, J. Toole, V. Sokolov, I. Frolov, E. Carmack, F. McLaughlin, K. Shimada, R. Woodgate, and T. Weingartner, 2009: The Arctic Ocean [in "State of the Climate in 2008"]. *Bulletin of the American Meteorological Society*, 90, S1-S196.

Reynolds, R. W., N. A. Rayner, T. M. Smith, D. C. Stokes, and W. Wang, 2002: An improved in situ and satellite SST analysis for climate. *J. Climate*, 15, 1609-1625.

Reynolds, R. W., T. M. Smith, C. Liu, D. B. Chelton, K. S. Casey, and M. G. Schlax, 2007: Daily high-resolution-blended analyses for sea surface temperature. *J. Climate*, 20, 5473-5496.

Simmonds, I., 2013: [The Arctic] Sidebar 5.1: The extreme storm in the Arctic Basin in August 2012 [in "State of the Climate in 2012"]. *Bulletin of the American Meteorological Society*, 94(8), S114-S115.

Steele, M., W. Ermold, and J. Zhang, 2008: Arctic Ocean surface warming trends over the past 100 years. *Geophys. Res. Lett.*, 35, L02614, doi:10.1029/2007GL031651.

Timmermans, M.-L., I. Ashik, Y. Cao, I. Frolov, R. Ingvaldsen, T. Kikuchi, R. Krishfield, H. Loeng, S. Nishino, R. Pickart, B. Rabe, I. Semiletov, U. Schauer, P. Schlosser, N. Shakhova, W.M. Smethie, V. Sokolov, M. Steele, J. Su, J. Toole, W. Williams, R. Woodgate, J. Zhao, W. Zhong, and S. Zimmermann, 2013: [The Arctic] Ocean Temperature and Salinity [in "State of the Climate in 2012"]. *Bulletin of the American Meteorological Society*, 94(8), S128-S130.

Timmermans, M.-L., and 21 others, 2014: [The Arctic] Ocean Temperature and Salinity [in "State of the Climate in 2013"]. *Bulletin of the American Meteorological Society*, 95, S128-S132.

Zhang J., R. Lindsay, A. Schweiger, and M. Steele, 2013: The impact of an intense summer cyclone on 2012 Arctic sea ice retreat. *Geophys. Res. Lett.*, 40, 720-726, doi:10.1002/grl.50190.

Arctic Ocean Primary Productivity

K. E. Frey¹, J. C. Comiso², L. W. Cooper³, R. R. Gradinger⁴,
J. M. Grebmeier³, S.-I. Saitoh⁵, J.-É. Tremblay⁶

¹Graduate School of Geography, Clark University, Worcester, MA, USA

²Cryospheric Sciences Laboratory, NASA Goddard Space Flight Center, Greenbelt, MD, USA

³Chesapeake Biological Laboratory, University of Maryland Center for Environmental Science, Solomons, MD, USA

⁴Institute of Marine Research, Tromsø, Norway

⁵Graduate School of Fisheries Sciences, Hokkaido University, Hokkaido, Japan

⁶Québec-Océan and Takuvik, Biology Department, Université Laval, Québec City, QC, Canada

December 2, 2014

Highlights

- Recent satellite-based studies of the entire Arctic Ocean indicate that the greatest increases in primary production between 1998 and 2010 have been in the East Siberian, Laptev and Chukchi seas. In 2014, anomalously high chlorophyll-*a* concentrations were observed during June, July and August, particularly in the Kara and Laptev seas.
- The response of primary production to recent sea ice decline, and thereby increased light availability, has been regionally variable and highly dependent upon the distribution of nutrients in the euphotic zone throughout the Arctic Ocean.
- Recent sea ice retreat has revealed important impacts on the timing of phytoplankton blooms throughout the Arctic Ocean, including more frequent secondary blooms during the autumn.



Primary productivity is the rate that atmospheric or aqueous carbon dioxide is converted by autotrophs (primary producers) to organic material. It occurs most commonly by photosynthesis, i.e., with light as an energy source, but also by chemosynthesis, i.e., through inorganic chemical reactions. Primary production is a key process on Earth, as the producers form the base of the entire food web, both on land and in the oceans. Nearly all photosynthesis in the oceans is by algae, and measurements of chlorophyll can serve as a proxy for the amount of algal biomass present as well as overall plant health. The oceans play a significant role in global carbon budgets via photosynthesis, as approximately half of all global net annual photosynthesis occurs in them, with ~10-15% of production occurring on the continental shelves alone (Müller-Karger et al. 2005). As primary production is strongly dependent upon light availability and the presence of nutrients, rates are highly seasonal in the Arctic region. In particular, the melting and retreat of sea ice during spring strongly drive primary production in the Arctic Ocean and its adjacent shelf seas by enhancing light availability (Frey et al. 2011).

Recent declines in minimum Arctic sea ice extent (see the essay on [Sea Ice](#)) have contributed substantially to shifts in primary productivity throughout the Arctic Ocean. Studies using Sea-viewing Wide Field-of-view Sensor (SeaWiFS) and Moderate Resolution Imaging Spectroradiometer (MODIS) across the entire Arctic Ocean reveal that the Barents and

Greenland seas are the most productive marine environments in the Arctic, whereas the East Siberian and Chukchi seas are the least productive (Petrenko et al. 2013). However, the greatest increases in primary production during 1998-2010 occurred in the East Siberian Sea (+112.7%), Laptev Sea (+54.6%) and Chukchi Sea (+57.2%) (Petrenko et al. 2013). In addition, more regionally-specific studies in the Eurasian Arctic show that increases in production are also linked to sea ice decline in the southern Fram Strait (Cherkasheva et al. 2014) and the Barents Sea (Dalpadado et al. 2014). These observed positive trends in production may have been even greater, were it not for concomitant increasing trends in cloudiness (and related negative impacts on primary production due to reduced solar radiation) across the Arctic Ocean and adjacent shelf seas during 1998-2010 (Bélanger et al. 2013).

The most recent year of the satellite record (2014) shows anomalously high chlorophyll-*a* concentrations, mainly in the Kara and Laptev seas during June, July and August (**Fig. 6.1**). Chlorophyll-*a* concentrations are shown here to illustrate direct measurements of ocean color rather than further processing the data into primary production rates and using model output for illustration. The highest rates of change in the 2003-2014 MODIS-Aqua satellite record occur in the Laptev and Kara seas (particularly for comparisons focused on August), which is consistent with the steepest trends identified by Petrenko et al. (2013) utilizing SeaWiFS and MODIS-Aqua data. Some of the highest anomalies in chlorophyll-*a* concentrations in 2014 are observed in the Laptev Sea (**Fig. 6.2**), where increases in chlorophyll biomass might be linked to declining sea ice cover, particularly during June and July.

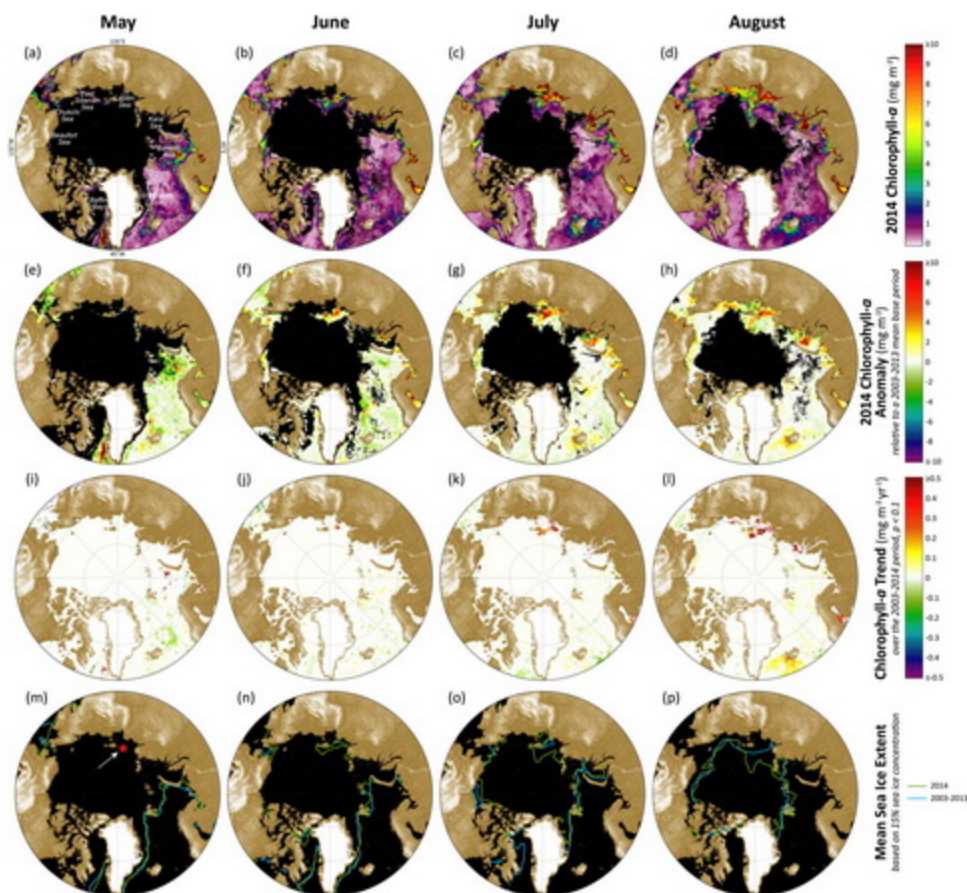


Fig. 6.1. Satellite-based chlorophyll-*a* data for the pan-Arctic region from the MODIS-Aqua platform (MODIS-Aqua Reprocessing 2013.1; <http://oceancolor.gsfc.nasa.gov/>). Chlorophyll-*a* concentrations are shown here (rather than further processing the time series into rates of primary production) to foster direct measurements of ocean color and minimize the use of modeled output. Mean monthly chlorophyll-*a* concentrations during 2014 are shown for (a) May, (b) June, (c) July, and (d) August. Monthly anomalies of chlorophyll-*a* concentrations for 2014 (relative to a 2003-2013 mean base period) are also shown (e-h). A base period of 2003-2013 was chosen to maximize its length relative to the short satellite-based time series derived from MODIS-Aqua. Theil-Sen median trends (2003-2014) in chlorophyll-*a* concentrations for each of the four months (i-l); only those trends that are statistically significant ($p < 0.1$, using the Mann-Kendall test for trend) are shown. Black areas (a-h) denote a lack of data owing to either clouds or sea ice. Sea ice extent (designated by a 15% sea ice concentration threshold) based on SSM/I data (Cavalieri et al. 1996, Maslanik and Stroeve 1999, Comiso and Nishio 2008) for 2003-2013 and 2014 is shown for each of the four months (m-p). The white arrow and red star in (m) indicate the location for the time series in **Fig. 6.2**.

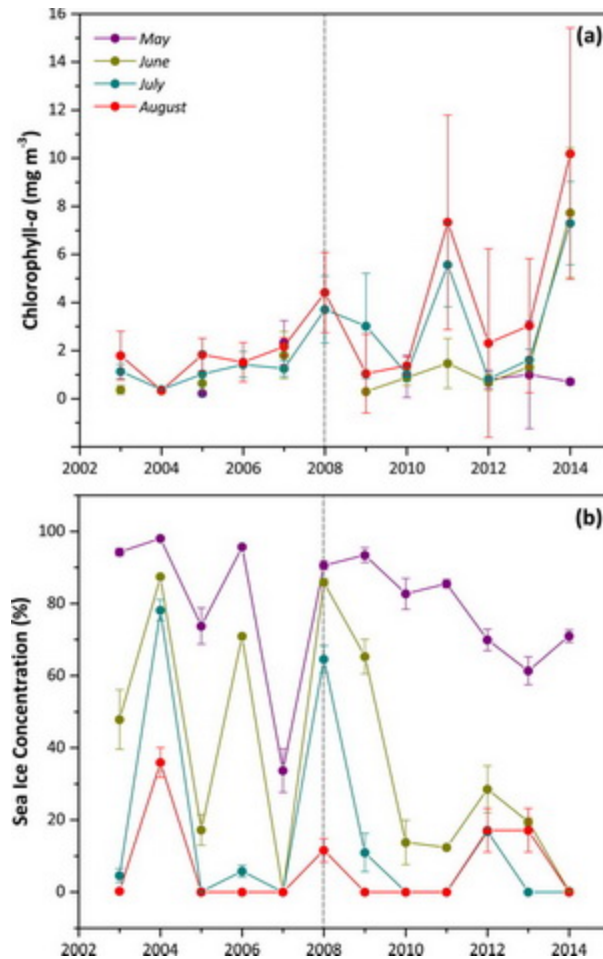


Fig. 6.2. Mean monthly (a) chlorophyll-*a* concentrations (based on MODIS-Aqua satellite data) and (b) sea ice concentrations (based on SSM/I satellite data) for a ~5625 km² region centered on anomalously high 2014 chlorophyll-*a* concentrations in the Laptev Sea (the location is marked with a white arrow and red star in **Fig. 6.1m**). The vertical dashed line at 2008 marks a threshold, after which sea ice declines precipitously and remains low in the region. After 2008, chlorophyll-*a* concentrations also show general increasing trends during June, July and August.

Despite the temporal shifts described in the previous paragraph, the prevailing spatial patterns of higher production on the shelves and lower production in the deep basin, driven by the distribution of sea ice and nutrients, appears to persist (Ulfsbo et al. 2014). Challenges remain, however, with linking satellite-based surface chlorophyll-*a* values to standing stocks of depth-integrated chlorophyll biomass or primary productivity rates, including confounding signals from river turbidity in coastal regions (e.g., Demidov et al. 2014) and chlorophyll maxima deeper than satellite sensor capabilities (Ardyna et al. 2013). Efforts to improve satellite retrieval algorithms based on *in situ* observations in all regions of the Arctic Ocean are essential because of regional variability in the optical properties of surface waters (Cota et al. 2004).

Loss of sea ice, facilitating the increased availability of solar radiation will not affect primary productivity rates in the absence of sufficient nutrients for production. Better knowledge of nutrient distributions across the Arctic Ocean is critical for understanding how climate warming,

sea ice decline, and subsequent light availability will affect primary production in future scenarios (e.g., Popova et al. 2010). To this end, Codispoti et al. (2013) have compiled a new, geographically extensive database of nitrate, nitrite and phosphate measurements to produce a climatology of net community production (NCP) estimates across the Arctic over the past several decades, ranging from (highest to lowest): (a) ~70-100 g C m⁻² in the Bering and southern Chukchi seas; (b) ~30-40 g C m⁻² in the Nordic/Barents Sea and Canadian Archipelago; (c) ~10-15 g C m⁻² in the southern Beaufort, East Siberian, Laptev, Kara, and northern Chukchi seas, and the Eurasian Basin and Greenland Shelf; and (d) ~1-5 g C m⁻² in the northern Beaufort Sea and Amerasian Basin.

Other recent studies further emphasize the importance of nutrient availability as a critical driver for primary production in Arctic Ocean environments. For example, Monier et al. (2014) observe that areas affected by river discharge, e.g., the Mackenzie River plume, experience a deepening of chlorophyll maxima in the water column because the fresh water displaces more nutrient-rich waters to lower depths. Furthermore, using time series data and an approach similar to that of Codispoti et al. (2013), Bergeron and Tremblay (2014) documented heterogeneous temporal trends in two geographically separate oceanographic settings (the southern Beaufort Sea and Baffin Bay) (**Fig. 6.3**). In that study, increases in nutrient drawdown (i.e., increases in net production) in the southern Beaufort Sea coincided with a deepening of the nitracline during the study period (2003-2011), suggesting that diatoms associated with subsurface chlorophyll maxima were consuming nutrients over a greater depth of the water column (**Figs. 6.3a and 6.3c**). In contrast, decreases in nutrient drawdown (i.e., decreases in net production) in Baffin Bay seem to be related to freshening and increased stratification of the water column during the study period (1997-2011) (**Figs. 6.3b and 6.3d**). In turn, impacts of reduced availability of nutrients owing to freshening of the surface water column have been shown to increase the abundance of small phytoplankton in the water column (Li et al. 2009, Lee et al. 2013, Yun et al. 2014). This finding has important implications for carbon turnover rates and vertical pathways of carbon flow in the Arctic Ocean system. Lalande et al. (2014) suggest that available nutrient concentrations have had strong impacts on how recent sea ice decline has affected carbon cycling, with low export fluxes of organic carbon from surface waters in the Arctic Ocean central basin (despite increased light availability during unprecedented sea ice loss in 2012). These low export fluxes imply that carbon export was limited by nutrient supply during summer 2012.

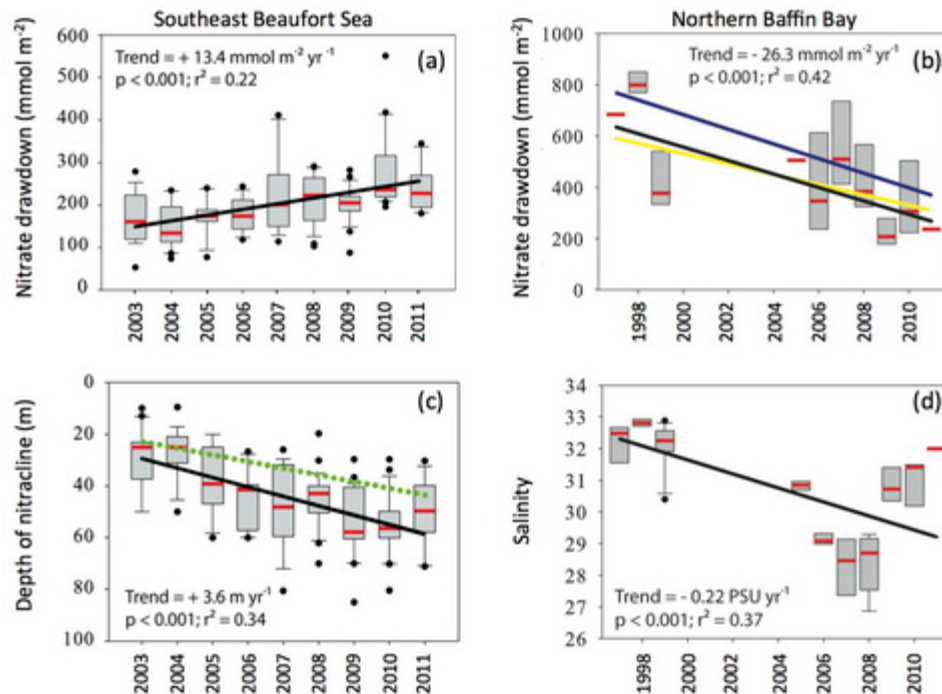


Fig. 6.3. Box plots of seasonal nitrate (NO_3^-) drawdown integrated across the water column for two disparate oceanographic settings, (a) Beaufort Sea and (b) Baffin Bay, where each box represents 50% of the observations, red marks indicate median values, whiskers provide ranges for the upper/lower quartiles, and circles indicate extreme values. Increases in the Beaufort Sea coincide with deepening of the nitracline, i.e., the water-column depth layer associated with rapid changes in nitrate or nutrients (c), suggesting that subsurface maxima are now consuming nutrients over a greater depth of the water column. Decreases in Baffin Bay are likely due to freshening and increased stratification of the water column (d). Modified from Bergeron and Tremblay (2014).

Recent seasonal sea ice retreat has shown important impacts on the timing of phytoplankton blooms across the Arctic, including the remarkable inter-annual differences in small-cell phytoplankton community structure across the northern Chukchi Sea (Fujiwara et al. 2014), where haptophytes (e.g., unicellular algae, including coccolithophorids) dominated in warm surface waters during 2008, while prasinophytes (e.g., unicellular green algae, including flagellates) dominated in cold water during 2009 and 2010 (when sea ice retreated ~1-2 months later than in 2008). Interestingly, Ji et al. (2013) have found that the timing of sea ice retreat has a strong effect on the timing of pelagic phytoplankton peaks over a large portion of the Arctic marginal seas, but weak or no impact on the timing of ice-algae peaks in the same regions.

Recent observed shifts in the timing of phytoplankton blooms also include the unexpected development of a secondary bloom in the autumn (Ardyna et al. 2014). This secondary bloom coincides with delayed formation of sea ice and longer exposure of the sea surface to wind stress, which presumably weakened vertical stratification and allowed nutrients to return to the euphotic zone. Between 1998 and 2012, a significant shift from a flat pattern of production to one and two annual phytoplankton blooms has occurred (**Fig. 6.4a**). In most of the Arctic Ocean and its marginal seas, autumn/secondary blooms have become more prevalent over the last 15 years, particularly in the Siberian sector: East Siberian Sea (+56%), Laptev Sea (+56%), Kara

Sea (+48%) and central Arctic Ocean/Eurasian Basin (+70%) (**Fig. 6.4b**), where trends in delayed sea ice formation during autumn have been most dramatic. Ardyna et al. (2014) also showed that during September (at sea ice minimum), the number of stormy days (defined using a wind speed threshold of 10 m s^{-1}) in the Arctic Ocean region has doubled over the last decade alone, which implicates wind-mixing as a potential driver of the rising prevalence of this secondary autumn bloom. Wind-mixing by polar cyclones acting on open waters has also been identified as another physical mechanism for promoting production in otherwise oligotrophic waters (e.g., Pozdnyakov et al. 2014, Zhang et al. 2014).

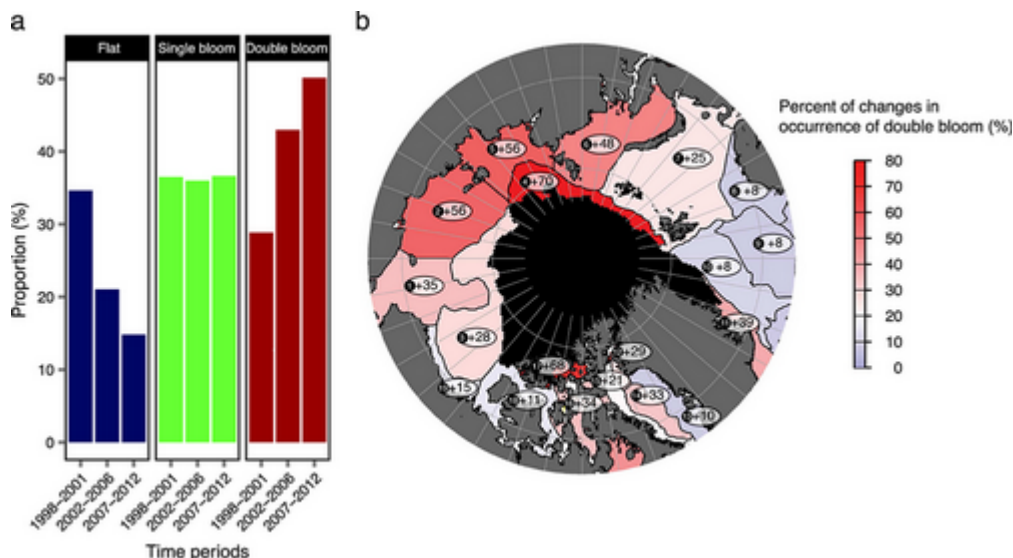


Fig. 6.4. Shifts in Arctic phytoplankton phenology above the Arctic Circle ($>66.58^{\circ}\text{N}$). (a) Histogram showing three different types of annual phytoplankton bloom cycles for three time periods (1998-2001, 2002-2006, and 2007-2012). (b) Percent change in autumn/secondary bloom occurrence between two periods (1998-2001 versus 2007-2012) for 19 discrete Arctic regions. The minimum September sea ice extent in 2012 is indicated in black. From Ardyna et al. (2014).

Impacts of recent sea ice decline on ice algae have also been substantial and have important implications for carbon fluxes in the Arctic Ocean system. Measurements of particulate organic carbon (POC) in the Chukchi Sea and western Arctic Ocean show that POC from sea ice floes (both sea ice and melt ponds) was $\sim 3\text{-}5\%$ of the total POC pool in the euphotic water column (Lee et al. 2014), which could be an important contributor of carbon via connections to higher trophic levels. Boetius et al. (2013) observed widespread deposition of ice algal biomass (primarily the diatom *Melosira arctica*, which grows as meter-long filaments anchored under ice floes) to the deep sea floor of the central Arctic Ocean basin (**Fig. 6.5**). At the time of observation (August-September 2012), the deposition of ice algae on the sea floor (stations of 3500-4400 m water depth) had a median of $\sim 9 \text{ g C m}^{-2}$. Although high biomass of *M. arctica* on sea ice is well known, measurements of oxygen penetration depths indicated that these high exports of sea ice algae all the way to the sea floor may have been rare in such deep, high-arctic waters before the record sea ice extent minimum of 2012. A related study of *M. arctica* indicated that melted sea ice, surface water warming, grazing and nutrient depletion can all lead to loss of buoyancy and deposition of *M. arctica* biomass to the deep sea (Fernández-Méndez

et al. 2014). Opportunistic megafauna (e.g., holothurians/sea cucumbers) were observed to feed on the deposited *M. arctica* biomass (Boetius et al. 2013), indicating clear and novel effects of declining sea ice cover in the central Arctic Ocean basin on pelagic-benthic coupling of carbon and food web dynamics throughout the region. Continued monitoring of environmental change and primary production in the Arctic Ocean marine system is critical for understanding overall carbon cycling and food web dynamics throughout the region.

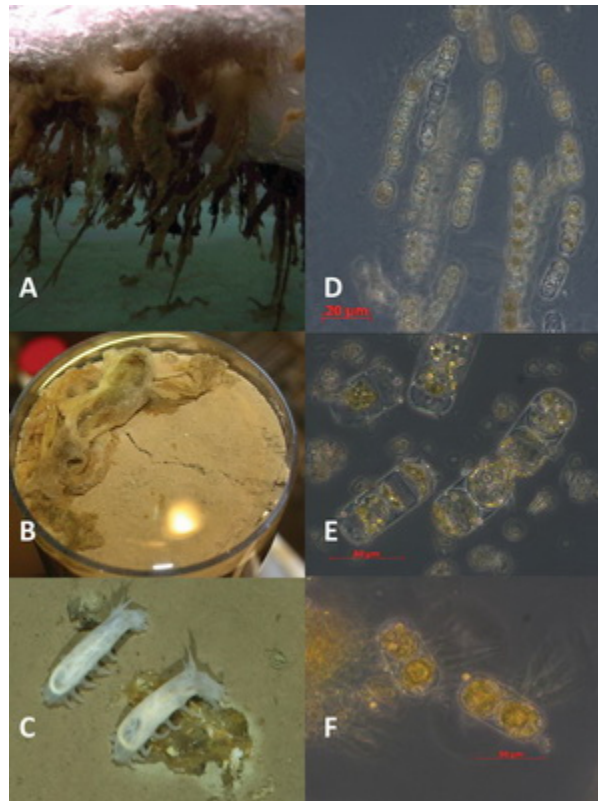


Fig. 6.5. (a) Strands (~20 cm) of the diatom *Melosira arctica* under sea ice; (b) recovered from the sea floor; and (c) photographed *in situ* with *Kolga hyaline* (sea cucumbers) grazing on deposits. (d to f) Microscopic images of *Melosira* cells from (a), (b) and (c), respectively. From Boetius et al. (2013).

References

- Ardyna, M., M. Babin, M. Gosselin, E. Devred, S. Bélanger, A. Matsuoka, and J.-É. Tremblay, 2013: Parameterization of vertical chlorophyll a in the Arctic Ocean: impact of the subsurface chlorophyll maximum on regional, seasonal, and annual primary production estimates. *Biogeosciences*, 10, 4383-4404, doi:10.5194/bg-10-4383-2013.
- Ardyna, M., M. Babin, M. Gosselin, E. Devred, L. Rainville, and J.-É. Tremblay, 2014: Recent Arctic Ocean sea ice loss triggers novel fall phytoplankton blooms. *Geophysical Research Letters*, 41, doi:10.1002/2014GL061047.

Bélangier, S., M. Babin, and J.-É. Tremblay, 2013: Increasing cloudiness in Arctic damps the increase in phytoplankton primary production due to sea ice receding. *Biogeosciences*, 10(6), 4087-4101, doi:10.5194/bg-10-4087-2013.

Bergeron, M., and J.-É. Tremblay, 2014: Shifts in biological productivity inferred from nutrient drawdown in the southern Beaufort Sea (2003-2011) and northern Baffin Bay (1997-2011), Canadian Arctic. *Geophysical Research Letters*, 41, 3979-3987, doi:10.1002/2014GL059649.

Boetius, A., S. Albrecht, K. Bakker, C. Bienhold, J. Felden, M. Fernández-Méndez, S. Hendricks, C. Katlein, C. Lalande, T. Krumpfen, M. Nicolaus, I. Peeken, B. Rabe, A. Rogacheva, E. Rybakova, R. Somavilla, F. Wenzhöfer and RV Polarstern ARK27-3-Shipboard Science Party, 2013: Export of algal biomass from the melting Arctic sea ice. *Science*, 339(6126), 1430-1432, doi:10.1126/science.1231346.

Cavalieri, D. J., C. L. Parkinson, P. Gloersen, and H. Zwally, 1996 (updated yearly): *Sea Ice Concentrations from Nimbus-7 SMMR and DMSP SSM/I-SSMIS Passive Microwave Data*. [2003-2013]. Boulder, Colorado USA: NASA DAAC at the National Snow and Ice Data Center.

Cherkasheva, A., A. Bracher, C. Melsheimer, C. Koeberle, R. Gerdes, E. M. Noethig, E. Bauerfeind, and A. Boetius, 2014: Influence of the physical environment on polar phytoplankton blooms: A case study in the Fram Strait. *Journal of Marine Systems*, 132, 196-207, doi:10.1016/j.jmarsys.2013.11.008.

Codispoti, L. A., V. Kelly, A. Thessen, P. Matrai, S. Suttles, V. Hill, M. Steele, and B. Light, 2013: Synthesis of primary production in the Arctic Ocean: III. Nitrate and phosphate based estimates of net community production. *Progress in Oceanography*, 110, 126-150, doi:10.1016/j.pocean.2012.11.006.

Comiso, J. C., and F. Nishio, 2008: Trends in the sea ice cover using enhanced and compatible AMSR-E, SSM/I and SMMR data. *Journal of Geophysical Research*, 113, CO2S07, doi:10.1029/2007JC004257.

Cota, G., G. Wang, and J. C. Comiso, 2004: Transformation of global satellite chlorophyll retrievals with a regionally tuned algorithm. *Remote Sensing of the Environment*, 90, 373-377.

Dalpadado, P., K. R. Arrigo, S. S. Hjollo, F. Rey, R. B. Ingvaldsen, E. Sperfeld, G. L. van Dijken, L. C. Stige, A. Olsen, and G. Ottersen, 2014: Productivity in the Barents Sea - Response to Recent Climate Variability, *Plos One*, 9(5), doi:10.1371/journal.pone.0095273.

Demidov, A. B., S. A. Mosharov, and P. N. Makkaveev, 2014: Patterns of the Kara Sea primary production in autumn: Biotic and abiotic forcing of subsurface layer. *Journal of Marine Systems*, 132, 130-149, doi:10.1016/j.jmarsys.2014.01.014.

- Fernández-Méndez, M., F. Wenzhöfer, I. Peeken, H. L. Sørensen, R. N. Glud, and A. Boetius, 2014: Composition, buoyancy regulation and fate of ice algal aggregates in the central Arctic Ocean. *PLoS One*, 9(9), doi:10.1371/journal.pone.0107452.
- Frey, K. E., D. K. Perovich, and B. Light, 2011: The spatial distribution of solar radiation under a melting Arctic sea ice cover. *Geophysical Research Letters*, 38, L22501, doi:10.1029/2011GL049421.
- Fujiwara, A., T. Hirawake, K. Suzuki, I. Imai, and S.-I. Saitoh, 2014: Timing of sea ice retreat can alter phytoplankton community structure in the western Arctic Ocean. *Biogeosciences*, 11, 1705-1716, doi:10.5194/bg-11-1705-2014.
- Ji, R., M. Jin, and O. Varpe, 2013: Sea ice phenology and timing of primary production pulses in the Arctic Ocean. *Global Change Biology*, 19(3), 734-741, doi:10.1111/gcb.12074.
- Lalande, C., E.-M. Noethig, R. Somavilla, E. Bauerfeind, V. Shevchenko, and Y. Okolodkov. 2014: Variability in under-ice export fluxes of biogenic matter in the Arctic Ocean. *Global Biogeochemical Cycles*, 28(5), 571-583, doi:10.1002/2013gb004735.
- Lee, S. H., B. K. Kim, H.-T. Joo, J. W. Park, J. H. Lee, H.-M. Joo, D. B. Lee, C.-K. Kang, and S.-H. Kang, 2014: Carbon accumulation of sea ice floes in the Arctic Ocean. *Deep-Sea Research II*, in press, <http://dx.doi.org/10.1016/j.dsr2.2013.12.021>.
- Lee, S. H., M. S. Yun, B. K. Kim, H. Joo, S.-H. Kang, C. K. Kang, and T. E. Whitledge, 2013: Contribution of small phytoplankton to total primary production in the Chukchi Sea, *Continental Shelf Research*, 68, 43-50, doi:10.1016/j.csr.2013.08.008.
- Li, W. K. W., F. A. McLaughlin, C. Lovejoy, and E. C. Carmack, 2009: Smallest algae thrive as the Arctic Ocean freshens. *Science*, 326, 539.
- Maslanik, J. and J. Stroeve, 1999 (updated daily): *Near-Real-Time DMSP SSM/I-SSMIS Daily Polar Gridded Sea Ice Concentrations*. [2014]. Boulder, Colorado USA: NASA DAAC at the National Snow and Ice Data Center.
- Monier, A., J. Comte, M. Babin, A. Forest, A. Matsuoka, and C. Lovejoy, 2014: Oceanographic structure drives the assembly processes of microbial eukaryotic communities. *The International Society for Microbial Ecology Journal*, 1-13, doi:10.1038/ismej.2014.197.
- Müller-Karger, F. E., R. Varela, R. Thunell, R. Luerssen, C. Hu, and J. J. Walsh, 2005: The importance of continental margins in the global carbon cycle. *Geophysical Research Letters*, 32, L01602, doi:10.1029/2004GL021346.

Petrenko, D., D. Pozdnyakov, J. Johannessen, F. Counillon, and V. Sychov, 2013: Satellite-derived multi-year trend in primary production in the Arctic Ocean. *International Journal of Remote Sensing*, 34, 3903-3937, <http://dx.doi.org/10.1080/01431161.2012.762698>.

Popova, E. E., A. Yool, A. C. Coward, Y. K. Aksenov, S. G. Alderson, B. A. de Cuevas, and T. R. Anderson, 2010: Control of primary production in the Arctic by nutrients and light: insights from a high resolution ocean general circulation model. *Biogeosciences*, 7, 3569-3591, doi:10.5194/bg-7-3569-2010.

Pozdnyakov, D., D. Tang, L. Bobylev, P. Golubkin, E. Zabolotskikh, D. Petrenko, and E. Morozov, 2014: A pilot satellite-based investigation of the impact of a deep polar cyclone propagation on the phytoplankton chlorophyll spatial and temporal dynamics in the Arctic Ocean. In *Typhoon Impact and Crisis Management, Advances in Natural and Technological Hazards Research*, edited by D. L. Tang and G. J. Sui (eds.), pp. 241-251, Springer-Verlag Berlin Heidelberg, doi:10.1007/978-3-642-40695-9_11.

Ulfsbo, A., N. Cassar, M. Korhonen, S. van Heuven, M. Hoppema, G. Kattner, and L. G. Anderson, 2014: Late summer net community production in the central Arctic Ocean using multiple approaches. *Global Biogeochemical Cycles*, in press, doi:10.1002/2014GB004833.

Yun, M. S., T. E. Whitledge, M. Kong, and S. H. Lee, 2014: Low primary production in the Chukchi Sea shelf, 2009. *Continental Shelf Research*, 76, 1-11, doi:10.1016/j.csr.2014.01.001.

Zhang, J., C. Ashjian, R. Campbell, V. Hill, Y. H. Spitz, and M. Steele, 2014: The great 2012 Arctic Ocean summer cyclone enhanced biological productivity on the shelves. *Journal of Geophysical Research-Oceans*, 119(1), 297-312.

Tundra Greenness

H. E. Epstein¹, U. S. Bhatt², M. K. Raynolds³, D. A. Walker³, P. A. Bieniek²,
C. J. Tucker⁴, J. Pinzon⁴, H. Zeng⁵, G. J. Jia⁵, K. C. Guay⁶, S. J. Goetz⁶

¹Department of Environmental Sciences, University of Virginia, Charlottesville, VA, USA

²Geophysical Institute, University of Alaska Fairbanks, Fairbanks, AK, USA

³Institute of Arctic Biology, University of Alaska Fairbanks, Fairbanks, AK, USA

⁴Biospheric Science Branch, NASA Goddard Space Flight Center, Greenbelt, MD, USA

⁵Institute of Atmospheric Physics, Chinese Academy of Sciences, Beijing, China

⁶Woods Hole Research Center, Falmouth, MA, USA

December 2, 2014

Highlights

- Peak tundra greenness (MaxNDVI) was still relatively high in 2013 for North America and the Arctic as a whole, indicating a continued trend in increasing vegetation productivity since satellite observations began in 1982.
- Temporally-integrated greenness (TI-NDVI, sum of the bi-weekly growing season values) had historically low values in 2013 for both Eurasia and the Arctic as a whole, suggesting a shorter growing season.
- During the latter half of the remote sensing record (1999-2013), there has been a substantial increase in the areas of tundra with declining TI-NDVI, i.e., there has been a "browning" of the tundra, suggesting a longer-term decline in growing season length.

Arctic tundra vegetation has been increasing its above-ground biomass, i.e. "greening", over at least the past several decades. This increase has implications for numerous aspects of terrestrial arctic ecosystems, including atmospheric carbon dioxide uptake through photosynthesis, surface energy and water exchanges, plant-herbivore interactions, and active layer/permafrost dynamics, as well as feedbacks to regional and global climate. The vegetation changes are neither spatially homogenous throughout the Arctic nor temporally consistent. Satellite remote sensing has provided the tool for examining the spatio-temporal patterns of arctic tundra vegetation dynamics.

The Global Inventory Modeling and Mapping Studies (GIMMS3g) dataset (GIMMS 2013) is a biweekly, maximum-value-composited, Normalized Difference Vegetation Index (NDVI) time series derived largely from Advanced Very High Resolution Radiometer (AVHRR) sensors aboard NOAA satellites. GIMMS3g provides a >30-year record (starting in 1982) of remote sensing data, from which vegetation greenness indices are calculated, such as MaxNDVI (maximum annual value) and Time Integrated NDVI (TI-NDVI, sum of the biweekly growing season values of NDVI) (Raynolds et al. 2012).

In 2013 (data for 2014 were not available at the time of writing), peak tundra greenness (MaxNDVI) was relatively high for North America and for the Arctic as a whole; 2013 ranked 4th

for both regions over the 32-year record. However, MaxNDVI was only slightly above the mode for Eurasia (ranked 13th). TI-NDVI for 2013 was greater than the mode for North America (11th), but for Eurasia and the Arctic as a whole, we observed some of the lowest values in the record (31st and 26th, respectively) (**Fig. 7.1**).

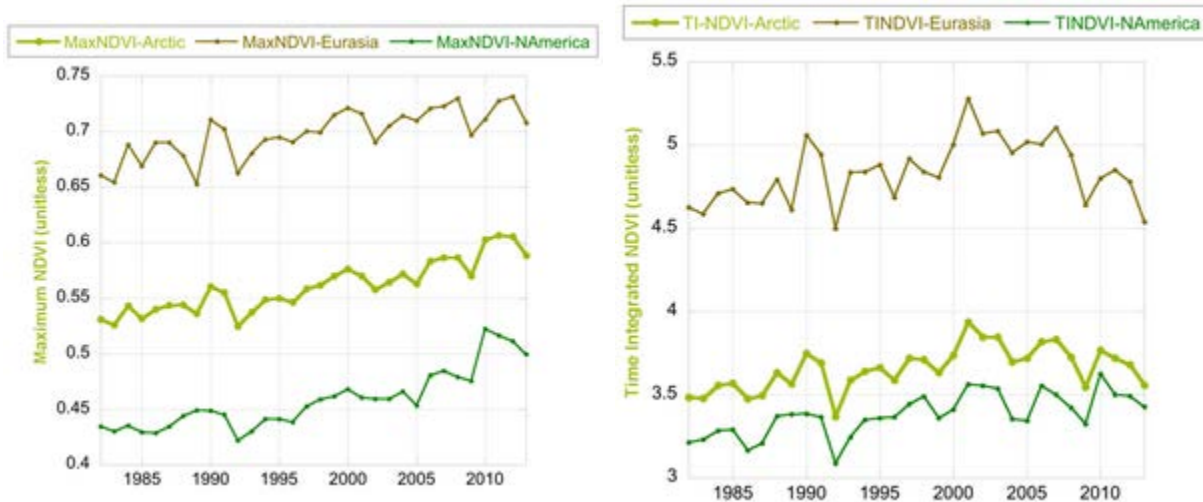


Fig. 7.1. (left) MaxNDVI and (right) TI-NDVI for North American, Eurasia and the Arctic as a whole over the 32-year (1982-2013) satellite remote sensing record.

Trends over the entire period 1982-2013 continue to show increases in tundra greenness, with MaxNDVI exhibiting high values through the early 2010s. MaxNDVI is strongly correlated with above-ground tundra biomass (Raynolds et al. 2012, Epstein et al. 2012); the 32-year trend in MaxNDVI indicates an average above-ground tundra biomass increase of approximately 20%, from $\sim 357 \text{ g m}^{-2}$ to 430 g m^{-2} .

There are some notable changes in the latter part of the record, particularly with respect to TI-NDVI (**Fig. 7.1**). Splitting the record at its midpoint (1998) reveals the temporal change. During the period 1982-1998, both MaxNDVI and TI-NDVI generally increased in the Arctic, indicating greater peak productivity and increased greenness over the entire growing season, respectively. During the period 1999-2013, however, there were decreasing trends in TI-NDVI, i.e., "browning", over large geographic areas, suggesting a decrease in growing season length; MaxNDVI declines of similar magnitude did not occur. It is possible that "browning" in some areas of the Low Arctic could be due to permafrost degradation and subsequent hydrological changes (Jorgenson et al. 2001, Frost and Epstein 2014). During the latter period in Eurasia, decreases in MaxNDVI and TI-NDVI match areas with declining summer air temperatures (Bhatt et al. 2013). Bjerke et al. (2014) also noted that anomalous weather events, such as extreme cold or heat and strong storms, as well as pest outbreaks, have led to historically low vegetation productivity in the Nordic Arctic Region.

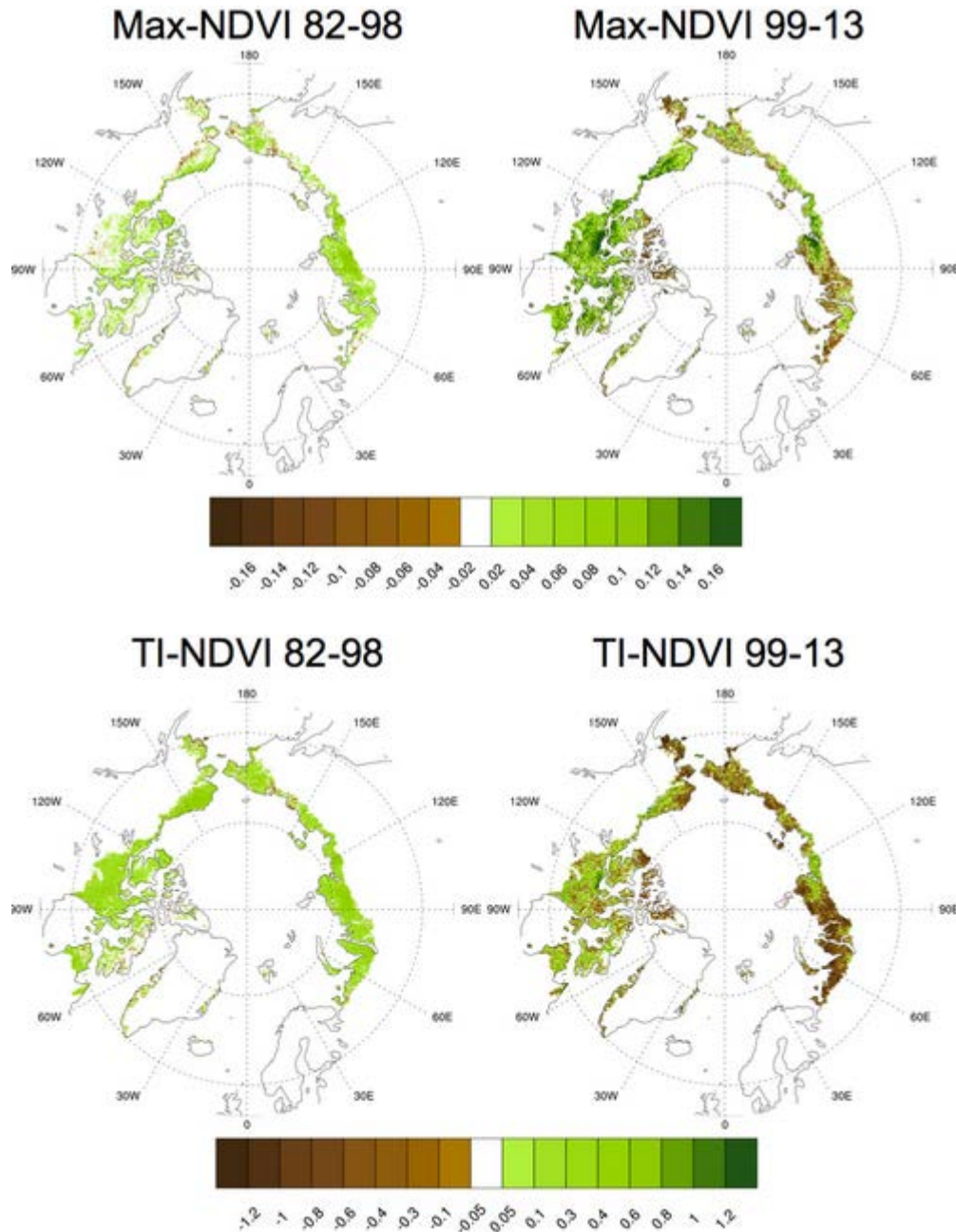


Fig. 7.2. Trends in magnitude for (top left) MaxNDVI for 1982-1998 and (top right) MaxNDVI 1999-2013 and (bottom left) TI-NDVI for 1982-1998 and (bottom right) TI-NDVI 1999-2013.

Trends of TI-NDVI from 1999-2013 show the largest declines at the start of the growing season. In fact, Zeng and Jia (2013) found, using Moderate Resolution Imaging Spectroradiometer (MODIS) data for 2000-2010 in the Yamal Peninsula region of northwestern Siberia, that the start of the growing season became later over the course of the decade. Further, the delay in the onset of vegetation increased at lower latitudes. The causes of reduced TI-NDVI and their relationship to, for example, the changing snow cover (see the essay on [Terrestrial Snow Cover](#)) have yet to be determined for the Arctic tundra as a whole.

Finally, recent studies indicate that arctic tundra greening trends, at least in the more southern arctic tundra, are strongly linked to the expansion of woody vegetation (Urban et al. 2014) and particularly the spread of tall shrubs (Frost and Epstein 2014, Frost et al. 2014). Frost and Epstein found that tall shrub and tree cover, primarily alder and larch, respectively, increased up to 26% in 9 of 11 forest-tundra ecotones across Siberia since the late 1960s. This expansion of woody vegetation has been shown to alter ecosystem processes, such as the surface energy balance (Myers-Smith and Hik 2013) and plant litter decomposition rates (DeMarco et al. 2014). Several recent studies note that consumption of plants by herbivores may be a mechanism whereby increases in woody vegetation cover across landscapes are constrained (Christie et al. 2014, Plante et al. 2014, Ravolainen et al. 2014). However, this is limited by the production of chemical compounds by individual woody plant species that deter herbivores (Bryant et al. 2014).

References

- Bhatt, U. S., D. A. Walker, M. K. Raynolds, P. A. Bieniek, H. E. Epstein, J. C. Comiso, J. E. Pinzon, C. J. Tucker, and I. V. Polyakov, 2013: Recent declines in warming and arctic vegetation greening trends over pan-Arctic tundra. *Remote Sensing* (Special NDVI3g Issue), 5, 4229-4254; doi:10.3390/rs5094229.
- Bjerke, J. W., S. R. Karlsen, K. A. Høgda, E. Malnes, J. U. Jepsen, S. Lovibond, D. Vikhamar-Schuler, and H. Tømmervik, 2014: Record-low primary productivity and high plant damage in the Nordic Arctic Region in 2012 caused by multiple weather events and pest outbreaks. *Environmental Research Letters*, 9, 084006.
- Bryant, J. P., K. Joly, F. S. Chapin, D. L. DeAngelis, and K. Kielland, 2014: Can antibrowsing defense regulate the spread of woody vegetation in the arctic tundra? *Ecography*, 37, 204-211.
- Christie, K. S., R. W. Reuss, M. S. Lindberg, and C.P. Mulder, 2014: Herbivore influence on growth, reproduction, and morphology of a widespread arctic willow. *PLoS One*, 9, e101716.
- DeMarco, J., M. C., Mack, and M. S. Bret-Harte, 2014: Effects of arctic shrub expansion on biophysical vs. biogeochemical drivers of litter decomposition. *Ecology*, 95, 1861-1875.
- Epstein, H. E., M. K. Raynolds, D. A. Walker, U. S. Bhatt, C. J. Tucker, and J. E. Pinzon, 2012: Dynamics of aboveground phytomass of the circumpolar arctic tundra over the past three decades. *Environmental Research Letters*, 7, 015506.
- Frost, G. V. and H. E. Epstein, 2014: Tall shrub and tree expansion in Siberian tundra ecotones since the 1960s. *Global Change Biology*, 20, 1264-1277.
- Frost, G. V., H. E. Epstein, and D. A. Walker, 2014: Regional and landscape-scale variability of Landsat-observed vegetation dynamics in northern Siberian tundra. *Environmental Research Letters*, 9, 025004.

Myers, I. H., and D. S. Hik, 2014: Shrub canopies influence soil temperature but no nutrient dynamics: An experimental test of tundra snow-shrub interactions. *Ecology and Evolution*, 3, 3683-3700, doi: 10.1002/ece3.710.

Global Inventory Modeling and Mapping Studies (GIMMS). Available online:

http://gcmd.nasa.gov/records/GCMD_GLCF_GIMMS.html.

Plante, S., E. Champagne, P. Ropars, S. Boudreau, E. Levesque, B. Tremblay, and J. P. Tremblay, 2014: Shrub cover in northern Nunavik: Can herbivores limit shrub expansion? *Polar Biology*, 37, 611-619.

Ravolainen, V. T., K. A. Brathen, N. G. Yoccoz, J. K. Nguyen, and R. A. Ims, 2014: Complementary impacts of small rodents and semi-domesticated ungulates limit tall shrub expansion in the tundra. *Journal of Applied Ecology*, 51, 234-241.

Raynolds M. K., D. A. Walker, H. E. Epstein, J. E. Pinzon, and C. J. Tucker, 2012: A new estimate of tundra-biome phytomass from trans-Arctic field data and AVHRR NDVI. *Remote Sensing Letters*, 3, 403-411.

Urban, M., M. Forkel, J. Eberle, C. Huettich, C. Schmullius, and M. Herold, 2014: Pan-Arctic climate and land cover trends from multi-variate and multi-scale analyses (1981-2012). *Remote Sensing*, 6, 2296-2316.

Zeng, H., and G. Jia, 2013: Impacts of snow cover on vegetation phenology in the Arctic from satellite view. *Advances in Atmospheric Sciences*, 30, 1421-1432.

Polar Bears: Status, Trends and New Knowledge

D. Vongraven¹, G. York²

¹Norwegian Polar Institute, Fram Centre, Tromsø, Norway

²Polar Bears International, Bozeman, MT, USA

December 2, 2014

Highlights

- A decline in survival of female polar bears of all age classes, from 1194 to 806, between 1987 and 2011 in western Hudson Bay was due to earlier sea ice break-up in the spring and later freeze-up in the autumn.
- In 2010, polar bear numbers in the southern Beaufort Sea appeared to stabilize at 900 bears following a period of low survival during 2004-2006 that led to a 25-50% decline in abundance. However, survival of sub-adult bears declined during the entire period.
- Polar bear condition and reproductive rates have also declined in the southern Beaufort Sea, unlike in the adjacent Chukchi Sea, immediately to the west, where they have remained stable for 20 years. There are also now twice as many ice-free days in the southern Beaufort Sea as there are in the Chukchi Sea.
- Genetic studies indicate that polar bears have been through long and dramatic periods of population decline during the last one million years, and that during periods with little sea ice there have been multiple episodes of interbreeding between polar bears and brown bears.



Introduction

Polar bears (*Ursus maritimus*) have a pan-arctic distribution that is influenced by the distribution and availability of sea ice. Sea ice provides the primary platform on which polar bears travel, hunt, mate and, in some areas, den. Polar bears rely on ice-associated seals for a majority of their energetic needs, i.e., food, such as ringed seals, bearded seals, harp seals, hooded seals, and, to a lesser extent, on other marine mammals, e.g., walrus and whales.

The primary habitat for polar bears and their prey, sea ice, is declining rapidly in extent in all seasons, and particularly in summer, with concurrent and even more dramatic reductions in total volume (Laxon et al. 2013). Since the satellite record began in 1979, minimum sea ice extent has declined 13.3% per decade (see the essay on [Sea Ice](#)). Given the close association between polar bears, their primary prey and sea ice, climate warming remains the most significant threat to the long-term survival of this species (Stirling and Derocher 1993, Amstrup et al. 2008, 2010).

Population Status

The IUCN/SSC-PBSG (International Union for Conservation of Nature/Species Survival Commission-Polar Bear Specialist Group, <http://pbsg.npolar.no>) assesses the status of the 19 recognized polar bear sub-populations at 4-year intervals, but annually since 2013. The most recent population trend assessment by region, completed in December 2013, is illustrated in **Fig. 8.1**.

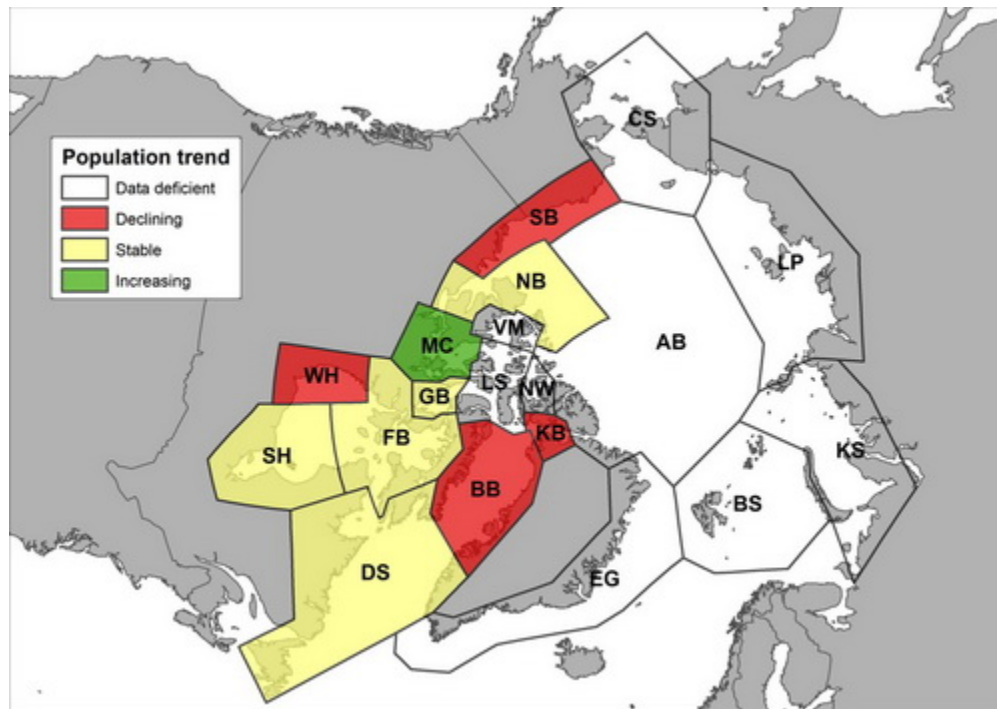


Fig. 8.1. Population trend assessment for all 19 acknowledged polar bear sub-populations assessed in 2013 by the IUCN/SSC-PBSG. Abbreviations: AB: Arctic Basin; BB: Baffin Bay; CS: Chukchi Sea; DS: Davis Strait; EG: East Greenland; FB: Fove Basin; GB: Gulf of Boothia; KB: Kane Basin; KS: Kara Sea; LS: Lancaster Sound; LP: Laptev Sea; MC: M'Clintock Channel; NB: northern Beaufort Sea; NW: Norwegian Bay; SB: southern Beaufort Sea; SH: southern Hudson Bay; VM: Viscount Melville; WH: western Hudson Bay.

It should be noted that monitoring data are increasingly dated in many areas or simply missing altogether due to infrequent or non-existent population assessments, lack of monitoring policies and focus, and funding challenges. Hence the large swath of data deficient zones from East Greenland eastward through Eurasian waters to the Chukchi Sea (**Fig. 8.1**). Also, **Fig. 8.1** does not show important demographic trends, such as survival, body condition and reproduction, from the populations where data are available. Vital rates are generally easier to obtain over long periods of time, provide important indices for population health, and are key factors in calculating population persistence over time.

New Analysis of Long Term Data Sets

In the three most studied polar bear populations (the southern Beaufort Sea, western Hudson Bay and Barents Sea; **Fig. 8.1**), where long term data sets are available, negative relationships have been noted between changes in sea ice availability and declines in body condition, survival and reproduction. In the southern Beaufort Sea and western Hudson Bay, these changes in vital rates have led to declining populations (Derocher et al. 2011, Hunter et al. 2007, Regehr et al. 2007a, 2007b). Here, we report on western Hudson Bay, the southern Beaufort Sea and, for comparison with the latter region, the adjacent Chukchi Sea (**Fig. 8.1**). These three regions were chosen for Arctic Report Card 2014 because they have the most peer-reviewed studies in recent years, which have contributed most to current understanding of polar bear ecology and the response to climate warming.

Western Hudson Bay. New analysis for the period 1984-2011 for western Hudson Bay polar bears indicates that survival of female polar bears of all age classes was significantly correlated with sea ice conditions, particularly with the timing of sea ice break-up in the spring and freeze-up in the autumn (Lunn et al. 2014). This outcome is consistent with previous findings that link body condition and survival of polar bears with impacts of climate warming, and illustrates polar bears' reliance on sea ice habitat. The survival of male polar bears, however, was not correlated with sea ice conditions. This may reflect higher mortality for males being linked directly to people rather than natural causes; approximately 73% of all mortality for young male bears was due to a sex-selected subsistence harvest.

Lunn et al. (2014) confirmed the declining trend in the size of the western Hudson Bay population, from 1,194 in 1987 to 806 in 2011, as noted in an earlier analysis (Regehr et al. 2007a), though estimates of abundance were slightly lower due to updated statistical analyses. One significant caveat was noted by Lunn et al. (2014): the available data were not collected in a manner optimal for estimating abundance. The primary goal of the Lunn et al. study was to calculate vital rates and demographic trends for the region. Estimates of population growth rate were also derived and, for the decade 2001-2011, the growth rate for female polar bears in western Hudson Bay was 1.02 (95% confidence interval = 0.98-1.06). The stable to positive population trend for females may be related to recent short-term stability in the long-term observed and forecast trend toward earlier sea ice break-up in the bay. The population abundance estimate for 2011 was 806 (95% Bayesian 3 credible interval of 653-984), which is lower than, but consistent with, the abundance estimate of 1,030 (95% confidence interval = 745-1406) from a 2011 aerial survey of western Hudson Bay (Stapleton et al. 2014). The two methods for estimating abundance used different spatial and temporal coverage of the region. Consequently, the effective study population considered by each approach is different.

Chukchi Sea and southern Beaufort Sea. A new study of the Chukchi Sea population suggests that the body condition and reproductive rates for polar bears in the area were stable between 1986-1994 and 2008-2011 (Rode et al. 2013). This is in contrast to the adjacent southern Beaufort Sea population, which has experienced recent declines in both condition and survival. Comparing sea ice conditions in the two regions, there were twice as many days with

no ice in the southern Beaufort Sea than in the Chukchi Sea. Chukchi Sea polar bears from this study period were physically larger, in better body condition and had higher reproduction rates than adjacent southern Beaufort Sea bears. Southern Beaufort Sea and Chukchi Sea bears had similar diets, but twice as many bears were fasting during spring in the southern Beaufort Sea compared to the Chukchi Sea. Comparing Chukchi Sea data from the late 1980's with the new information from this study (2008-2011), body size, condition and recruitment in the Chukchi Sea did not decline, notwithstanding a 44-day increase in days with no ice (Rode et al. 2013). In the southern Beaufort Sea, the narrow continental shelf, low overall productivity and proportionately greater number of days without sea ice, has led to nutritional stress resulting in reduced condition and survival rates, particularly of sub-adult bears, and an overall 40% decline to 900 individuals between 2001 and 2010, respectively (Regehr et al. 2008, Bromaghin et al. in press). In contrast, greater availability of prey (both abundance and variety) in the Chukchi Sea, a vast continental shelf area, and fewer ice-free days, may have allowed Chukchi Sea polar bears to avoid critical energetic thresholds at present. These findings are consistent with predictions that the near-term effects of global warming on polar bear populations are expected to differ in time and space, depending largely on regional variation in productivity and physical oceanography (Rode et al. 2013).

Polar Bear Genetics

A recently published analysis of Arctic-wide polar bear genetics over the last two decades evaluated whether genetic diversity and structure have changed, how current genetic patterns compare with historic information, and whether genetic demography changed with fluctuations in climate over time (Peacock et al. in press). The analysis defined four "population" clusters that correspond well with eco-regions described by Amstrup et al. (2008): the eastern Polar Basin, western Polar Basin, Canadian Arctic Archipelago and Southern Canada. The new research provides evidence for recent directional gene flow from southern Canada and the eastern Polar Basin towards the Canadian Arctic Archipelago, an area theorized to be future refugia for sea ice dependent species as climate-induced habitat decline continues (Durner et al. 2009, Hamilton et al. 2014). The analyses of mitochondrial DNA provided additional evidence that both the Canadian Arctic Archipelago and the Barents Sea (two areas of High Arctic islands) might have functioned as past refugia for polar bears. Additionally, comparison of mitochondrial DNA data from polar and brown bear (*Ursus arctos*) suggested unique demographic responses between the two species in response to historic climate variation. Finally, the analysis indicates that the genetic structure of polar bears is limited and developed recently, in contrast to brown bears. It also found no genetic evidence of recent hybridization between the species in their large, circumpolar sample, supporting the idea that recently observed hybrids represent local phenomena. (Peacock et al. in press)

Polar Bear Evolution

There have been substantial new additions to our knowledge of the evolutionary history of polar bears as a species. Genetic analyses suggest a range of possible ages for the polar bear lineage, from 110,000-130,000 years (Lindqvist et al. 2010) to 300,000-900,000 years (Hailer et

al. 2012) and even 4-5 million years (Miller et al. 2012). Miller et al. (2012) also proposed that polar bears have been through a long and dramatic period of population decline during the last million years. They further suggested that (1) there have been multiple periods of interbreeding between polar bears and brown bears, during periods with little sea ice and lower glacier coverage, when ranges of the two species overlapped to a greater degree, and (2) earlier studies that concluded there had been recent splits between the species in fact identified periods following hybridization and not actual speciation. The close relationship between polar bears and brown bears, and hybridization between the species was also noted in recent studies by Cahill et al. (2013) and Cronin et al. (2014).

References

Amstrup, S. C., B. G. Marcot and D. C. Douglas, 2008: A Bayesian network modeling approach to forecasting the 21st century worldwide status of polar bears. In *Arctic Sea Ice Decline: Observations, Projections, Mechanisms, and Implications*, Geophysical Monograph Series 180, edited by E. T. DeWeaver, C. M. Bitz, and L.-B. Tremblay, American Geophysical Union, Washington DC, Geophysical Monograph 180, 213-268.

Amstrup, S. C., E. T. DeWeaver, D. C. Douglas, B. G. Marcot, G. M. Durner, C. M. Bitz, and D. A. Bailey, 2010: Greenhouse gas mitigation can reduce sea-ice loss and increase polar bear persistence. *Nature*, 468, 955-960.

Bromaghin, J., S. Amstrup, T. McDonald, I. Stirling, A. Derocher, E. Richardson, E. Regehr, D. Douglas, G. Durner, and T. C. Atwood, in press: Polar bears in the Beaufort Sea: Population decline and stabilization in the 2000s. *Ecological Applications*, <http://dx.doi.org/10.1890/14-1129.1>.

Cahill, J. A., R. E. Green, T. L. Fulton, M. Stiller, F. Jay, N. Ovshyanikov, R. Salamzade, J. St. John, I. Stirling, M. Slatkin, and B. Shapiro, 2013: Genomic evidence for island population conversion resolves conflicting theories of polar bear evolution. *Plos Genetics*, 9, e1003345.

Cronin, M. A., G. Rincon, R. W. Meredith, M. D. MacNeil, A. Islas-Trejo, A. Canovas, and J. F. Medrano, 2014: Molecular phylogeny and SNP variation of polar bears (*Ursus maritimus*), brown bears (*U. arctos*), and black bears (*U. americanus*) derived from genome sequences. *Journal of Heredity*, 105, 312-323.

Derocher, A. E., M. Andersen, Ø. Wiig, J. Aars, E. Hansen, and M. Biuw, 2011: Sea ice and polar bear den ecology at Hopen Island, Svalbard. *Marine Ecology Progress Series*, 441, 273-297.

Durner, G. M., and 16 others, 2009: Predicting 21st-century polar bear habitat distribution from global climate models. *Ecological Monographs*, 79, 25-58. <http://dx.doi.org/10.1890/07-2089.1>.

Hailer, F., V. E. Kutschera, B. M. Hallström, D. Klassert, S. R. Fain, J. A. Leonard, U. Arnason, and A. Janke, 2012: Nuclear genomic sequences reveal that polar bears are an old and distinct bear lineage. *Science*, 336, 344-347.

Hamilton, S. G., L. Castro de la Guardia, A. E. Derocher, V. Sahanatien, B. Tremblay, and D. Huard, 2014: Projected polar bear sea ice habitat in the Canadian Arctic Archipelago. *PLoS ONE*, 9(11), e113746. doi:10.1371/journal.pone.0113746.

Hunter, C. M., H. Caswell, M. C. Runge, E. V. Regehr, S. C. Amstrup, and I. Stirling, 2007: Polar bears in the Southern Beaufort Sea II: Demography and population growth in relation to sea ice conditions. Administrative Report, US Geological Survey, Reston, Virginia, 46 pp.

Laxon, S. W., K. A. Giles, A. L. Ridout, D. J. Wingham, R. Willatt, R. Cullen, R. Kwok, A. Schweiger, J. Zhang, C. Haas, S. Hendricks, R. Krishfield, N. Kurtz, S. Farrell, and M. Davidson, 2013: CryoSat-2 estimates of Arctic sea ice thickness and volume. *Geophysical Research Letters*, 40, 1-6.

Lindqvist, C., S. C. Schuster, Y. Z. Sun, S. L. Talbot, J. Qi, A. Ratan, L. P. Tomsho, L. Kasson, E. Zeyl, J. Aars, W. Miller, O. Ingolfsson, L. Bachmann, and Ø. Wiig, 2010: Complete mitochondrial genome of a Pleistocene jawbone unveils the origin of polar bear. *Proceedings of the National Academy of Sciences*, 107, 5053-5057.

Lunn, N. J., S. Servanty, E. R. Regehr, S. J Converse, E. Richardson, and I. Stirling, 2014: Demography and population status of polar bears in Western Hudson Bay, Canada. Environment Canada Research Report.

Miller, W., S. C. Schuster, A. J. Welch, A. Ratan, O. C. Bedoya-Reina, F. Zhao, H. L. Kim, S. C. Burhans, D. I. Drautz, N. E. Wittekindt, L. P. Tomsho, E. Ibarra-Laclette, L. Herrera-Estrella, E. Peacock, S. Farley, G. K. Sage, K. Rode, M. Obbard, R. Montiel, L. Bachmann, O. Ingolfsson, J. Aars, T. Mailund, Ø. Wiig, S. L. Talbot, and C. Lindqvist, 2012: Polar and brown bear genomes reveal ancient admixture and demographic footprints of past climate change. *Proceedings of the National Academy of Sciences*, 109(36): E2382-E2390.

Peacock, E., S. A. Sonsthagen, M. E. Obbard, A. Boltunov, E. V. Regehr, N. Ovsyanikov, J. Aars, S. N. Atkinson, G. K. Sage, A. G. Hope, E. Zeyl, L. Bachmann, D. Ehrich, K. T. Scribner, S. C. Amstrup, S. Belikov, E. Born, A. E. Derocher, I. Stirling, M. K. Taylor, Ø. Wiig, D. Paetkau, and S. L. Talbot, in press: Implications of the circumpolar genetic structure of polar bears for their conservation in a rapidly warming Arctic. *Plos One*.

Regehr, E. V., N. J. Lunn, S. C. Amstrup, and I. Stirling, 2007a: Effects of earlier sea ice breakup on survival and population size of polar bears in Western Hudson Bay. *Journal of Wildlife Management*, 71, 2673-2683.

Regehr, E. V., C. M. Hunter, H. Caswell, S. C. Amstrup, and I. Stirling, 2007b: Polar bears in the southern Beaufort Sea I: Survival and breeding in relation to sea ice conditions, 2001-2006. Administrative Report, U.S. Geological Survey, Reston, Virginia, 50 pp.

Rode, K. D., E. V. Regehr, D. C. Douglas, G. M. Durner, A. E. Derocher, G. W. Thiemann, and S. M. Budge, 2013: Variation in the response of an Arctic top predator experiencing habitat loss: Feeding and reproductive ecology of two polar bear populations. *Global Change Biology*, 20, 76-88.

Stapleton, S., S. Atkinson, D. Hedman, and D. Garshelis, 2014: Revisiting Western Hudson Bay: Using aerial surveys to update polar bear abundance in a sentinel population. *Biological Conservation*, 170, 38-47.

Stirling, I., and A. E. Derocher, 1993: Possible impacts of climatic warming on polar bears. *Arctic*, 46, 240-245.

Climate and Herbivore Body Size Determine How Arctic Terrestrial Ecosystems Work

P. Legagneux^{1,2}, G. Gauthier¹, N. Lecomte^{2,3,4}, N. M. Schmidt⁵, D. Reid⁶,
M.-C. Cadieux¹, D. Berteaux², J. Bêty², C. J. Krebs⁷, R. A. Ims³, N. G. Yoccoz³,
R. I. G. Morrison⁸, S. J. Leroux⁹, M. Loreau¹⁰, D. Gravel¹¹

¹Département de Biologie and Centre d'études nordiques, Université Laval, Québec City, QC, Canada

²Université du Québec à Rimouski and Centre d'études nordiques, Rimouski, QC, Canada

³Department of Arctic and Marine Biology, University of Tromsø, Tromsø, Norway

⁴Department of Biology, University of Moncton, Moncton, NB, Canada

⁵Arctic Research Centre, Aarhus University, Aarhus, Denmark

⁶Wildlife Conservation Society Canada, Whitehorse, YT, Canada

⁷Department of Zoology, University of British Columbia, Vancouver, BC, Canada

⁸National Wildlife Research Centre, Environment Canada, Carleton University, Ottawa, ON, Canada

⁹Department of Biology, Memorial University of Newfoundland, St John's, NL, Canada

¹⁰Centre for Biodiversity Theory and Modelling, CNRS, Moulis, France

¹¹Département de Biologie, Université du Québec à Rimouski, Rimouski, QC, Canada

December 2, 2014

Arctic ecosystems are particularly vulnerable to climate change. Scientists are beginning to understand how various animal species can cope with such changes, but scaling this up to the level of entire ecosystems is challenging. Understanding the dominant relationships among species is a prerequisite to determine what controls the food web structure and ecosystem services, such as the exploitation of natural resources, that benefit people.

Both food resources and predator abundance and diversity can shape relationships among species in an ecosystem. Determining how much each component controls the food web in the tundra remains controversial. To address this debate, how food webs vary across a broad geographic scale was investigated during International Polar Year (2007-2009) in Canada, Greenland, Norway and Russia (Legagneux et al. 2014). This was accomplished by gathering data on primary production, species abundance and diet composition at 7 circumpolar study sites spread over a wide range of latitudes covering a distance of 1,500 km and encompassing large climatic differences (**Fig. 9.1a**).

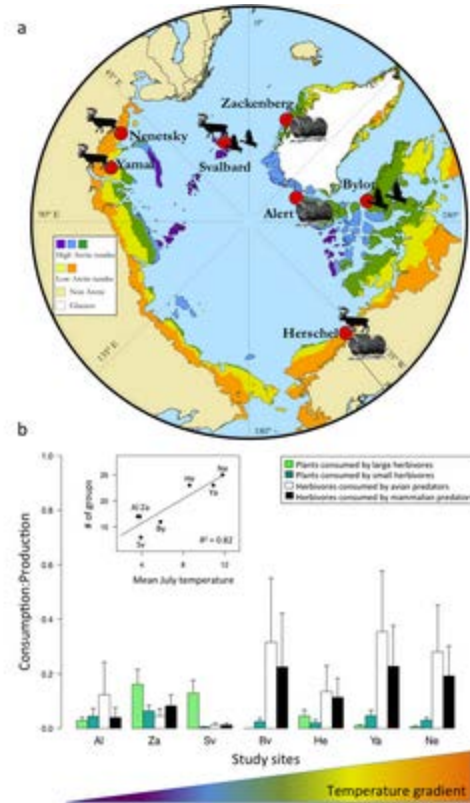


Fig. 9.1. Consumption rates at seven Arctic tundra study sites. (a) The study sites are identified by red dots on a map of bioclimatic zones from high to low Arctic tundra. The pictograms represent the most abundant herbivores (muskoxen; caribou/reindeer and geese) at each site. (b) Median consumption rates (consumption:production ratios) at each study site. Consumption rates of plants were divided according to the size of herbivores consuming them and consumption rates of herbivores according to the predator types. Sites are ranked in increasing order of average July air temperature. The insert graph shows that the number of species (or group of species) increased with air temperature.

Legagneux et al. (2014) found air temperature was strongly correlated with the strength of food web interactions: predation by Arctic foxes, small mustelids (e.g., stoat, which is known to cause cycles in some lemming populations (Gilg et al. 2003)), and birds of prey on small herbivores (lemmings, voles and ptarmigan) intensified at warmer sites in conjunction with reduced consumption rate of annual plant growth (**Fig. 9.1b**). Predator-prey interactions thus appear to be the dominant interaction of the tundra food web, compared to herbivore-plant interactions, except in the High Arctic where there plant productivity is lower and the food chain is more simple than at lower Arctic latitudes. Moreover, as reported by Hansen et al. (2013), in the High Arctic, extreme winter weather conditions, such as rain-on-snow events, have the potential to indirectly drive the population dynamics of overwintering vertebrates. These patterns may allow improved predictions of how climate change will affect whole food webs.

Another key result was that predation intensity varied according to the body size of herbivores in the ecosystem, with large herbivores (caribou and muskoxen) mostly escaping strong limitation by predators, unlike small herbivores. Interestingly, similar patterns had previously been reported for the food web of the African savannas. The Arctic study suggests, for the first time,

that some general principles govern terrestrial ecosystems with simple vegetation structure. The study also highlights the value of international collaboration to better understand ecosystem function, especially in polar environments.

References

Gilg, G., I. Hanski, and B. Sittler, 2003: Cyclic dynamics in a simple vertebrate predator-prey community. *Science*, 302, 866-868, doi:10.1126/science.1087509.

Hansen, B. U., V. Grøtan, R. Aanes, B.-E. Sæther, A. Stien, E. Fuglei, R. A. Ims, N. G. Yoccoz, and Å. Ø. Pedersen, 2013: Climate events synchronize the dynamics of a resident vertebrate community in the High Arctic. *Science*, 339, 313-315, doi:10.1126/science.1226766.

Legagneux, P., G. Gauthier, N. Lecomte, N. M. Schmidt, D. Reid, M.-C. Cadieux, D. Berteaux, J. Bêty, C. J. Krebs, R. A. Ims, N. G. Yoccoz, R. I. G. Morrison, S. J. Leroux, M. Loreau, and D. Gravel, 2014: Arctic ecosystem structure and functioning shaped by climate and herbivore body size. *Nature Climate Change*, 4, 379-383, doi:10.1038/nclimate2168.

Depicting Arctic Change: Dependence on the Reference Period

J. Walsh

International Arctic Research Center, University of Alaska Fairbanks, Fairbanks, AK, USA

December 2, 2014

Global and regional variations of climate over periods of a season to a decade are often characterized as departures (anomalies) from "normals", i.e., the mean values (averages) for a given reference period. A similar approach is used in tracking variations of weather, which are generally referenced to "normals" for 30-year periods. The use of a 30-year reference period is the standard recommended by the World Meteorological Organization and adopted by the NOAA National Climatic Data Center. A 30-year reference period represents a compromise between (a) longer record lengths that are less sensitive at inter-annual to decadal-scale variations (because they include more such variations) but can be affected by trends, and (b) shorter record lengths that are less sensitive to trends but are more sensitive to inter-annual to decadal variations. The changing network of observing stations also constrains the choice of reference periods to several decades or less.

The 30-year "normals" are typically updated at the start of a new decade by operational agencies such as NOAA. For example, the present "normals" are for the 1981-2010 period, which replaced the 1971-2000 reference period after 2010. Even though such an updating of normals retains 66% of the years in the preceding 30-year period, the updates often result in non-negligible changes of the reference-period means.

Further complicating the use of reference periods is the fact that some observational records are too short to allow the calculation of 30-year averages. Users of such records must choose shorter reference periods, for which the averages are affected even more than 30-year averages by decadal-scale natural variability compared to 30-year averages. The lack of availability of 30 years of data creates challenges when describing and comparing changes using datasets of different lengths.

Arctic change is occurring rapidly, especially in the post-2000 period (AMAP 2012). The changes of the past decade are large enough that they can affect the 30-year means to which variations of climate are referenced. The rapid changes are such that a year that is cooler than the average for the most recent period of 10, 20 or even 30 years can actually be warmer than averages from the 20th Century.

The pan-Arctic temperatures shown in **Fig. 10.1** provide an excellent example of the sensitivity to the reference period. The 1981-2010 average temperature is about 1°C warmer than the 1961-1990 average used to compute the departures from average in **Fig. 10.1**. Therefore, if **Fig. 10.1** had been referenced instead to the 1981-2010 average, the values on the y-axis

would be shifted upwards by about 1°C. With this upward shift, the temperatures of the 1980s, which are shown in **Fig. 10.1** as about 0.5°C warmer than the 1961-1990 average, would have negative departures from the 1981-2000 average. In other words, the 1980s were warmer than the 1961-1990 average but colder than the 1981-2010 average.

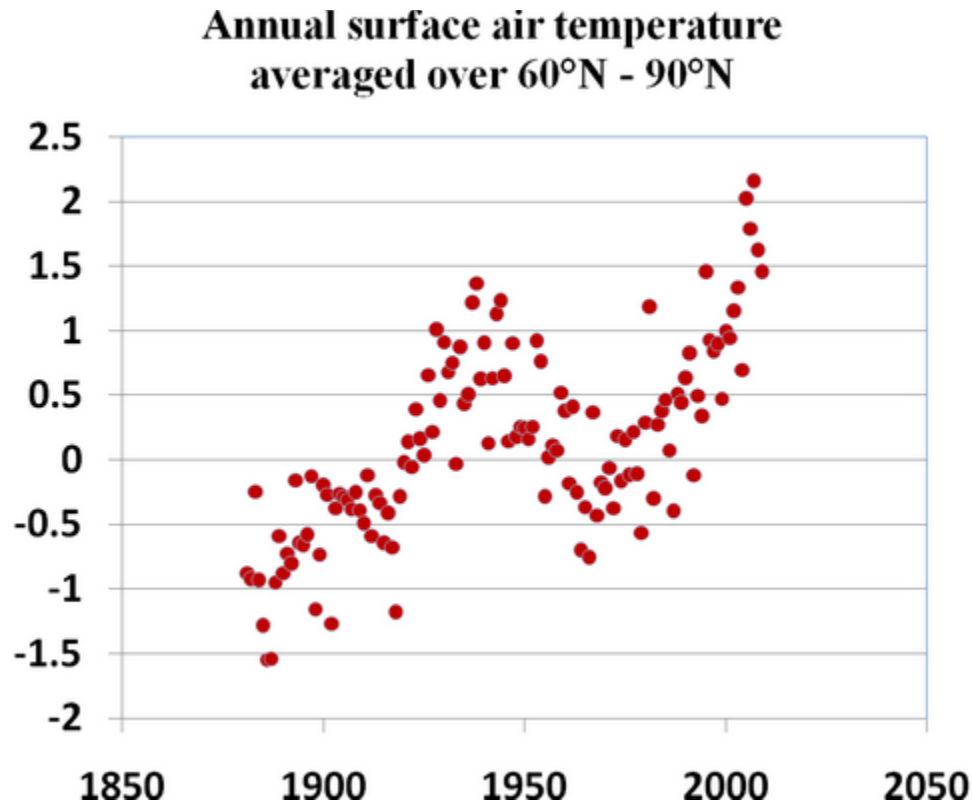


Fig. 10.1. Yearly mean temperatures for 1880-2009 averaged over the region of 60-90°N. Values are plotted as departures from the mean for 1961-1990. Source: AMAP (2012).

Given the rapidity of recent Arctic changes and the increasing importance of the forced component (change driven by external forcing, mainly greenhouse gases and aerosols), one may argue that the use of reference periods is becoming outdated, especially with the availability of statistical tools for variational time series analysis (spectral techniques, rank correlation methods, etc.). However, reference periods continue to pervade weather and climate analyses and products. For example, the monthly and seasonal outlooks issued by the NOAA Climate Prediction Center are presented in terms of probabilities of "above-normal" and "below-normal" terciles (values that partition the data into three groups, each containing one-third of the total number of observations), which are defined on the basis of 30-year reference periods. Moreover, many of the time series and changes presented in the most recent U.S. National Climate Assessment (USGCRP 2014) are relative to reference periods, and the choice of optimal reference periods in such assessments is generally not straightforward.

To illustrate the impact of the reference period at particular locations, **Fig. 10.2a** shows the changes in the 30-year mean temperatures for Alaskan weather stations when the reference

period was changed from 1971-2000 to 1981-2010. This 10-year update increased the 30-year "normal" temperatures in most months at most stations, as the decade of the 2000s was generally warmer than the decade of the 1970s in Alaska. In some instances, the "normals" increased by 1-2°C. The decade of the 2000s was also generally wetter than the decade of the 1970s in Alaska, so the 30-year reference-period precipitation means also increased; **Fig. 10.2b** shows that the changes in the reference-period precipitation means exceeded 30% at some locations, especially in the cold season.

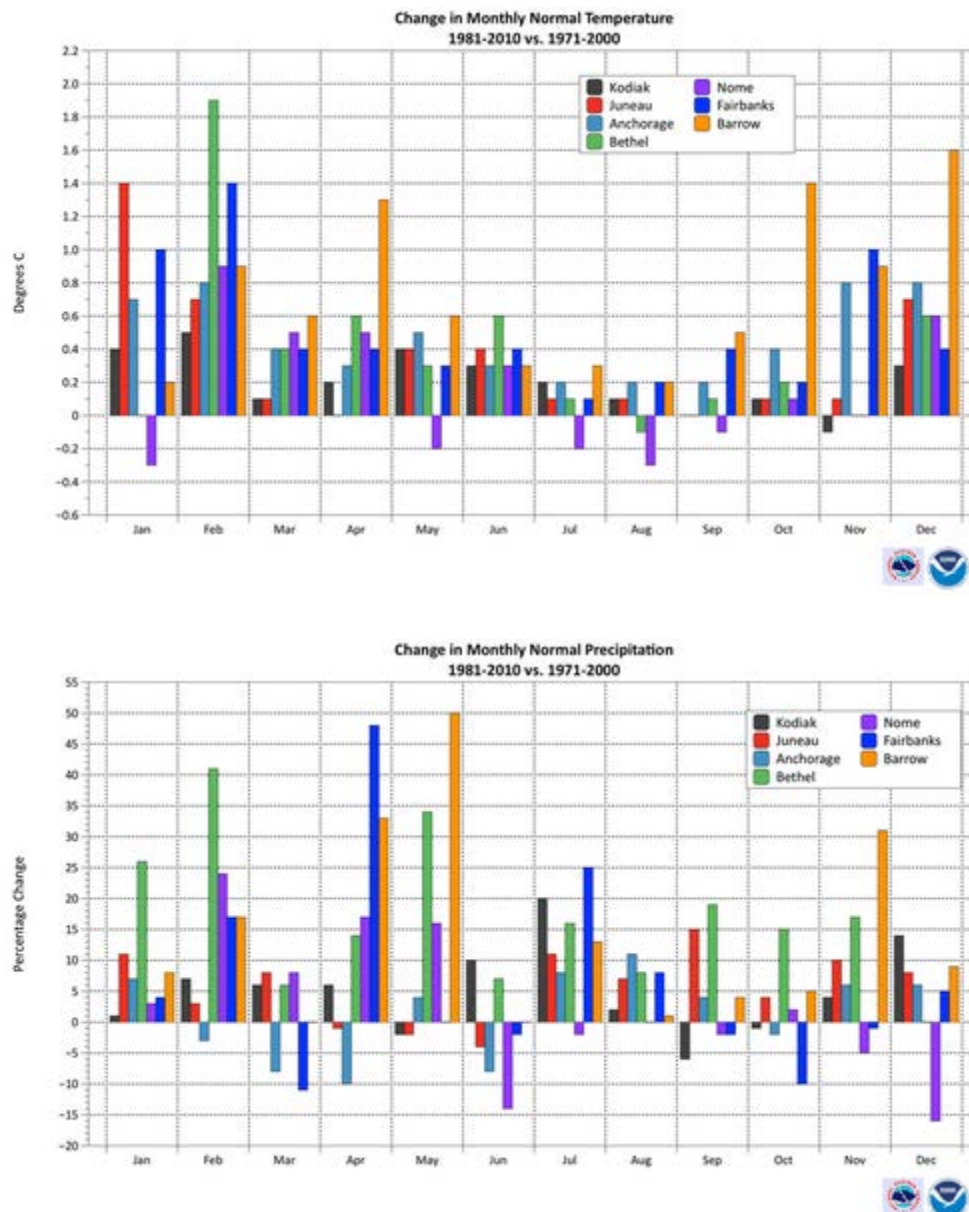


Fig. 10.2. Changes in (a, top) 30-year normals of monthly surface air temperature and (b, bottom) monthly precipitation at major observing locations in Alaska when the reference period used to compute normals changed from 1971-2000 to 1981-2010. Source: NOAA National Weather Service, Fairbanks Forecast Office (C. Bogel and R. Thoman, NOAA/NWS Alaska Region).

In the cases of both temperature and precipitation (**Figs. 10.2a and 10.2b**), the changes due to the shift in the reference period are comparable to the changes expected over multi-decadal periods in climate model simulations under greenhouse forcing scenarios. For example, the Third U.S. National Climate Assessment (USGCRP 2014, p. 28-29) shows projected precipitation changes of 20-30% over much of Alaska in all seasons by the late 21st Century under the A2 scenario. The projected late-century warming under the same scenario is 3-5°C over much of Alaska.

While **Fig. 10.2** depicts changes in means for individual calendar months, even the annual mean temperatures are affected substantially by the post-2000 warming. **Figure 10.3a** shows the departure of the annual mean temperatures of 2001-2013 from the mean for the 1971-2000 reference period. Annual means for the most recent 13 years exceeded those of the reference period by 1-2°C over most of the Arctic, where the warming was clearly amplified relative to lower latitudes. The warming is even greater in the winter season (**Fig. 10.3b**), when it ranges from 2-4°C over much of the Atlantic sector of the Arctic.

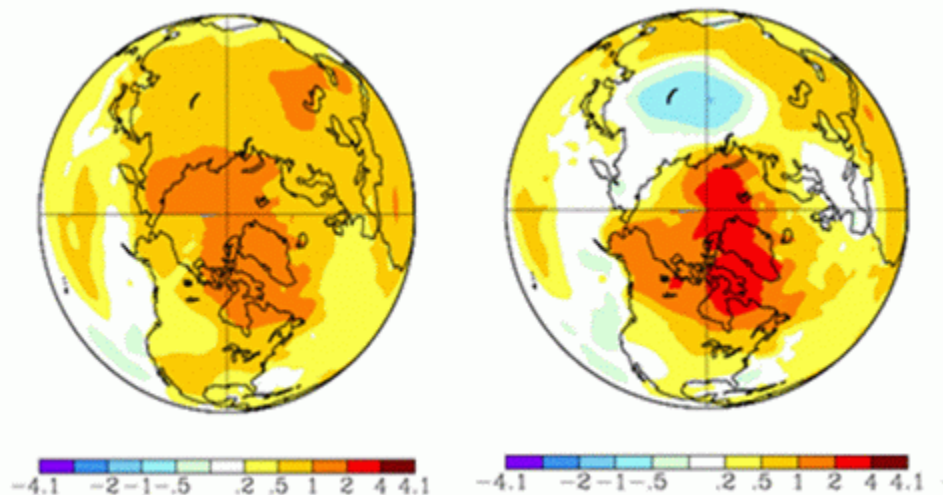


Fig. 10.3. Differences between (a) annual mean air temperatures of 2001-2013 and 1971-2000, and (b) winter (December-February) temperatures of 2001-2013 and 1971-2000. Source: NASA Goddard Institute for Space Studies, <http://data.giss.nasa.gov/gistemp/maps/>.

Figure 10.4 compares the departures from normal of the 2001-2013 autumn air temperatures from the means for two 30-year reference periods: 1971-2000 and 1981-2010. Autumn is a season of significantly reduced sea ice extent in the recent decade (Cavaliere and Parkinson 2012) and the season in which air temperatures appear to be most affected by the loss of sea ice (Overland and Wang 2010). Relative to the 1971-2000 reference period, approximately half the Arctic Ocean was more than 4°C above "normal" during 2001-2013. However, relative to the 1981-2010 reference period, essentially none of the Arctic Ocean had temperature departures as large as 4°C. Temperature anomalies over some northern land areas exceeded 2°C relative to their 1971-2000 means, while there were no substantial areas as much as 2°C warmer than

the means for the later period (1981-2010). The extent to which the autumn temperatures of 2001-2013 were anomalous clearly depends on the choice of reference period.

Departures from normal temperature, Sep-Nov 2001-2013

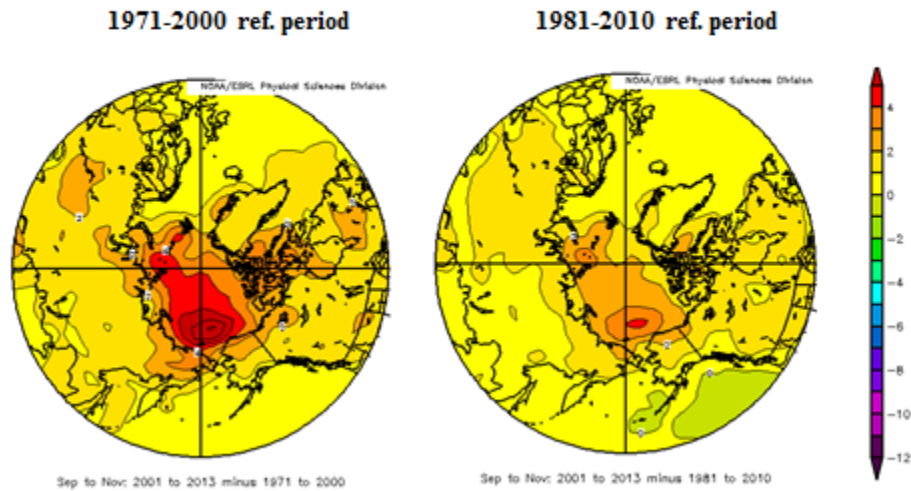


Fig. 10.4. Departures of autumn (September–November) air temperatures for 2001–2013 from the means of the 30-year reference periods (a, left) 1971–2000 and (b, right) 1981–2010.

Source: NOAA Earth System Research Laboratory,
<http://www.esrl.noaa.gov/psd/data/reanalysis/reanalysis.shtml>.

Multi-decadal variability is also a characteristic of temperatures in middle latitudes, although the amplitude of multi-decadal variations averaged over comparable areas is smaller in middle than in high latitudes. This variability creates challenges for the establishment of statistical significance of trends in the Arctic and, as shown here, the quantitative description of anomalies (or any departures from normal) in the Arctic. While the focus here has been Arctic temperature (and precipitation, to a lesser extent), the challenges inherent in the choice of a reference period extend to other climate variables in the Arctic and in any other region that is undergoing rapid change.

In conclusion, calculating, and especially communicating, anomalies of climate variables depend strongly on the choice of the reference period. While a 30-year window was intended to provide a slowly varying reference period, this is not the case for the Arctic where major changes have been observed in the 2000–2010 decade. There is no formal way to resolve this issue, other than to state clearly the reference period chosen to calculate any anomaly value.

References

AMAP. 2012. Arctic Climate Issues, 2011: *Changes in Arctic Snow, Water, Ice and Permafrost*. Arctic Monitoring and Assessment Programme, Oslo, 2011, 97 pp. Available at <http://www.amap.no/swipa/>.

Cavalieri, D. J., and C. L. Parkinson, 2012: Arctic sea ice variability and trends, 1979-2010. *The Cryosphere*, 6, 881-889, doi:10.5194/tc-6-881-2012.

Overland, J. E., and M. Wang, 2010: Large-scale atmospheric circulation changes are associated with the recent loss of Arctic sea ice. *Tellus*, 62A, 1-9.

USGCRP, 2014: U.S. National Climate Assessment, 2014: *Global Climate Change Impacts in the United States*. U.S. Global Change Research Program, Washington, DC. Available at <http://nca2014.globalchange.gov/downloads>.